NORTHWESTERN UNIVERSITY

Functional Maps of the Intact and Transected Lumbosacral Spinal Cord in the Decerebrate Cat Using Subdural Electrical Stimulation

A DISSERTATION

SUBMITTED TO THE GRADUATE SCHOOL
IN PARTIAL FULFILLMENT OF THE REQUIREMENTS

for the degree

DOCTOR OF PHILOSOPHY

Field of Neuroscience

By

Jacqueline Patterson

EVANSTON, ILLINOIS

September 2022

Abstract

Electrical spinal cord stimulation is an emerging treatment for spinal cord injury that can improve walking and bladder control, among many other functions. While the anatomical location of the motor pools for muscles involved in locomotion in the lumbosacral cord has been identified, the map of the functional output of subdural electrical stimulation of the lumbosacral cord in both the intact and transected states is still relatively unknown. This represents a significant gap in knowledge in spinal cord injury rehabilitation. Our first goal was to determine what hindlimb muscles are activated by subdural electrical stimulation of the intact lumbar spinal cord of the cat. Our second goal was to determine how those patterns of activation are affected by transection. In eight decerebrate cats with intact spinal cords, eight locations were stimulated starting from the caudal portion of lumbar segment L3 to the border of sacral segments S1 and S2. Stimulation was repeated 15 times at each location at 1 Hz with stimulation amplitudes high enough to evoke muscle responses without causing tissue injury. Electromyography (EMG) was measured in nine hindlimb muscles: tibialis anterior, soleus, lateral gastrocnemius, medial gastrocnemius, sartorius, vastus lateralis, biceps femoris posterior, gluteus medius, and pectineus. EMG peak to peak amplitude of the short-latency response (presumably monosynaptic), and rectified integrated EMG of the long latency response were used to assess muscle response. The spinal cord was then transected above L3, and this protocol was then repeated. In the intact cord, for most muscles, the most effective stimulus was at or near the motor pool. However, some muscles, including the sartorius, were also strongly activated outside of their motor pools. After transection, there was an overall significant change in the responses at both short and long latencies. On an individual muscle basis, the intact and transected responses largely overlapped at earlier latencies, but during the longest latency window, a few muscles had significant differences between the intact and transected responses at multiple stimulation locations. These results suggest that subdural electrical stimulation in the intact cord results in muscle activity that largely

aligns with but is broader than the motor pools, and that changes in the acute transected cord. Further research is needed to understand how the maps are affected by chronic spinal cord injury.

Acknowledgment

This dissertation would not have been possible without the amazing community of people surrounding me. To CJ, for being a great advisor who values living a vibrant life alongside doing great science. To Vicki and Monica, for being supportive committee members and making this work better. To Matthieu and Amr, for being both great teachers and fun people to do science with. To Netta and Theresa, for being supportive mentors over the years. To my parents, who cultivated an environment where my curiosity and confidence could grow and have supported me through all the twists and turns. To my sisters, who taught me how to communicate quickly and effectively in order to be heard in a house of four girls. To Lydia, Shannon, and Kaitlyn, who have taught me so much about what it means to be human and have journeyed alongside me through every up and down of grad school. To Mary and Vatsala, who gave me the courage to speak up and out and buoyed me through every crisis. To all my classmates, to be in the same boat as you for the past six years has been an honor. To Terry, for climbing mountains with me and keeping me well fed and laughing to every summit and back. To Cleo, for being pure joy and pure menace. To my therapist, who provided the space for me to heal and grow. And finally to all of my friends, who have been my greatest inspirations and greatest supports through the past six years.

List of Abbreviations

BF	Biceps Femoris Posterior
EMG	Electromyography
GM	Gluteus Medius
LG	Lateral Gastrocnemius
MG	Medial Gastrocnemius
PT	Pectineus
PIC	Persistent Inward Current
RIEMG	Rectified Integrated Electromyography
SR	Sartorius
SCI	Spinal Cord Injury
SCS	Spinal Cord Stimulation
SL	Soleus
TA	Tibialis Anterior
VL	Vastus Lateralis

Table of Contents

List of Tables, Illustrations, Figures, and Graphs

I. Background and Rationale

Spinal Cord Injury

Prevalence, Causes, and Costs

Spinal Cord Injury (SCI) is prevalent, costly, and debilitating, making SCI research urgent and necessary. There are an estimated 294,000 people living with SCI in the United States, with about 17,800 new cases per year (Anon 2020; Hachmann et al. 2021). People who suffer a spinal cord injury are typically young—the average age is 43—meaning that research that improves outcomes will improve individuals' quality of life over a greater span of their lives (Anon 2020). SCI can result in paralysis, spasticity, bladder infections, bowel issues, and cardiac and respiratory dysfunction, all of which greatly impact individuals physiologically, psychologically, socially, and economically (Hachmann et al. 2021; Silva et al. 2014).

The leading cause of SCI is vehicle crashes, followed by falls, then violence (primarily gunshot wounds), and then sports (Anon 2020). While SCI impacts people of all races, socioeconomic status, etc., it disproportionately affects some communities more than others (Anon 2020). Black people are disproportionately affected by SCI, with 24% of SCIs occurring in non-Hispanic Black people, which is much higher than the proportion of non-Hispanic Black people in the general population (13%) (Anon 2020). This is likely due to systemic oppressive systems that have led to a higher proportion of Black people in low-wage manual jobs that have greater risk of vehicle accidents and falls, as well as a higher proportion of Black people experiencing poverty that contributes to gun violence. Therefore, work to dismantle systemic oppression and poverty is a key public health aspect of preventing spinal cord injury.

The estimated lifetime costs of health care and living expenses (not including loss in wages, productivity, etc.) for someone with an SCI is $1.2 - $5.1 million (Anon 2020). The average hospital

stay post injury is 11 days, followed by an average rehab stay of 31 days; both averages have decreased over the years, with a contributing factor being limits in what insurance will cover (Anon 2020). 30% of people with SCI are hospitalized one or more times in any given year following the injury, with the average hospital stay being 18 days (Anon 2020). Additional health care costs include wheelchairs and other mobility aids, health aides, additional rehabilitation, medications, and more. On top of that, only 18% of people with SCI are employed one year following the injury, compared to 67% before the injury, and that only increases to 32% 40 years after the injury (Anon 2020). Devastatingly, the average remaining years of life for people with SCI has not improved since the 1980s and is significantly below the life expectancy of people without SCI (Anon 2020).

Physiology

When SCI occurs, there is the primary injury as a result of the impact, followed by a secondary injury that results from a biological cascade of events (e.g. inflammatory response, excitotoxicity, thrombosis, etc.) over minutes and weeks that leads to further damage (Silva et al. 2014). Supraspinal input is cut off to the cord below the level of injury, and without excitatory monoaminergic input, motoneuron excitability is promptly and drastically diminished (Heckman et al. 2009a). At the same time, with the loss of monoaminergic input comes the disinhibition of spinal interneurons (Heckman et al. 2009a). Even still, with the reduced motoneuron excitability, extension reflexes are almost nonexistent, and flexion reflexes become greatly weakened (Heckman et al. 2009a). Over a century of research has established that basic neural circuits needed for standing and locomotion exists within the lumbosacral cord, and remain intact (albeit depressed) below the level of the SCI (Musienko et al. 2012). The challenge then is to transform (i.e. increase the excitability of) these intact circuitries into functional states (Musienko et al. 2012).

Treatments

In an effort to increase the excitability of these spinal circuits, multiple strategies have been investigated: electrical stimulation of muscles and dorsal roots, epidural and intraspinal electrical spinal cord stimulation, pharmacological agents, stem cells, and implantable polymer scaffolds (Hachmann et al. 2021; Musienko et al. 2012; Silva et al. 2014). With all the treatments available and still in development, there is no cure and recovery of full mobility is rare (Hachmann et al. 2021). For individuals with paraplegia, restoring their ability to walk is typically the number one priority, while individuals with tetraplegia prioritize hand and arm function (Hachmann et al. 2021).

Spinal Cord Physiology

Structure

The spinal cord is comprised of a variety of neurons that each play an important role in motor output. The cord consists is divided into the cervical, thoracic, lumbar, and sacral sections, which each contain segments along their length (Hochman 2007). Each segment consists of white matter, which is composed of axons traveling within and between segments, and grey matter, which is composed of cell bodies. The three classes of cells in the spinal cord that will be explored herein: sensory afferents, interneurons, and motoneurons.

Sensory Afferents

Sensory afferents enter the cord via the dorsal root, and their cell bodies lie in the dorsal root ganglion. In the motor system, these afferents include Ia, which encode muscle velocity, II, which encode muscle length, and Ib, which encode muscle force (Hochman 2007; Vincent et al. 2017). The Ib afferents synapse in the dorsal horn, whereas the Ia and II afferents synapse in the dorsal or ventral horn either with interneurons or directly with motoneurons (Brown 1981; Nichols et al. 1999; Vincent et al. 2017). Afferents have many collaterals and may enter the spinal cord segments away from where they ultimately synapse. For example, afferent collaterals projecting

from L2 through L4 spinal segments to at least S1 have been discovered by electrophysiology and axonal degeneration studies (Imai and Kusama 1969; Wall and Werman 1976). It has also been shown that dorsal horn interneurons respond to input from afferents that enter the cord up to three segments away (Mendell et al. 1978).

Interneurons

The gray matter also consists of interneurons, whose main function is to integrate information from afferents and descending input (Jankowska 1992). Ia inhibitory interneurons are directly activated by Ia afferents and supraspinal input and target motoneurons (Jankowska 1992). Their cell bodies are in the same segment as the entering Ia afferents, but in a different segment than the antagonist motoneurons they synapse with (Brown 1981). They are inhibited by Renshaw cells (Jankowska 1992). Ia afferents have been shown to adjust motoneuron excitability during movement, including during muscle stretch, postural reflexes, and fictive locomotion (Jankowska 2001). Ib is a second type of interneuron receives convergent input from Ib afferents, spindle afferents, and descending pathways to coordinate the activity of muscles across joints (Jankowska 1992; Jankowska and Edgley 2010). Just as afferents may exist in different segments from the motoneuron they synapse with, so may interneurons. Last order interneurons tend to be in the same segments as the motoneurons they synapse with, but have also been found up to four segments rostral (Jankowska 1992).

Motoneurons

Motoneurons are located in the ventral horn and send their axons through the ventral root to activate muscles. These neurons integrate information from supraspinal input, afferents, and interneurons.

Spinal stimulation as a treatment for different things

History

Electrical stimulation, as introduced above as a treatment for spinal cord injury, was first indicated to augment motor outputs in 1871 (Nagel et al. 2017). Spinal cord stimulation (SCS) was first introduced as a treatment for chronic neuropathic pain in 1967 and has since become a standard of care (Nagel et al. 2017; Thiriez et al. 2014). Today, at least 35,000 stimulators are implanted annually for chronic pain (Kumar and Bishop 2009). In 1973, a person with multiple sclerosis receiving SCS for pain reported major improvements in mobility, speech, and swallowing (Cook and Weinstein 1973). The researchers went on to implant SCS devices in additional patients and in 1979 reported 99 of the first 204 patients receiving SCS improved (Cook et al. 1979). Since then, clinical trials testing SCS in other movement disorders have emerged (Thiriez et al. 2014). One 1997 study followed 1336 patients with cerebral palsy, dystonia, torticollis, multiple sclerosis, spinocerebellar degeneration, spinal cord injury, and traumatic brain injury over two and a half decades (Waltz 1997). The majority of these participants showed moderate to great improvement (Waltz 1997). In 2002, epidural stimulation was demonstrated for the first time to facilitate motor improvements in individuals with incomplete SCI (Herman et al. 2002).

Urination

In people with SCI, SCS is being tested for impairments with urination and bowel movements. Sacral anterior root stimulation has been shown to be effective for improving bowel and bladder emptying in thousands of people with SCI (Martens and Heesakkers 2011). However, this treatment requires sensory deafferentation to prevent bladder reflex contractions, which permanently damages reflex erection, reflex urination and any pelvic sensation (Bourbeau et al. 2020). An alternative approach is being tested that electrically blocks the pudendal nerves or sacral roots; fortunately, this approach does not require sensory deafferentation and appears to

have similar results to the first approach (Boger et al. 2012). Lumbosacral cord SCS to improve bladder and bowel control is in the initial stages of testing and shows promising results as well (Gad et al. 2014).

Spasticity

Studies examining SCS for spasticity are less conclusive, with some showing promising results and others no evidence of improvement (Nagel et al. 2017).

Potential

SCS has been implemented as a therapy for over fifty years. However, there is still much research to be done before it is implemented as a standard of care for movement impairments, and particularly standing and walking, following spinal cord injury. Current implementation of SCS in SCI will be explored further in the final section of this chapter.

Types of Stimulation

This SCS used to treat different conditions can actually be subdivided into four types of stimulation: epidural, transcutaneous, subdural, and intraspinal. While stimulation can occur directly at the muscles, spinal stimulation is much more fatigue resistant and also has added autonomic benefits: it can improve bladder control, sexual function, and temperature regulation with motor training (Bourbeau et al. 2020; Darrow et al. 2019; Holinski et al. 2016). Further, spinal stimulation, as opposed to muscle stimulation, can assist with remodeling neural pathways with rehabilitation, building functional pathways rather than maladaptive pathways (Ievins and Moritz 2017). The four types of spinal stimulation described herein differ in their location of application, mechanisms, and outcomes.

Cutaneous

Cutaneous spinal stimulation has electrodes placed on the skin above the vertebrae (Ievins and Moritz 2017). Its effects depend on body position, with varying levels of current needed to elicit movement depending on if the body is prone, standing, or supine due to the context dependent nature of spinal pathways (Danner et al. 2016; Dimitrijevic et al. 1986). The mechanism by which this stimulation elicits movement is by way of increasing the baseline level of excitability to enable remaining supraspinal or sensory input to elicit movement (Edgerton et al. 2008). High frequency stimulation allows for higher currents to be applied without skin damage or discomfort, and has been shown to activate the lumbar cord in both individuals with SCI and individuals with intact spinal cords (Gerasimenko et al. 2015a). Cutaneous stimulation over the thoracic spinal cord has resulted in improvements in spasticity and improved stepping in people with SCI (Hofstoetter et al. 2014, 2015; Minassian et al. 2016). Similarly, when applied over the cervical spinal cord, cutaneous stimulation has bene shown to improve hand and arm function (Gerasimenko et al. 2015b). Cutaneous stimulation is especially attractive as it does not require surgery, but as it is a newer technology, more research is needed to understand and improve its effectiveness.

Epidural

Epidural stimulation has electrodes placed on the dorsal surface of the cord above the dura (Hachmann et al. 2021; Ievins and Moritz 2017). The 1967 experiment referenced earlier in which SCS used to treat pain also improved movement in a person with multiple sclerosis specifically used epidural stimulation (Shealy et al. 1967b). Stimulation caused a buzzing sensation that relieved pain for 5-15 minutes, and it was proposed that the stimulation inhibited pain signals by activating larger sensory fibers and quieting smaller pain fibers (Shealy et al. 1967a). Since 1967, additional evidence supporting epidural stimulation’s effectiveness has been reported (Ievins and Moritz 2017). Epidural stimulation in individuals with multiple sclerosis has been shown to improve spasticity, motor function, and sensory function (Cook and Weinstein 1973). Epidural stimulation

in individuals with spinal cord injury and individuals with multiple sclerosis has been shown to improve motor function and bladder control (Campos et al. 1981). In animal models, epidural stimulation has been shown to induce stepping movements in decerebrated cats and to improve locomotion in non-human primates with spinal cord injuries (Capogrosso et al. 2016; Iwahara et al. 1992).

Suprathreshold epidural stimulation can be used to directly activate neurons, and subthreshold stimulation can be used to increase the excitability of neurons so that supraspinal and sensory inputs can bring neurons above threshold and induce movements (Ievins and Moritz 2017). Subthreshold epidural stimulation in the rat spinal cord has been shown to induce movement when there is also proprioceptive inputs (Gad et al. 2013).

Epidural stimulation has also been shown to be effective in improving human motor behaviors (Ievins and Moritz 2017; Mushahwar 2000). Suprathreshold epidural stimulation has been shown to induce lower limb extension in individuals with SCI, which was hypothesized to be due to the activation of sensory afferents which in turn activated the necessary neural network (Jilge et al. 2004). It has also helped individuals with complete and incomplete SCI make volitional movements in both the upper and lower limbs (Angeli et al. 2014; Harkema et al. 2011; Lu et al. 2016). In some cases, the motor improvements outlast the period of stimulation (Lu et al. 2016). Individuals with complete spinal cord injury have also been shown to produce muscle activity but not movement with epidural stimulation, which demonstrates that even with complete injuries, spared pathways can still trigger movements (Moss et al. 2011).

Subdural

Subdural stimulation has electrodes implanted under the dura but not yet in the spinal cord. This technique is less invasive than intraspinal stimulation, but may still offer more specificity than

cutaneous or epidural stimulation (Sharpe and Jackson 2014). Subdural stimulation has been shown to elicit locomotion in cats (Iwahara et al. 1992). Subdural stimulation of the cervical cord in sedated monkeys functionally activated muscles and showed great rostrocaudal specificity (Kato et al. 2020). The current understanding of subdural spinal stimulation is incomplete, and research on it is still less common. Therefore, further research is needed to understand the mechanisms underlying subdural stimulation and how it can be implemented following SCI.

Intraspinal

Intraspinal stimulation has electrodes implanted within the spinal cord (Ievins and Moritz 2017). It is hypothesized the intraspinal stimulation directly activates motoneurons, as well as propriospinal neural networks that coordinate limb movements (Ievins and Moritz 2017). As of now, intraspinal studies in humans are rare, but there has been some extensive study in animal models (Ievins and Moritz 2017). When applied to the ventral spinal cord, its been shown to directly activate motoneurons or ventral root axons, evoking single joint movements, including stepping, reaching, and grasping (Holinski et al. 2016; Moritz et al. 2007; Mushahwar et al. 2002; Mushahwar and Horch 1998a; Saigal et al. 2004; Zimmermann et al. 2011). In rats and cats, intraspinal stimulation of the lumbosacral cord has produced weight-bearing standing and stepping (Mushahwar 2000; Sharpe and Jackson 2014). Intraspinal stimulation in the cervical cord in monkeys produces EMG responses in upper limb muscles, and when multiple electrodes are stimulated, grasping and reaching movements can be elicited (Moritz et al. 2007; Zimmermann et al. 2011). Studies in rodents have demonstrated motor improvements that outlast the stimulation period (McPherson et al. 2015; Mondello et al. 2014). As will be described in a future section on spinal cord mapping, extensive mapping of the lumbosacral spinal cord has been performed using intraspinal stimulation in cats.

Conclusion

Currently, no type of stimulation fully restores mobility in the long term, and so extensive research is still need to further develop these technologies. Gaps remain in our understanding of the mechanism, and so research to unveil the underlying mechanisms of this stimulation is a foundational step. Nonetheless, all stimulation types show therapeutic potential.

Mapping in Cats

In 1892, Sherrington first described a rostrocaudal distribution of motoneuron pools from the organization of ventral roots innervating hindlimb muscles (Sherrington 1892). In 1951, Romanes discovered that motoneurons innervating each cat hindlimb muscle are arranged in columns in the ventral horn, and that muscles acting on the same joints are organized in the same longitudinal columns (Romanes 1951, 1964). Since then, our knowledge of the rostrocaudal longitudinal organization of the cat lumbosacral cord has greatly increased, particularly with the development of the method of intraspinal microstimulation. Study after study has shown that while there may be variation in the absolute position of the functional map of the lumbosacral cord, the relative positions between motor pools and functional responses are consistent (Mushahwar 2000; Vanderhorst and Holstege 1997). Further, functional responses appear to align well with the anatomical motor pools (Mushahwar 2000). Additionally, the dimensions of the functional activation pools also aligned well with the dimensions of the anatomical motor pool (Mushahwar 2000).

A few trends have been defined. First, the more rostral a muscle is in the hindlimb, the more rostral its motoneurons are in the spinal cord (Vanderhorst and Holstege 1997; Yakovenko et al. 2002). Second, the more anterior a muscle is within the hindlimb, the more rostral its motoneurons are (Vanderhorst and Holstege 1997). For instance, hip flexors are anterior to hip extensors in

the hindlimb, and therefore hip flexor motoneurons are more rostral than hip extensor motoneurons in the cord; however, knee extensors are anterior to the knee flexors in the hindlimb, and therefore knee extensor motoneurons are more rostral than knee flexor motoneurons in the cord (Vanderhorst and Holstege 1997; Yakovenko et al. 2002). Finally, the more distal a muscle is in the hindlimb, the more caudal its motoneurons are in the cord (Vanderhorst and Holstege 1997). Its also been found that the caudal half of the lumbosacral cord contains many more motoneurons than the rostral half, and that most of these motoneurons innervate extensors (Vanderhorst and Holstege 1997; Yakovenko et al. 2002). In fact, more than 80% of flexor motoneurons are in the rostral half of the lumbosacral cord (Yakovenko et al. 2002). Overall, in cats, the general rostrocaudal organization of the hind limb with lumbosacral spinal stimulation appears to be: hip flexors activated by the most rostral stimulation, followed by knee extensors, then ankle flexors, hip extensors, toe flexors, ankle extensors, and finally knee flexors being most caudal.

Mapping in Other Animals

Overall, research shows that a similar rostrocaudal arrangement of hindlimb motor pools exists in the frog, pigeon, chick, rat, rabbit, guinea pig, dog, cat, rhesus monkey, macaque, gorilla, and human (Vanderhorst and Holstege 1997). This is true, even as the function of the hindlimb varies greatly across animals; e.g. rhesus monkeys and frogs use their hindlimbs very differently and even rhesus monkeys and cats, both quadrupedal, vary greatly in their hindlimb placement and function during locomotion (Cruce 1974; Toossi et al. 2019). In all species, there was found to be variability between animals within a species, but a general order of rostrocaudal organization. In the rhesus monkey, intraspinal stimulation built a map as follows from rostral to caudal: hip flexors, then knee extensors, then ankle flexors, then hip extensors, then toe flexors, then ankle extensors, then knee flexors (Toossi et al. 2019). This functional rostrocaudal arrangement has

also been shown to align with the anatomical rostrocaudal arrangement (Toossi et al. 2019). That said, despite a similar rostrocaudal organization of functional maps, the dimensions of cord that evoke different motor patterns varies between animals. For example, knee extension is evoked in a larger portion of the lumbosacral cord in monkeys compared to cats, while knee flexion is evoked in a smaller portion in monkeys compared to cats (Toossi et al. 2019).

Applications in Humans

Research to further understand the functional organization of the spinal cord will help improve electrical stimulation as a treatment for spinal cord injury. As electrical stimulation improves in its precision, it will become more efficacious in restoring mobility. Herein, the current landscape of electrical stimulation as a treatment in human spinal cord injury is explored.

Epidural Stimulation

As previously described, in 1967, the field saw the first evidence of improved motor behaviors during epidural stimulation that was applied to treat pain in an individual with multiple sclerosis (Hachmann et al. 2021; Shealy et al. 1967a, 1967b). In the 1970s, 80s, and 90s, further research demonstrated epidural stimulation modulated the motor system, and even improved voluntary motor, bladder, and bowel function in some participants (Dimitrijevic et al. 1986; Dooley 1976; Hachmann et al. 2021). In 1998, Dimitrijevic et al. showed that lumbar epidural stimulation induced rhythmic flexion-extension patterns in paraplegic individuals, providing evidence of central pattern generators in humans that remained intact and functional with stimulation (Dimitrijevic et al. 1998). Shortly after, Herman et al. demonstrated that epidural implants in people with SCI could improve motor function (Carhart et al. 2004; Herman et al. 2002; Huang et al. 2006). In 2011, Harkema et al. showed for the first time that epidural stimulation could resptore stepping and weight-bearing standing in individuals with motor complete SCI (Harkema et al.

2011). In 2014, Angeli et al. showed that voluntary motor control could be restored relatively quickly in individuals with motor and sensory complete injuries (Angeli et al. 2014). Rejc et al. later reported full weight-bearing overground standing with only a handrail for balance in these same individuals (Rejc et al. 2015). They found that individualized, higher frequencies resulted in better standing (Rejc et al. 2015). Interestingly, they found that step-training led to poorer standing performance in most individuals, suggesting that motor learning and plasticity may be task-specific, and rehabilitation protocols may impair some motor behaviors (Rejc et al. 2017b). Then, Rejc et al. found one individual could maintained volitional control even after the stimulator was turned off, suggesting the stimulation and rehabilitation triggered plasticity (Rejc et al. 2017a). In 2018, Angeli et al. showed that epidural stimulation allowed for overground walking with assistive devices in individuals with incomplete SCI, and weight-supported treadmill stepping in an individual with complete SCI (Angeli et al. 2018). In 2019, Darrow et al. demonstrated for the first time the restoration of volitional control during the first application of epidural stimulation, meaning without prior rehabilitation and training (Darrow et al. 2019). In 2020, Peña Pino et al. showed restoration of volitional control in individuals with both complete and incomplete SCI, and that half of individuals maintained volitional control when stimulation was turned off, although with less fidelity than when stimulation was on (Peña Pino et al. 2020).

In total, epidural stimulation has improved significantly over the past few decades in its efficacy in improving motor behaviors for individuals with SCI. Alongside improvements in voluntary control, these decades of research have also showed improvements in bladder and bowel control, sexual function, blood pressure regulation, and more autonomic functions (Hachmann et al. 2021). The number of individuals tested is still small, and a complete restoration of function has yet to be achieved. Therefore, further research is necessary to improve the efficacy of epidural spinal stimulation to improve movement after SCI.

Intraspinal Stimulation

While epidural spinal stimulation has had decades of implementation and innovation in humans, intraspinal stimulation has yet to be implemented in humans. Intraspinal stimulation has been studied extensively in small animal models, and is slowly being tested in large animal models (e.g. pigs) and non-human primates. Before intraspinal stimulation can be safely and effectively be implemented in individuals with SCI, it first must be proven successful in these large animal models and non-human primates.

Limited studies in nonhuman primates with SCI have shown that intraspinal stimulation of the cervical spinal cord produces EMG responses in upper limb muscles (Moritz et al. 2007). Cervical intraspinal stimulation has also been shown to elicit functional hand movement in nonhuman primates, and multiple intraspinal electrodes can be combined to produce reaching and grasping movements (Nishimura et al. 2013; Zimmermann et al. 2011).

Cutaneous and Subdural Stimulation

As of now, there is little to no research on the implementation of cutaneous and spinal stimulation in individuals with SCI. Further research is needed.

II. Functional Map of the Intact Lumbosacral Cord

Abstract

Direct electrical stimulation of the spinal cord shows promise as a therapy for patients with motor impairments after spinal cord injury. While the anatomical location of the motor pools for muscles involved in locomotion in the lumbosacral cord has been identified, the map of the functional output of subdural electrical stimulation of the lumbosacral cord is still relatively unknown. This represents a significant gap in knowledge in spinal cord injury rehabilitation. Our goal was to determine what hindlimb muscles are activated by subdural electrical stimulation of the lumbar spinal cord of the cat. In eight decerebrate cats with intact spinal cords, eight locations were stimulated starting from the caudal portion of lumbar segment L3 to the border of sacral segments S1 and S2. Stimulation was repeated 15 times at each location at 1 Hz with stimulation amplitudes high enough to evoke muscle responses without causing tissue injury. Electromyography (EMG) was measured in nine hindlimb muscles: tibialis anterior, soleus, lateral gastrocnemius, medial gastrocnemius, sartorius, vastus lateralis, biceps femoris posterior, gluteus medius, and pectineus. EMG peak to peak amplitude of the short-latency response (presumably monosynaptic), and rectified integrated EMG of the long latency response were used to assess muscle response. For the short latency response, the most rostrally responding muscles were sartorius, pectineus, and vastus lateralis; the remaining muscles responded more caudally. For most muscles, the most effective stimulus was at or near the motor pool. However, some muscles, including the sartorius, were also strongly activated outside of their motor pools. For the long latency response, sartorius, pectineus, and vastus lateralis responded most rostrally, then tibialis anterior, followed by the remaining muscles more caudally. These results suggest that subdural electrical stimulation of the spinal cord evokes muscle responses that largely align with motor pools but can also activate some muscles outside the anatomical location of their motor pools.

Introduction

Spinal cord injury (SCI) impacts an estimated 282,000 people in the United States and can lead to impairments in mobility and even paralysis (Ievins and Moritz 2017). While SCI disrupts the connection between supraspinal and spinal neurons, spinal networks below the level of the injury largely remain intact (Musienko et al. 2012). This makes the spinal cord an excellent therapeutic target, as sensorimotor pathways are preserved allowing for potential movement generation (Ievins and Moritz 2017).

Electrical stimulation targeting these intact networks shows therapeutic promise to help restore sensorimotor function. Advances in spinal electrical stimulation over the past few decades have produced functional improvement in locomotion, breathing, bladder function, and pain management (Angeli et al. 2014; Jilge et al. 2004; Martens and Heesakkers 2011; Nagel et al. 2017; Toossi et al. 2019). Plus, compared with stimulation of muscles and peripheral nerves, spinal electrical stimulation is incredibly fatigue resistant, allowing animals to stand and walk longer (Ievins and Moritz 2017; Toossi et al. 2019).

Currently, the spinal cord stimulators used clinically are either transcutaneous, meaning above the skin, or implanted epidurally, meaning dorsal to the dura matter, which is separated from the spinal cord by cerebrospinal fluid (Anderson et al. 2019). In the 1960s and 1970s, some spinal stimulators were implanted intradurally, but development then fixated on epidural stimulation as it is easier to implant and prevents cerebrospinal fluid leakage (Anderson et al. 2019; Holland et al. 2020). The downside of epidural stimulators, however, is that they are separated from the spinal cord by the electrically resistant dura and the cerebrospinal fluid. Hence, modeling studies have shown that more than 95% of their power is dissipated before reaching the cord (Holland et al. 2020). This is a fundamental limitation of epidural spinal

stimulators that prevents selective stimulation of deeper spinal neural networks, and may contribute to suboptimal efficacy of these stimulators to restore mobility (Anderson et al. 2019; Holland et al. 2020). Additionally, while cerebrospinal fluid leakage was a previous risk, technological neurosurgical advances can prevent this leakage (Holland et al. 2020). Therefore, subdural stimulators prove to be a promising avenue in the development of more effective spinal stimulators for the treatment of paralysis after spinal cord injury, among other disorders and diseases (Anderson et al. 2019).

In order to deliver precisely targeted stimuli, a detailed functional map of the spinal cord is needed. Research across decades has produced a detailed anatomical map of motor pools in the cat (Yakovenko et al. 2002). Additionally, numerous studies have functionally mapped the lumbosacral spinal cord in cats using intraspinal stimulation (Mushahwar 2000; Mushahwar and Horch 1998b; Vanderhorst and Holstege 1997). Currently, there are no studies that have functionally mapped the lumbosacral cord in cats using subdural stimulation. The map using subdural stimulation may differ from the intraspinal map because subdural stimulation recruits fibers differently than intraspinal stimulation: its stimuli dissipate through tissue andfluid before reaching the ventral horn. Modeling has demonstrated that epidural stimulation, which also dissipates through the cerebrospinal fluid and white matter, does not penetrate spinal cord structures, and therefore does not activate motoneurons directly but instead indirectly via activation of sensory afferents (Capogrosso et al. 2013). Therefore, a question that arises is whether afferent entry to the cord aligns with the anatomical motor pools. If this is the case, subdural stimulation could evoke motor output aligned with the anatomical map.

Building a functional map of the spinal cord with subdural stimulation is essential to its development as a clinical tool in the treatment of paralysis after spinal cord injury and other disorders. The goal of this study was to map the lumbosacral cord in the decerebrate cat using

subdural stimulation. This was achieved using custom-engineered electrodes sitting on dorsal columns spanning segments L3 to S2. Activity in the hindlimb muscles was measured to chart if there were optimal stimulation locations to activate individual muscles or muscle groups. The data show that although muscle-specific activation using surface stimulation is difficult to accomplish, It is possible to attain joint-selective targeting.

Methods

Animals

All experimental procedures were approved by the Institutional Animal Care and Use Committee of Northwestern University. All animals were obtained from a designated breeding establishment for scientific research. Before the experiments, animals were housed and fed within designated areas, which were monitored daily by veterinary staff and trained personnel. The current data set is compiled from 8 adult cats of either sex weighing between 2.5 and 5.0 kg. All animals underwent acute terminal experiments, in which initial surgical procedures were done under deep gaseous anesthesia obtained by a mixture of isoflurane, nitrous oxide, and oxygen. Before data collection, a precollicular decerebration was performed. This allowed the discontinuation of anesthesia, thus warranting that spinal circuits responded fully to electrical stimulation without being suppressed by anesthesia.

Surgical preparation

Anesthesia. Anesthesia was induced in a clear cylindrical chamber with a gaseous mixture (4% isoflurane in a 1:3 mixture of O_2 and N_2O) and continued with a face mask until a tracheal tube was inserted and secured. Afterwards, isoflurane was reduced to 1.5 – 3 % and gases were delivered through the tracheal tube for the duration of initial procedures. The right common carotid artery and right jugular vein were cannulated to monitor arterial blood pressure and administer

intravenous fluids, respectively. Throughout the experiment, arterial blood pressure, heart rate, respiratory rates, reflexes, and muscle tone were recorded every 15 minutes, and used to adjust the level of anesthesia.

EMG recordings. The animal was transferred to a stereotaxic frame (Kopf) for further surgery. The animal's hindlimbs were positioned and rigidly clamped with the ankle at about 90° relative to the tibia, the knee at 130°, and the hip at 105°. Stainless steel fine wire EMG electrodes (A-M Systems, Washington USA) were inserted into nine muscles in the left hindlimb: medial gastrocnemius (MG), lateral gastrocnemius (LG), soleus (SL), tibialis anterior (TA), gluteus medius (GM), sartorious (SR), vastus lateralis (VL), biceps femoris posterior (BF), and pectineus (PT). The EMG data was recorded using custom-built differential amplifiers and were digitized at 10 KHz per channel using a power 1401 board (CED, UK). The data was acquired through SPIKE2 software (CED, UK) and stored on a computer for offline analysis.

Stimulation locations. A dorsal laminectomy was performed to expose the lumbosacral spinal cord between L3 and S2. The dura was incised and retracted to expose the spinal cord tissue and allow identification of exact location of dorsal root entry zones. A Microscribe G2X Digitizer was used to record the 3D location of the identifiable dorsal root entry zones (L3-S2) as well as the border of laminectomy. Great care was taken not to damage the cord during these recordings. These digitally-recorded locations were used to guide the placement of the stimulation electrode.

Decerebration. Once these above-mentioned initial procedures are completed, a precollicular decerebration was performed while the deep anesthetic plane is maintained. All anterior forebrain structures were removed via an aspirator and replaced with saline-soaked cotton to control bleeding. At this point, animals were considered to have complete lack of sentience (Silverman et al. 2005), and anesthesia was gradually discontinued (Silverman et al. 2005). The preparation

was left to recover for about 60 minutes before data collection commenced. Details of these procedures are provided in previous publications (Lee and Heckman 1998).

Electrical stimulation

Stimulus generation and delivery. Electrical stimulation was generated by a custom-built voltage-controlled current source (VCCS) driven by an NI DAQ card. Stimulation was delivered to spinal tissue through a custom-built silver ball bipolar electrode. The voltage command and the delivered current on the spinal cord were measured, and simultaneously recorded into SPIKE2 at 20 KHz to ensure accurate delivery of intended stimuli. The stimulation electrode was fitted in a spring-loaded mechanism to minimize damage to spinal cord whenever vertical movements occurred.

Stimulus parameters. 1 Hz square wave electrical stimulation of 1 ms duration was applied to individual dorsal root entry zones. The 1 ms pulse duration was chosen to ensure activation of different different afferent types and stronger muscle responses. The stimulation amplitude was increased gradually starting at 5 μA until we observed EMG activity within one of the 9 muscles. This amplitude was noted as the response threshold at that stimulation location. The amplitude was then increased to 2, 5, and 10 times that response threshold or until a response plateau was reached but below any risk of tissue damage. Using the measured range, threshold to plateau, we designed a stimulation sequence covering that range. Each stimulation amplitude was repeated 5 times at each location, and the average EMG response of each muscle was used for analysis. The electrode was then moved to a new dorsal root entry zone and the protocol was repeated.

Data Analysis

The raw time series data from each muscle was split according to stim amplitude and position, to windows of ±0.5 s centered around the stimulus time. Trials with spontaneous muscle activity 10 ms pre-stimulus through 4 ms post-stimulus were excluded.

The goal of this experiment was to map how different muscles responded to stimulation at different spinal locations. To this end, both the short latency and long latency responses were

measured in the nine hindlimb muscles using custom Matlab software (The MathWorks, Natick, MA). The short latency response was quantified as the maximum peak to peak response within 12 ms post-stimulus. The long latency response was quantified as the rectified integrated EMG (RIEMG) for two windows: 12-30 ms and 30-400 ms.

Statistical Analysis. The distribution of outcomes of interest was explored through the density plots. Side-by-side boxplots were generated to compare outcomes of interest across stim location and muscle. Generalized linear mixed models were fit on log transformed outcomes for all animals, with fixed effects of muscle, stimulation position, the interaction between muscle and stim position, as well as a random intercept of animal and muscle within animal effect. ANOVA was conducted to test the significance of the interaction term. Outcomes of interest were peak to peak response within the first 12 ms, RIEMG for 12-30 ms, and RIEMG for 30-400 ms. The analysis was performed for both normalized and unnormalized data.

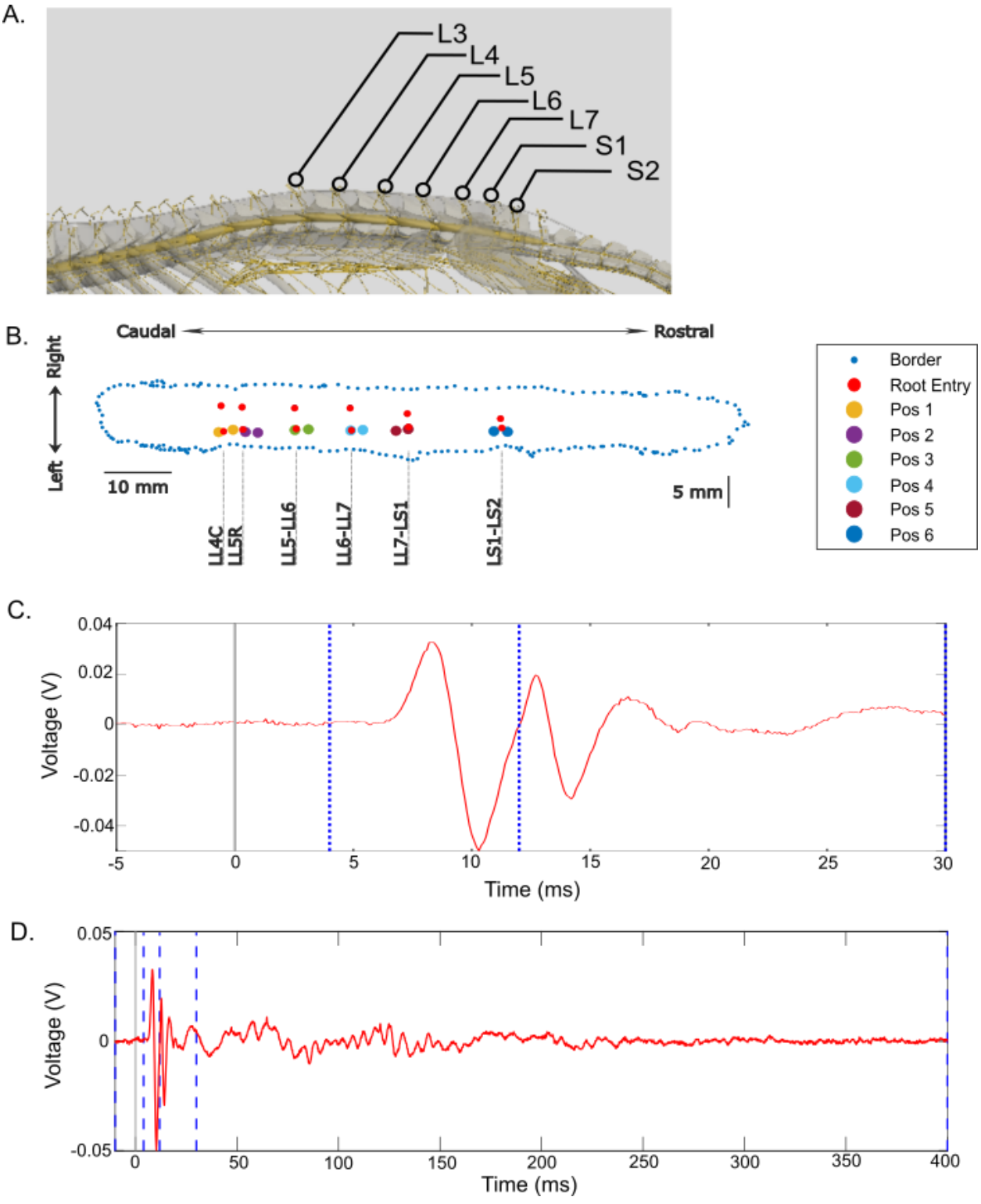

Figure 1. Methods. A) Schematic of cat vertebrae and labeled dorsal roots of the cat lumbosacral cord. B) Microscribe data of one cat's cord. The blue border indicates the edges of the exposed cord. Red dots indicate the dorsal root entry zones. The different color dots indicate the position of the electrode when

stimulating the different roots. C) EMG of a single trial. Blue dotted lines indicate the beginning and end of the different analysis windows—short latency, long latency (12-30 ms), and long latency (30-400 ms).

Results

Short Latency Response

Rostrocaudal Distribution of Short Latency Responses. The first goal of this component of the experiments was to create a map of the rostro-caudal arrangement of the short latency responses in the decerebrate cat. The short latency responses are likely to be monosynaptic, and thus reflect the direct activation of monosynaptic Ia afferents. To map the short latency response for each muscle, we measured the peak to peak EMG response within 4-12 ms post stimulation. Figure 2 shows the distribution of these peak to peak early responses. Trials were included regardless of whether activity surpassed the ten times baseline threshold; therefore, lower values indicate activity at that location was closer to baseline. Figure 2 A-B presents the raw data and Figure 2 C-D presents the log transformed data. To correct for non-normally distributed data, statistics were performed on the log transformed data. 95% confidence intervals are presented in Table 1. During the short latency window, the most rostrally responding muscles were the hip flexor SR, the hip adductor PT, and the knee extensor VL. The remainder of muscles studied responded to stimulation applied more caudally.

Map of Short Latency Responses Vs. Motor Pool Location. To compare the alignment of the short latency responses to the locations of motor pools, the mean responses for each muscle at different locations were compared to the anatomical location of that muscle's motor pool, as determined by Yakovenko et al. 2002. Figure 3 illustrates each muscle's functional map compared to its motor pool (red dots). Error bars indicate 95% confidence intervals, which are also listed in Table 1. Responses to stimulation were considered significantly different if their 95% confidence intervals did not overlap. When a location within a muscle's motor pool had a significantly greater

response compared to locations outside the motor pool, this was interpreted as the functional responses aligning with the anatomical motor pool (red dots with stars). If a location outside the motor pool had a significantly greater response compared to other locations outside the motor pool, this was interpreted as the functional responses being broader than the anatomical motor pool (black dots with stars).

All muscles had functional activity that aligned with their anatomical pools, although to different extents. Five muscles—SR, PT, SL, LG, and BF—had responses at least one locations outside the motor pool that were significantly greater compared to other locations. All other muscles had significantly greater responses at locations within the motor pool compared to other locations. VL and TA had significant responses at only one of the stimulation locations within their motor pools. The VL muscle, which has its motor pool spanning L5 and L6, responded significantly greater to stimulation at L6-L7 compared to L3C and L4R. The TA muscle, which has its motor pool spanning L6 and L7, responded significantly greater to stimulation at L7-S1 compared to L4R. MG, which has its motor pool spanning L7 and S1, was the only muscle that had significant responses to all locations within the motor pool and no significant responses at locations outside the motor pool, compared to other locations. SR, which has its motor pool spanning L5 and L6, had the broadest response, responding significantly to stimulation at L4C through L6-L7 compared to L7-S1 and S1-S2, and to stimulation at L3C and L4C compared to S1-S2. Further detail of how the functional responses of individual muscles compare to their anatomical motor pools can be found in Figure 3 and Table 1.

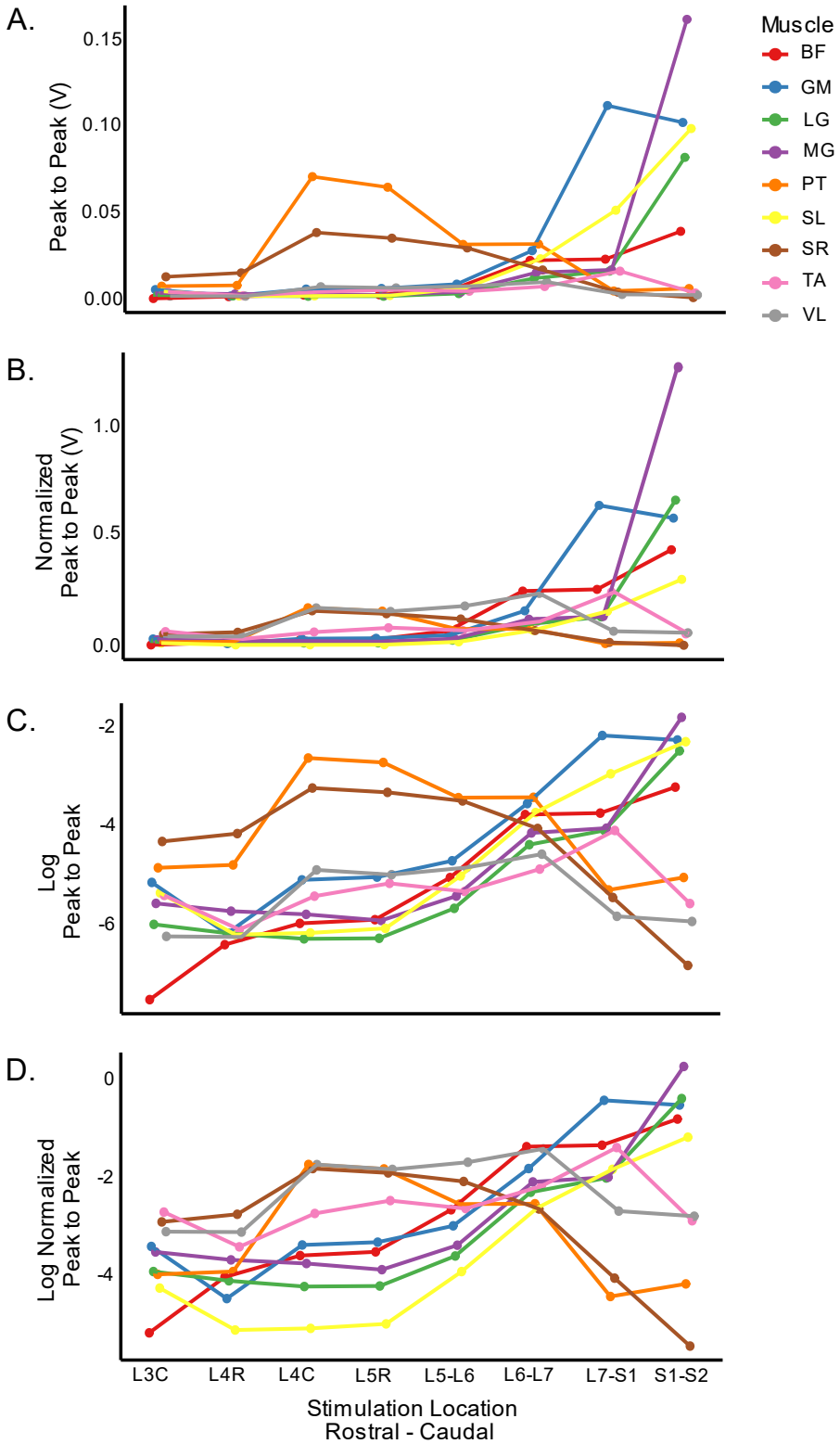

Figure 2. Rostrocaudal Distributions of Short Latency Responses. Each colored line represents the mean

peak to peak muscle response to electrical stimulation of the lumbosacral spinal cord across eight decerebrate cats. Stimulation locations are indicated on the x axis (L3C through S1-S2) and the peak to peak EMG response was measured from 4-12 ms in nine hindlimb muscles (colors, legend). Each subplot represents a different way of processing the data. A) Raw data. B) Normalized data. C) Log transformed data. D) Log transformed normalized data.

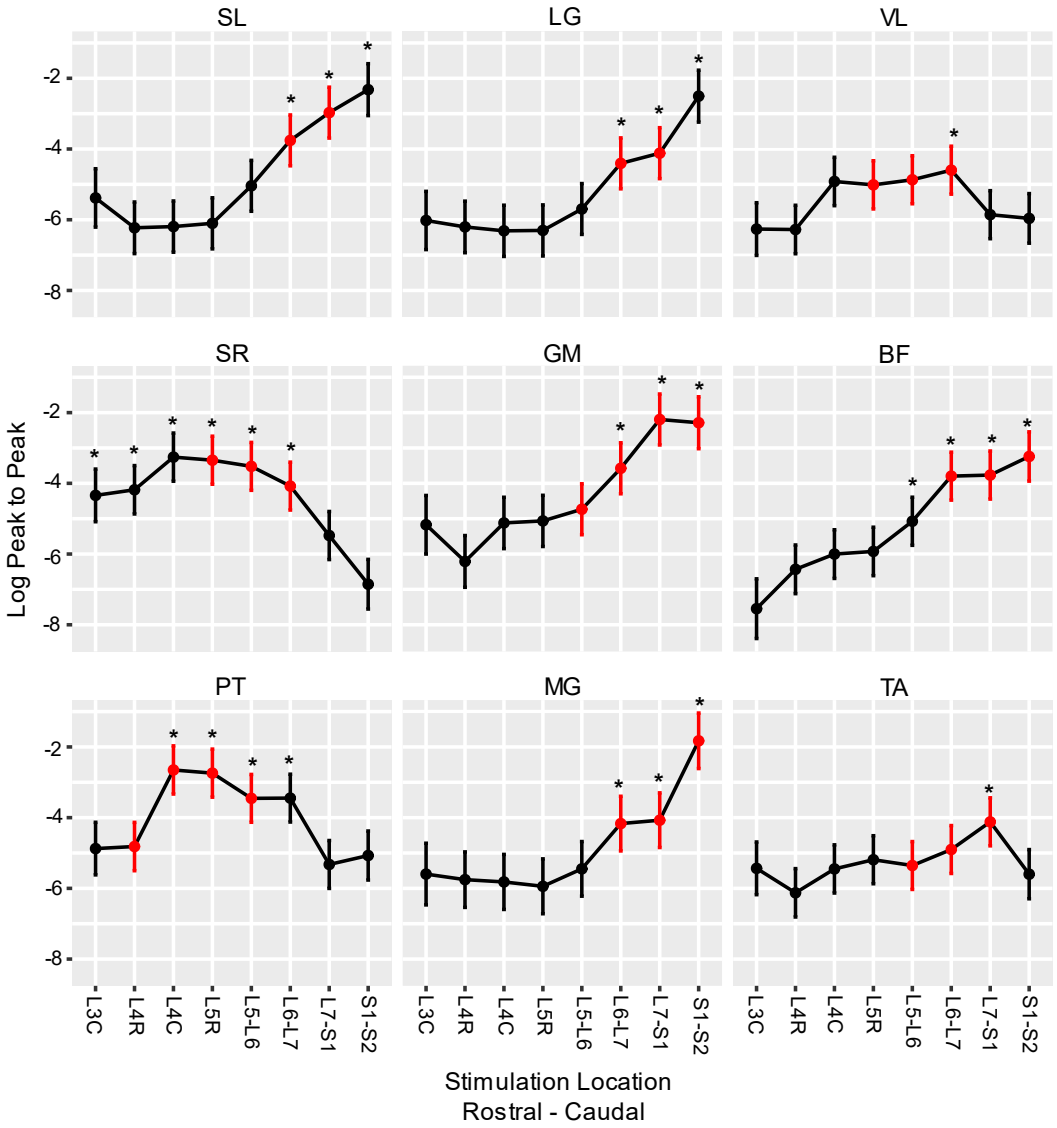

Figure 3. Individual Muscles' Rostrocaudal Distributions of Log Transformed Short Latency Response. Each subplot shows the mean peak to peak response of a different hindlimb muscle across eight decerebrate cats. Electrical stimulation was applied to the lumbosacral cord at locations indicated on the x axis (L3C through S1-S2) and the peak to peak EMG response was measured at 4-12 ms in nine hindlimb muscles. Error bars indicate 95% confidence intervals; lower and upper bounds are listed in Table 1. Responses to stimulation are significantly different if their 95% confidence intervals do not overlap. Stars indicate the response at that stimulation location is significantly different from at least one other location's response. To determine significance, generalized linear mixed models were fit on log transformed outcomes for all animals, with fixed effects of muscle, stim position and the interaction between muscle and stim

position, as well as a random intercept of animal and muscle within animal effect. ANOVA was conducted to test the significance of the interaction term. The anatomical locations of the motor pools are highlighted in red. This figure illustrates how the spread of significant responses compares to the anatomical motor pool.

Muscle	Stimulation Position	Log Peak to Peak	Confidence Interval Lower Bound	Confidence Interval Lower Bound	Raw Peak to Peak
SL	L3C	-5.383	-6.208	-4.558	0.00459
SL	L4R	-6.228	-6.957	-5.499	0.00197
SL	L4C	-6.194	-6.918	-5.470	0.00204
SL	L5R	-6.102	-6.824	-5.380	0.00224
SL	L5-L6	-5.041	-5.760	-4.322	0.00647
SL	L6-L7	-3.756	-4.475	-3.037	0.02338
SL	L7-S1	-2.971	-3.690	-2.251	0.05125
SL	S1-S2	-2.321	-3.054	-1.587	0.09818
LG	L3C	-6.021	-6.844	-5.198	0.00243
LG	L4R	-6.203	-6.932	-5.475	0.00202
LG	L4C	-6.314	-7.038	-5.590	0.00181
LG	L5R	-6.303	-7.025	-5.581	0.00183
LG	L5-L6	-5.696	-6.415	-4.977	0.00336
LG	L6-L7	-4.406	-5.126	-3.686	0.01220
LG	L7-S1	-4.118	-4.838	-3.397	0.01628
LG	S1-S2	-2.505	-3.239	-1.771	0.08168
VL	L3C	-6.264	-7.009	-5.520	0.00190
VL	L4R	-6.277	-6.961	-5.592	0.00188
VL	L4C	-4.918	-5.602	-4.234	0.00731
VL	L5R	-5.014	-5.695	-4.333	0.00664
VL	L5-L6	-4.869	-5.548	-4.191	0.00768
VL	L6-L7	-4.598	-5.276	-3.921	0.01007
VL	L7-S1	-5.857	-6.536	-5.178	0.00286
VL	S1-S2	-5.962	-6.663	-5.261	0.00257
SR	L3C	-4.341	-5.085	-3.597	0.01302
SR	L4R	-4.182	-4.866	-3.498	0.01527
SR	L4C	-3.258	-3.939	-2.578	0.03847
SR	L5R	-3.346	-4.025	-2.667	0.03522
SR	L5-L6	-3.520	-4.197	-2.843	0.02960
SR	L6-L7	-4.078	-4.755	-3.401	0.01694
SR	L7-S1	-5.476	-6.155	-4.796	0.00419
SR	S1-S2	-6.853	-7.555	-6.151	0.00106
GM	L3C	-5.171	-5.999	-4.343	0.00568

GM	L4R	-6.209	-6.940	-5.477	0.00201
GM	L4C	-5.120	-5.846	-4.394	0.00598
GM	L5R	-5.063	-5.786	-4.339	0.00633
GM	L5-L6	-4.733	-5.453	-4.013	0.00880
GM	L6-L7	-3.574	-4.295	-2.854	0.02804
GM	L7-S1	-2.194	-2.914	-1.474	0.11147
GM	S1-S2	-2.286	-3.020	-1.552	0.10167
BF	L3C	-7.545	-8.389	-6.701	0.00053
BF	L4R	-6.432	-7.120	-5.744	0.00161
BF	L4C	-6.001	-6.689	-5.313	0.00248
BF	L5R	-5.926	-6.611	-5.241	0.00267
BF	L5-L6	-5.073	-5.753	-4.393	0.00626
BF	L6-L7	-3.796	-4.474	-3.119	0.02246
BF	L7-S1	-3.766	-4.445	-3.087	0.02314
BF	S1-S2	-3.240	-3.937	-2.544	0.03916
PT	L3C	-4.875	-5.618	-4.131	0.00764
PT	L4R	-4.816	-5.500	-4.133	0.00810
PT	L4C	-2.651	-3.332	-1.970	0.07058
PT	L5R	-2.741	-3.420	-2.062	0.06451
PT	L5-L6	-3.454	-4.130	-2.778	0.03162
PT	L6-L7	-3.447	-4.123	-2.771	0.03184
PT	L7-S1	-5.324	-6.001	-4.647	0.00487
PT	S1-S2	-5.071	-5.764	-4.378	0.00628
MG	L3C	-5.596	-6.467	-4.724	0.00371
MG	L4R	-5.753	-6.538	-4.969	0.00317
MG	L4C	-5.818	-6.596	-5.040	0.00297
MG	L5R	-5.942	-6.717	-5.166	0.00263
MG	L5-L6	-5.448	-6.220	-4.676	0.00430
MG	L6-L7	-4.168	-4.941	-3.396	0.01548
MG	L7-S1	-4.072	-4.844	-3.299	0.01704
MG	S1-S2	-1.827	-2.611	-1.042	0.16090
TA	L3C	-5.434	-6.178	-4.689	0.00437
TA	L4R	-6.126	-6.809	-5.442	0.00219
TA	L4C	-5.450	-6.131	-4.769	0.00430
TA	L5R	-5.190	-5.869	-4.511	0.00557
TA	L5-L6	-5.354	-6.030	-4.677	0.00473
TA	L6-L7	-4.901	-5.578	-4.224	0.00744
TA	L7-S1	-4.119	-4.797	-3.440	0.01626
TA	S1-S2	-5.599	-6.294	-4.903	0.00370

Table 1. Short Latency Confidence Intervals. Each row outlines the mean log peak to peak, lower and upper bounds of the 95% confidence interval, as well as the raw mean peak to peak for each muscle and stimulation position for 8 decerebrate cats combined. Means and 95% confidence intervals determined by fitting generalized linear mixed models on log transformed outcomes for all animals, with fixed effects of muscle, stim position and the interaction between muscle and stim position, as well as a random intercept of animal and muscle within animal effect. The mean log peak to peak values for each muscle and stimulation location are displayed in Figure 2B and Figure 3. In Figure 3, the confidence interval lower and upper bounds are displayed as error bars. The raw peak to peak measurements are displayed in Figure 2A.

Long Latency Response

Another main goal of this experiment was to create a rostrocaudal map of long latency responses, and to compare these long latency responses to the anatomical motor pools. For the long latency responses, the outcome measure was the rectified and integrated EMG response (RIEMG) within two windows: Window I is 12-30 ms and Window II is 30-400 ms. The long latency responses are polysynaptic, so likely involve the local circuits that can also span multiple segments. Just as with the short latency response, we will describe the rostrocaudal distribution of responses, and then compare the responses to the location of the anatomical motor pool for each muscle.

Rostrocaudal Distribution of Long Latency Window I Responses. Figure 4 shows the rostrocaudal distribution of muscle activity at 12-30 ms. Figure 4 A-B presents the raw data and Figure 4 C-D presents the log transformed data. Statistics were performed on the log transformed data, and 95% confidence intervals are presented in Table 2. The most rostrally responding muscles were the hip flexor SR, the hip adductor PT, and the knee extensor VL. The ankle flexor TA responded to stimulation both more rostrally and caudally. The remainder of muscles studied responded to stimulation applied more caudally.

Comparison of Long Latency Window I Responses to Motor Pools. To determine whether the map of long latency responses and the anatomical map are aligned for each of the 9 muscles, responses were compared to the cat anatomical motor pool locations. Figure 5 illustrates each muscle's functional map compared to its motor pool. As for the short latency responses, error

bars indicate 95% confidence intervals, which are also listed in Table 2. Responses to stimulation are considered significantly different if their 95% confidence intervals do not overlap. As with the short latency response, when a location or locations within a muscle's motor pool has or have a significantly greater response compared to locations outside the motor pool, this was interpreted as the functional responses aligning with the anatomical motor pool.

As shown in Figure 5, all muscles had functional activity that aligned with their anatomical pools, although to different extents. Only two muscles—MG and GM—responded significantly greater at locations only within the motor pool, compared to other locations. MG again responded significantly to all locations within its motor pool and to no locations outside its motor pool. All other muscles had significant responses at locations both within and outside the motor pool. TA, SL, and LG had the greatest spread with each responding significantly to three locations outside their motor pools. In comparison, in the short latency window, TA had no significant responses outside its motor pool, and SL and LG had significant responses each at only one location outside its motor pool. In this way, there is a trend towards the functional maps broadening at longer latencies. Further detail of how the functional responses of individual muscles compare to their anatomical motor pools can be found in Figure 5 and Table 2.

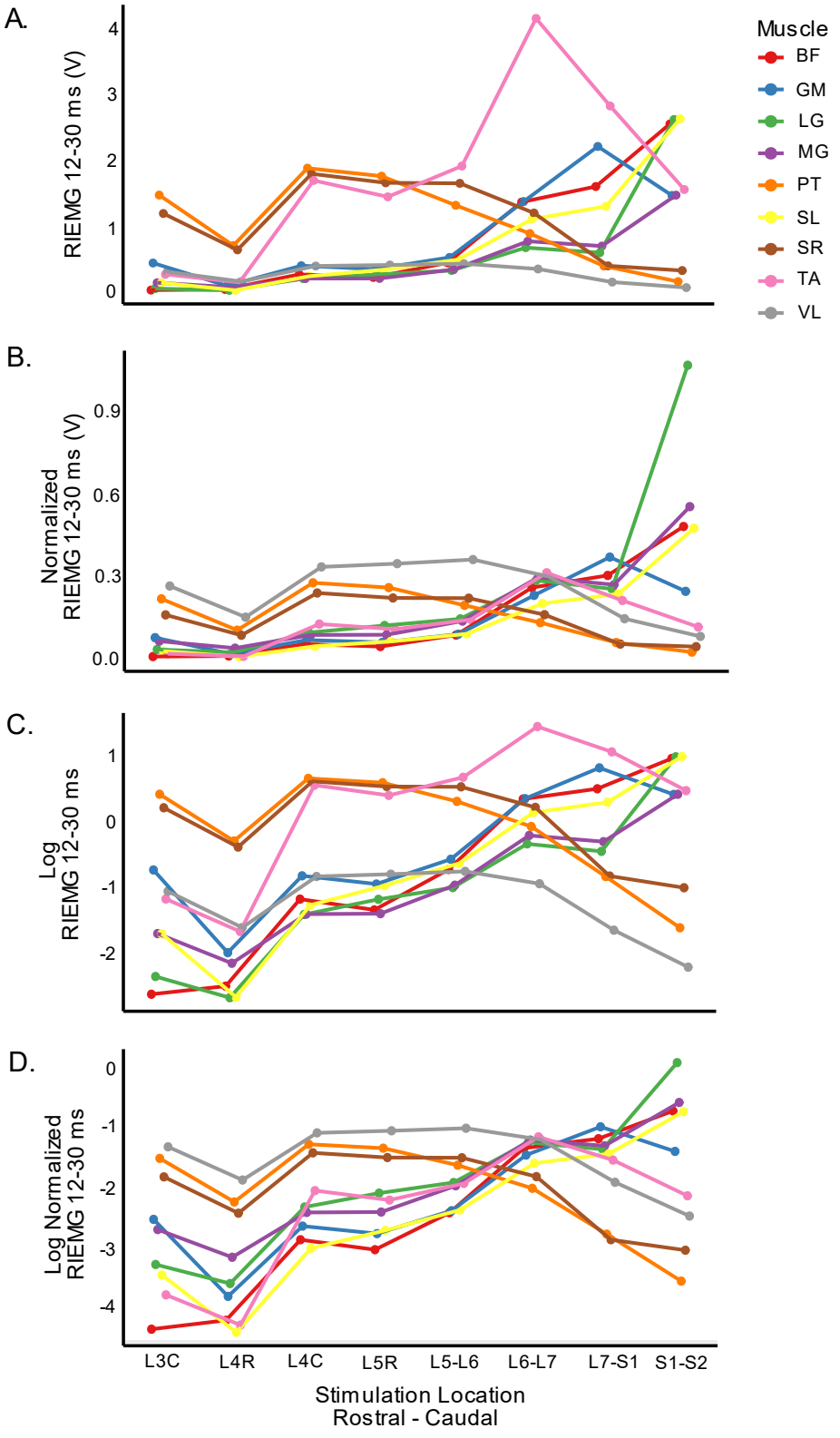
A.
RIEMG 12-30 ms (V)
0
1
2
3
4
B.
Normalized
RIEMG 12-30 ms (V)
0.0
0.3
0.6
0.9
C.
Log
RIEMG 12-30 ms
-2
-1
0
1
D.
Log Normalized
RIEMG 12-30 ms
-4
-3
-2
-1
0
L3C
L4R
L4C
L5R
L5-L6
L6-L7
L7-S1
S1-S2
Stimulation Location
Rostral - Caudal
Muscle
BF
GM
LG
MG
PT
SL
SR
TA
VL

Figure 4. Rostrocaudal Distributions of Long Latency (12-30 ms) Responses. Each colored line represents the mean RIEMG muscle response to electrical stimulation of the lumbosacral spinal cord across eight decerebrate cats. Stimulation locations are indicated on the x axis (L3C through S1-S2) and the RIEMG response was measured from 12-30 ms in nine hindlimb muscles (colors, legend). Each subplot represents a different way of processing the data. A) Raw data. B) Normalized data. C) Log transformed data. D) Log transformed normalized data.

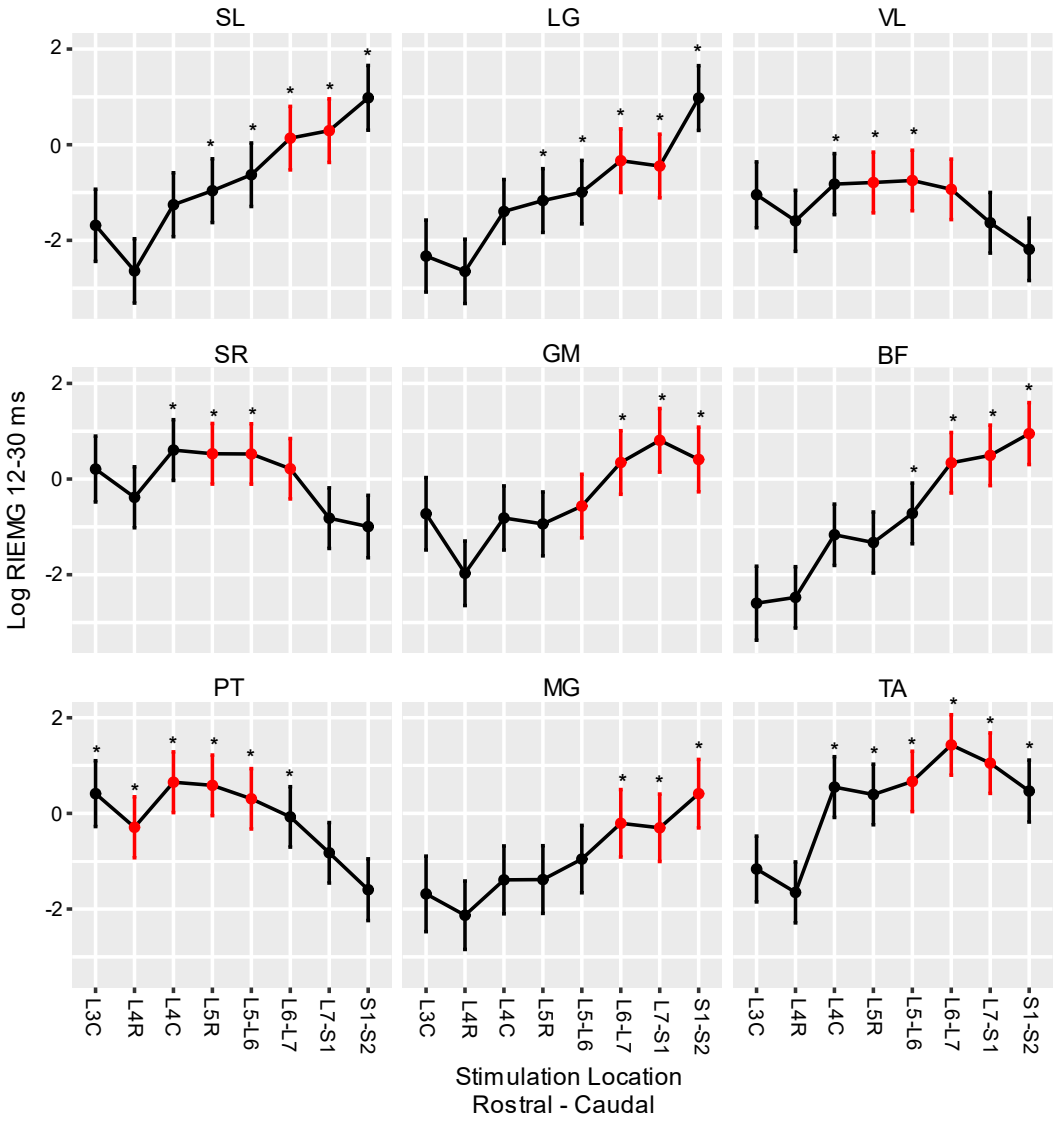

Figure 5. Individual Muscles' Rostrocaudal Distributions of Log Transformed Long Latency (12-30 ms) Response. Each subplot shows the mean RIEMG response of a different hindlimb muscle across eight decerebrate cats. Electrical stimulation was applied to the lumbosacral cord at locations indicated on the x axis (L3C through S1-S2) and the RIEMG response was measured at 12-30 ms in nine hindlimb muscles. Error bars indicate 95% confidence intervals; lower and upper bounds are listed in Table 2. Responses to stimulation are significantly different if their 95% confidence intervals do not overlap. Stars indicate the response at that stimulation location is significantly different from at least one other location's response. To determine significance, generalized linear mixed models were fit on log transformed outcomes for all

animals, with fixed effects of muscle, stim position and the interaction between muscle and stim position, as well as a random intercept of animal and muscle within animal effect. ANOVA was conducted to test the significance of the interaction term. The anatomical locations of the motor pools are highlighted in red. This figure illustrates how the spread of significant responses compares to the anatomical motor pool.

Muscle	Stimulation Position	Log RIEMG	Confidence Interval Lower Bound	Confidence Interval Lower Bound	RIEMG
SL	L3C	-1.686	-2.440	-0.931	0.18526
SL	L4R	-2.639	-3.311	-1.967	0.07143
SL	L4C	-1.255	-1.923	-0.587	0.28508
SL	L5R	-0.962	-1.628	-0.295	0.38213
SL	L5-L6	-0.628	-1.292	0.036	0.53366
SL	L6-L7	0.137	-0.527	0.801	1.14683
SL	L7-S1	0.294	-0.371	0.959	1.34178
SL	S1-S2	0.980	0.304	1.657	2.66446
LG	L3C	-2.329	-3.081	-1.576	0.09739
LG	L4R	-2.648	-3.320	-1.976	0.07079
LG	L4C	-1.396	-2.064	-0.728	0.24759
LG	L5R	-1.168	-1.834	-0.501	0.31099
LG	L5-L6	-0.992	-1.656	-0.328	0.37083
LG	L6-L7	-0.334	-0.999	0.331	0.71605
LG	L7-S1	-0.446	-1.111	0.220	0.64018
LG	S1-S2	0.976	0.299	1.653	2.65382
VL	L3C	-1.047	-1.736	-0.359	0.35099
VL	L4R	-1.592	-2.230	-0.954	0.20352
VL	L4C	-0.824	-1.462	-0.186	0.43867
VL	L5R	-0.790	-1.425	-0.155	0.45384
VL	L5-L6	-0.748	-1.381	-0.115	0.47331
VL	L6-L7	-0.933	-1.566	-0.301	0.39337
VL	L7-S1	-1.632	-2.266	-0.998	0.19554
VL	S1-S2	-2.188	-2.840	-1.536	0.11214
SR	L3C	0.209	-0.479	0.898	1.23244
SR	L4R	-0.382	-1.019	0.256	0.68250
SR	L4C	0.606	-0.029	1.241	1.83308
SR	L5R	0.529	-0.105	1.162	1.69723
SR	L5-L6	0.524	-0.107	1.156	1.68877
SR	L6-L7	0.215	-0.416	0.847	1.23986
SR	L7-S1	-0.818	-1.451	-0.184	0.44131
SR	S1-S2	-0.994	-1.646	-0.341	0.37009

GM	L3C	-0.726	-1.483	0.031	0.48384
GM	L4R	-1.970	-2.645	-1.296	0.13946
GM	L4C	-0.814	-1.484	-0.144	0.44308
GM	L5R	-0.938	-1.606	-0.270	0.39141
GM	L5-L6	-0.565	-1.230	0.100	0.56836
GM	L6-L7	0.346	-0.319	1.011	1.41340
GM	L7-S1	0.810	0.145	1.475	2.24791
GM	S1-S2	0.409	-0.267	1.086	1.50531
BF	L3C	-2.596	-3.369	-1.823	0.07457
BF	L4R	-2.474	-3.115	-1.833	0.08425
BF	L4C	-1.165	-1.806	-0.524	0.31192
BF	L5R	-1.327	-1.965	-0.689	0.26527
BF	L5-L6	-0.718	-1.353	-0.084	0.48773
BF	L6-L7	0.340	-0.292	0.973	1.40495
BF	L7-S1	0.495	-0.138	1.128	1.64050
BF	S1-S2	0.950	0.303	1.598	2.58571
PT	L3C	0.413	-0.275	1.101	1.51135
PT	L4R	-0.291	-0.928	0.347	0.74752
PT	L4C	0.652	0.017	1.286	1.91938
PT	L5R	0.586	-0.047	1.220	1.79679
PT	L5-L6	0.305	-0.326	0.936	1.35663
PT	L6-L7	-0.073	-0.704	0.558	0.92960
PT	L7-S1	-0.824	-1.456	-0.192	0.43867
PT	S1-S2	-1.596	-2.241	-0.951	0.20271
MG	L3C	-1.683	-2.473	-0.894	0.18582
MG	L4R	-2.130	-2.845	-1.414	0.11884
MG	L4C	-1.390	-2.100	-0.681	0.24908
MG	L5R	-1.384	-2.091	-0.676	0.25057
MG	L5-L6	-0.955	-1.660	-0.251	0.38481
MG	L6-L7	-0.207	-0.912	0.498	0.81302
MG	L7-S1	-0.301	-1.006	0.404	0.74008
MG	S1-S2	0.412	-0.303	1.128	1.50983
TA	L3C	-1.163	-1.851	-0.475	0.31255
TA	L4R	-1.652	-2.289	-1.015	0.19167
TA	L4C	0.550	-0.085	1.185	1.73325
TA	L5R	0.395	-0.238	1.029	1.48438
TA	L5-L6	0.668	0.037	1.299	1.95033
TA	L6-L7	1.431	0.799	2.063	4.18288
TA	L7-S1	1.050	0.418	1.683	2.85765
TA	S1-S2	0.467	-0.180	1.115	1.59520

Table 2. Long Latency Latency (12-30 ms) Confidence Intervals. Each row outlines the mean log RIEMG, lower and upper bounds of the 95% confidence interval, as well as the raw mean RIEMG for each muscle and stimulation position for 8 decerebrate cats combined. Means and 95% confidence intervals determined by fitting generalized linear mixed models on log transformed outcomes for all animals, with fixed effects of muscle, stim position and the interaction between muscle and stim position, as well as a random intercept of animal and muscle within animal effect. The mean log RIEMG values for each muscle and stimulation location are displayed in Figure 4B and Figure 5. In Figure 5, the confidence interval lower and upper bounds are displayed as error bars. The raw RIEMG measurements are displayed in Figure 4A.

Rostrocaudal Distribution of Long Latency Window II Responses. The rostrocaudal distribution of muscle activity in the later window of the long latency response, is displayed in Figure 6. This is muscle activity 30-400 ms following subdural spinal stimulation. The rostrocaudal trends observed at the earlier latencies were not as apparent during this latest window. No muscles tended to respond more to rostral stimulation compared to caudal stimulation. TA tended to respond more strongly to stimulation at more central locations compared to more rostral and more caudal locations. SL, LG, MG, GM, and BF tended to respond to more caudal stimulation. Table 3 includes details on mean EMG response and 95% confidence intervals.

Comparison of Long Latency Window II Responses to Motor Pools. Finally, we will explore how this later window of the long latency response aligns with the anatomical motor pools. As shown in Figure 7, three muscles—SR, PT, and VL—showed no significant difference in response to stimulation at any location compared to other locations. This is a new finding compared to the earlier windows, suggesting a further broadening of responses at this latest latency. Three muscles—TA, SL, and LG—showed significantly greater responses at locations both within and outside the motor pool compared to other locations. And three muscles-- MG, GM, and BF—showed significantly greater responses only at locations within the motor pool. Further detail of how the functional responses of individual muscles compare to their anatomical motor pools can be found in Figure 7 and Table 3.

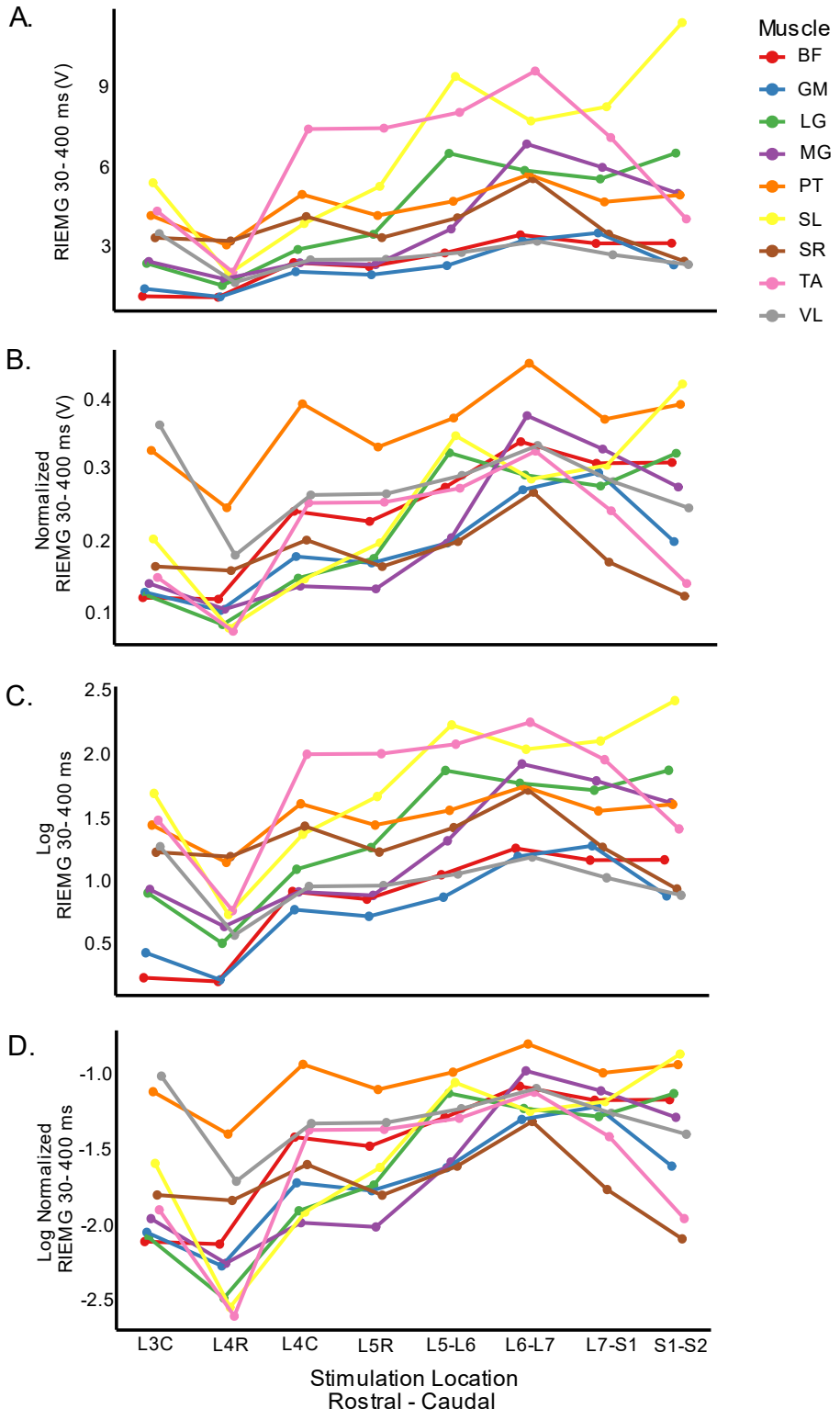
A.
RIEMG 30-400 ms (V)
9
6
3
B.
Normalized RIEMG 30-400 ms (V)
0.4
0.3
0.2
0.1
C.
Log RIEMG 30-400 ms
2.5
2.0
1.5
1.0
0.5
D.
Log Normalized RIEMG 30-400 ms
-1.0
-1.5
-2.0
-2.5
L3C
L4R
L4C
L5R
L5-L6
L6-L7
L7-S1
S1-S2
Stimulation Location
Rostral - Caudal
Muscle
BF
GM
LG
MG
PT
SL
SR
TA
VL

Figure 6. Rostrocaudal Distributions of Long Latency (30-400 ms) Responses. Each colored line represents the mean RIEMG muscle response to electrical stimulation of the lumbosacral spinal cord across eight decerebrate cats. Stimulation locations are indicated on the x axis (L3C through S1-S2) and the RIEMG response was measured from 30-400 ms in nine hindlimb muscles (colors, legend). Each subplot represents a different way of processing the data. A) Raw data. B) Normalized data. C) Log transformed data. D) Log transformed normalized data.

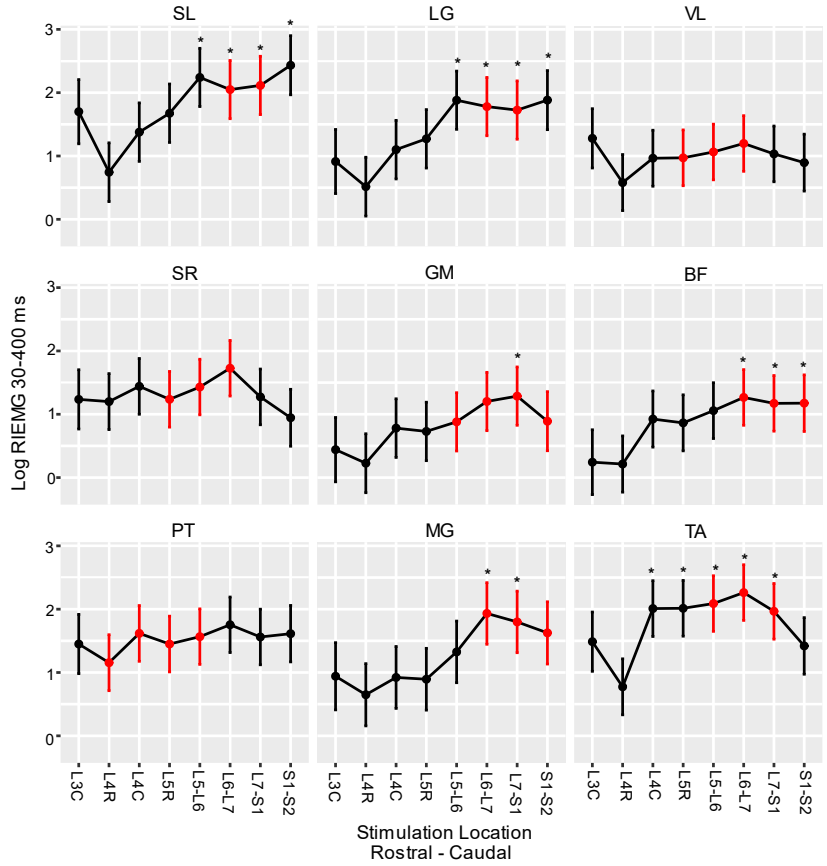

Figure 7. Individual Muscles' Rostrocaudal Distributions of Log Transformed Long Latency (30-400 ms) Response. Each subplot shows the mean RIEMG response of a different hindlimb muscle across eight decerebrate cats. Electrical stimulation was applied to the lumbosacral cord at locations indicated on the x axis (L3C through S1-S2) and the RIEMG response was measured at 30-400 ms in nine hindlimb muscles. Error bars indicate 95% confidence intervals; lower and upper bounds are listed in Table 2. Responses to stimulation are significantly different if their 95% confidence intervals do not overlap. Stars indicate the response at that stimulation location is significantly different from at least one other location's response. To determine significance, generalized linear mixed models were fit on log transformed outcomes for all animals, with fixed effects of muscle, stim position and the interaction between muscle and stim position, as well as a random intercept of animal and muscle within animal effect. ANOVA was conducted to test the

significance of the interaction term. The anatomical locations of the motor pools are highlighted in red. This figure illustrates how the spread of significant responses compares to the anatomical motor pool.

Muscle	Stimulation Position	Log RIEMG	Confidence Interval Lower Bound	Confidence Interval Lower Bound	RIEMG
SL	L3C	1.700	1.193	2.207	5.47395
SL	L4R	0.744	0.280	1.208	2.10434
SL	L4C	1.377	0.915	1.839	3.96299
SL	L5R	1.675	1.214	2.137	5.33880
SL	L5-L6	2.241	1.781	2.701	9.40273
SL	L6-L7	2.049	1.589	2.509	7.76014
SL	L7-S1	2.115	1.654	2.575	8.28959
SL	S1-S2	2.433	1.967	2.900	11.39301
LG	L3C	0.913	0.407	1.419	2.49179
LG	L4R	0.516	0.051	0.980	1.67531
LG	L4C	1.101	0.638	1.563	3.00717
LG	L5R	1.272	0.810	1.733	3.56798
LG	L5-L6	1.881	1.421	2.341	6.56006
LG	L6-L7	1.780	1.320	2.241	5.92986
LG	L7-S1	1.725	1.265	2.186	5.61252
LG	S1-S2	1.883	1.416	2.349	6.57319
VL	L3C	1.279	0.811	1.747	3.59304
VL	L4R	0.580	0.138	1.023	1.78604
VL	L4C	0.965	0.523	1.407	2.62479
VL	L5R	0.971	0.531	1.412	2.64058
VL	L5-L6	1.064	0.624	1.503	2.89794
VL	L6-L7	1.198	0.758	1.637	3.31348
VL	L7-S1	1.033	0.593	1.473	2.80948
VL	S1-S2	0.895	0.446	1.345	2.44734
SR	L3C	1.235	0.767	1.703	3.43838
SR	L4R	1.200	0.758	1.642	3.32012
SR	L4C	1.441	1.000	1.881	4.22492
SR	L5R	1.236	0.797	1.676	3.44182
SR	L5-L6	1.430	0.991	1.869	4.17870
SR	L6-L7	1.727	1.288	2.166	5.62376
SR	L7-S1	1.274	0.834	1.714	3.57512
SR	S1-S2	0.945	0.495	1.394	2.57281

GM	L3C	0.441	-0.067	0.949	1.55426
GM	L4R	0.227	-0.239	0.692	1.25483
GM	L4C	0.781	0.318	1.244	2.18365
GM	L5R	0.729	0.267	1.190	2.07301
GM	L5-L6	0.880	0.420	1.340	2.41090
GM	L6-L7	1.202	0.741	1.662	3.32676
GM	L7-S1	1.286	0.826	1.747	3.61828
GM	S1-S2	0.890	0.424	1.357	2.43513
BF	L3C	0.243	-0.269	0.755	1.27507
BF	L4R	0.214	-0.230	0.658	1.23862
BF	L4C	0.924	0.481	1.368	2.51935
BF	L5R	0.864	0.422	1.307	2.37263
BF	L5-L6	1.057	0.617	1.498	2.87772
BF	L6-L7	1.266	0.826	1.705	3.54664
BF	L7-S1	1.172	0.733	1.612	3.22844
BF	S1-S2	1.175	0.728	1.622	3.23814
PT	L3C	1.450	0.982	1.918	4.26311
PT	L4R	1.155	0.713	1.597	3.17402
PT	L4C	1.618	1.177	2.058	5.04299
PT	L5R	1.450	1.010	1.890	4.26311
PT	L5-L6	1.566	1.128	2.005	4.78746
PT	L6-L7	1.754	1.315	2.192	5.77767
PT	L7-S1	1.561	1.122	2.000	4.76358
PT	S1-S2	1.613	1.168	2.059	5.01784
MG	L3C	0.941	0.410	1.471	2.56254
MG	L4R	0.649	0.157	1.140	1.91363
MG	L4C	0.922	0.433	1.411	2.51431
MG	L5R	0.894	0.406	1.382	2.44489
MG	L5-L6	1.325	0.839	1.812	3.76219
MG	L6-L7	1.933	1.446	2.419	6.91021
MG	L7-S1	1.799	1.313	2.285	6.04360
MG	S1-S2	1.626	1.134	2.117	5.08350
TA	L3C	1.487	1.019	1.955	4.42380
TA	L4R	0.774	0.332	1.216	2.16842
TA	L4C	2.010	1.569	2.450	7.46332
TA	L5R	2.014	1.574	2.454	7.49323
TA	L5-L6	2.089	1.650	2.528	8.07683
TA	L6-L7	2.262	1.823	2.702	9.60227
TA	L7-S1	1.967	1.527	2.406	7.14920
TA	S1-S2	1.420	0.973	1.867	4.13712

Table 3. Long Latency Latency (12-30 ms) Confidence Intervals. Each row outlines the mean log RIEMG, lower and upper bounds of the 95% confidence interval, as well as the raw mean RIEMG for each muscle and stimulation position for 8 decerebrate cats combined. Means and 95% confidence intervals determined by fitting generalized linear mixed models on log transformed outcomes for all animals, with fixed effects of muscle, stim position and the interaction between muscle and stim position, as well as a random intercept of animal and muscle within animal effect. The mean log RIEMG values for each muscle and stimulation location are displayed in Figure 6B and Figure 7. In Figure 7, the confidence interval lower and upper bounds are displayed as error bars. The raw RIEMG measurements are displayed in Figure 6A.

Discussion

The goal of this study was to build the first functional map of the intact spinal cord using subdural stimulation of the lumbosacral spinal cord in the decerebrate cat. This functional map could be used to inform the development of better electrical stimulation infrastructure and protocols for the treatment of spinal cord injury. To build this map, electrical stimulation was applied at eight spinal locations ranging from L3-S2 while intramuscular EMG was recorded in nine hindlimb muscles. Our results demonstrate the rostro-caudal distribution of hindlimb EMG activity in response to lumbosacral subdural stimulation. For some muscles, these distributions closely parallel the distribution of the anatomical motor pool, while for others, these distributions appear broader, especially for responses with long latencies.

Rostrocaudal Organization of Short Latency Responses. Our results showed that in the decerebrate cat, short latency responses to subdural stimulation of the lumbosacral spinal cord largely aligned with the anatomical location of motor pools. In general, subdural stimulation in our unanesthetized cat preparation showed similar trends to intraspinal stimulation in the the anestetized cat. While we did not test for the anatomical motor pool, the functional output mainly aligned with the cat motor pool rostrocaudal organization described by Yakovenko et al. 2002. Generally, we found that hip flexors responded most rostrally, followed by hip adductors, and then the rest of the muscles overlapped more caudally. Even within the more rostrally activated

muscles, however, there was overlap. Previous work using intraspinal stimulation has found that the more distal a muscle is in the limb, the more caudal its motor pool is located in the cord, which generally aligns with our findings that muscles of the hip tend to be activated by more rostral stimulation, followed by muscles of the knee and ankle (Vanderhorst and Holstege 1997). Overall, intraspinal stimulation in monkeys and cats showed that hip flexors are activated by the most rostral stimulation, followed by knee extensors, then ankle flexors, hip extensors, toe flexors, ankle extensors, and finally knee flexors being most caudal (Toossi et al. 2019). The distributions of muscle responses in our study tended to be more overlapping than this discrete rostrocaudal order. This may be attributed to the suppressive effects of anesthesia in these other studies as well as less current spread with intraspinal stimulation.

Alignment of Short Latency Responses and Motor Pools. Our data show that the relative rostrocaudal positions of maximum muscle activation aligns with recent studies using intraspinal stimulation in rhesus monkeys. Toosi et al. (2019) showed in rhesus monkeys that hip flexors were activated most rostrally, followed by knee extensors (Toossi et al. 2019). Similarly, we found that the hip flexors SR and PT were both activated most rostrally. Likewise, Vanderhorst and Holstege (1997), using intraspinal stimulation in the unanesthized cat, observed SR to be the muscle activated by the most rostral stimulation. They also showed that SR motoneurons overlap with the knee extensor motoneurons, because SR is a knee extensor in addition to being a hip flexor (Vanderhorst and Holstege 1997). Similarly, we found that SR and the knee extensor VL are activated by stimulation at some overlapping spinal sections. The hamstrings muscle, BF, was previously described to be activated by stimulation of the caudal half of the lumbosacral cord, which matches our findings of BF activity at L5-L6 through S1-S2 (Vanderhorst and Holstege 1997). They showed the MG and SL to be activated by stimulation more caudally than the LG.

However, we found all three muscles to respond maximally to the most caudal position tested: S1-S2. Perhaps by stimulating even more caudally, we may have found a difference.

In accordance with these trends, our data demonstrated that some muscles have overlapping activation patterns. For instance, SR and PT tended to be activated by more rostral stimulation locations while SL, LG, MG, GM, BF, and TA tended to be activated by more caudal stimulation locations. Previous research shows that with intraspinal microstimulation, the gastrocnemius, BF, and TA are commonly activated together (Toossi et al. 2019). This is consistent with research in humans that shows heteronymous Ia afferent excitation and recurrent inhibition between the gastrocnemius and biceps femoris, and with research in cats that shows coactivation of the gastrocnemius and biceps femoris (Meunier et al. 1993; Rasmussen et al. 1978).

While the global functional maps largely align with the rostrocaudal organization of the anatomical map, there was still considerable spread. In other words, muscles were often activated by stimulation outside of their anatomical motor pools. First, it is important to discuss that spinal stimulation is more likely to activate sensory afferents than motoneurons and interneurons. Capogrosso et al. 2013 demonstrated that epidural electrical stimulation failed to activate motoneurons directly because it could not penetrate spinal cord structures. Sensory afferents, particularly Ia and Ib are larger in diameter, and thus depolarized at lower thresholds by electrical stimulation (Capogrosso et al. 2013). Even with intraspinal stimulation, which is more targeted than subdural stimulation, there is a bias towards the activation of sensory afferents as there are more afferent axons than motoneurons or interneurons near the electrode tip (Gaunt et al. 2006). Additionally, sensory afferents can pass through multiple spinal segments, sometimes to great lengths (Ishizuka et al. 1979). Guant et al. 2006 showed that intraspinal microstimulation at one location in the spinal cord activated afferent terminals along the entire length the lumbosacral

cord. In fact, activity was detected in dorsal root filaments up to 17 mm rostral to and caudal to a single stimulation site (Gaunt et al. 2006). This suggests that the intraspinal stimulation activated sensory afferents nearby the electrode which antidromically propagated back to their axons and via dorsal columns to the dorsal root filaments (Gaunt et al. 2006). Previous work helps to explain why that is. Studies using the tracer horseradish peroxidase demonstrated that sensory afferent collaterals enter the spinal cord gray matter at distances up to 10 mm rostral to and 5 mm caudal to their entry zones (Brown 1981). Further, electrophysiological and axonal degeneration research has demonstrated afferent collaterals projecting from L2-L4 spinal segments to at least the S1 spinal segment (Imai and Kusama 1969; Wall and Werman 1976). Additionally, afferents with entry points up to three segments away, have been shown to evoke responses in dorsal horn interneurons (Mendell et al. 1978). This explains why some muscles responded to our subdural stimulation outside the estimated boundaries of their anatomical motor pools. This spread has been shown to vary between muscles. For instance, the SR and TA demonstrated functional activity with stimulation of a greater range of lumbosacral locations than their anatomical motor pools, whereas the functional activity of the gastrocnemius is more aligned with its anatomical motor pools (Toossi et al. 2019). In sum, while specific locations on the cord were stimulated, that stimulation likely activates motoneurons and interneurons across several segments via activation of sensory afferents, thus resulting in spread in the global functional maps.

Comparing Short Latency Maps with Other Species. When the rostrocaudal arrangement of activity is compared between species, we see similarities as well. When comparing the anatomical motor pools of humans, monkeys, and cats, they all appear to have similar organization (Toossi et al. 2019). These anatomical motor pools have also been found to be in alignment with the functional output maps in monkeys and cats (Toossi et al. 2019).

Alignment of Long Latency Responses and Motor Pools. Our results showed that in the decerebrate cat, long latency responses to subdural stimulation of the lumbosacral spinal cord generally were evoked outside the anatomical motor pools and decreased in specificity with even longer latencies. This suggests that stimulation-induced action potentials propagated rostrally and caudally activating afferents, interneurons, and motoneurons along the lumbosacral cord. This finding aligns with previous work showing, at polysynaptic latencies, many muscles generating responses to focal spinal stimulation (Gaunt et al. 2006). Computer models show that epidural spinal stimulation, and likely subdural stimulation, directly activate Ia, Ib, and II fibers (Capogrosso et al. 2013). These afferents can activate polysynaptic pathways across multiple spinal segments contributing to the spread of response. Moreover, evidence from pharmacological experiments and computer simulations suggest that the polysynaptic responses are largely due to activation of interneurons by type-II fibers (Capogrosso et al. 2013; Jankowska 1992; Minassian et al. 2004). This leads to more muscles activated by stimulation at a particular location over longer latencies compared to shorter latencies. Previous studies have even shown that out of five hindlimb muscles recorded across multiple joints, all five showed activity in response to stimulation at a single location (Gaunt et al. 2006).

Limitations

The stimulation protocol selected for this study was chosen for its similarity to protocols used clinically. Other stimulation protocols varying in stimulation duration, frequency, and amplitude may activate different fibers and pathways resulting in different maps. Further research is needed to determine how varying subdural stimulation parameters affects the output maps. The muscles recorded here were selected to capture a range of joints and functions. For some joints and functions, however, only one muscle was tested, which does not give a robust description of the map and trends for that joint and function. Perhaps there are two to three different maps that

animals tend to display that contributes to this variance. Further testing on a significantly greater number of animals is needed to determine this. And finally, the spread of muscle responses in our study is due to apparent inherent lack of focal specificity of subdural stimulation, as compared for example to intraspinal stimulation. This spread might be reduced by using high-resolution multi-electrode arrays for stimulation in future work.

Clinical Relevance

Electrical spinal cord stimulation has the potential to improve function, particularly motor function, after spinal cord injury via bypassing the injury and directly activating intact spinal motor systems. While it has been implemented for decades in the treatment of chronic pain, it is still an emergent treatment when it comes to restoring motor function (e.g. treating spasticity, promoting weight bearing and ambulation, etc.) after spinal cord injury (Hamid and Hayek 2008; Nagel et al. 2017). A critical step in increasing our understanding of electrical spinal cord stimulation after spinal cord injury is to first understand its effects in the intact spinal cord. This study focused on building a functional output map of the lumbosacral cord stimulation in preparation large animal. We confirmed subdural stimulation in the decerebrate cat largely aligns with the functional maps of epidural and intraspinal stimulation in anesthetized cats and monkeys, as well as with the anatomical maps of cats, monkeys, and humans. Building from this intact map, future work can examine if and how spinal cord injury affects these maps which in turn will lead to more effective electro-therapeutic treatments for spinal cord injury.

Conclusions

In summary, our results demonstrate the rostro-caudal distribution of hindlimb EMG activity in response to lumbosacral subdural stimulation in the intact cord of decerebrate cats. This is the first functional map of the lumbosacral cord using subdural stimulation. Short latency responses

largely aligned with the anatomical motor pools, with some muscles having more spread. Long latency responses showed increasing spread with increasing latency. These results are in agreement with previous findings using epidural and intraspinal stimulation in anesthetized cats and monkeys. Future work will explore this rostro-caudal distribution of electrically-evoked activity following spinal injury.

III. Changes in the Functional Map of the Lumbosacral Cord with Transection

Abstract

Electrical spinal cord stimulation is an emerging treatment for spinal cord injury that can improve walking and bladder control, among many other functions. The effects of stimulation changes with stimulation location, and maps of these effects have been studied and described in many animals, including the cat. While the cat lumbosacral spinal cord has been both anatomically and functionally mapped in both its intact and transected state, there has yet to be a study comparing the functional mapping of a cord both before and after SCI. The goal of this study was to examine how the functional map of the lumbosacral spinal cord in the decerebrate cat changes with SCI. In eight decerebrate cats with intact spinal cords, eight locations were stimulated starting from the caudal portion of lumbar segment L3 to the border of sacral segments S1 and S2. Stimulation was done 15 times at each location at 1 Hz with stimulation amplitudes high enough to evoke muscle responses without causing tissue injury. EMG was measured in nine hindlimb muscles: soleus, tibialis anterior, lateral gastrocnemius, sartorius, medial gastrocnemius, vastus lateralis, biceps femoris posterior, gluteus medius, and pectineus. EMG peak to peak amplitude of the short-latency response (presumably monosynaptic), and rectified integrated EMG of the long latency response were used to assess muscle response. Then, the spinal cord was transected above L3 and the protocol was repeated to map the acute cord. Results showed that for most muscles at most stimulation locations, there was no significant difference between the intact and transected responses. This was true for both the short latency and long latency responses. These results suggest that subdural electrical stimulation in the acute transected cord largely has the same effects as in the intact cord. Further research is needed to understand how the maps are affected by chronic spinal cord injury.

Introduction

Electrical spinal cord stimulation shows massive potential as a treatment for spinal cord injury (SCI). Now a standard of care for the treatment of chronic pain, electrical spinal cord stimulation is still in its infancy for the treatment of SCI (Nagel et al. 2017; Thiriez et al. 2014). Decades of research has shown that electrical stimulation is effective at improving mobility as well as autonomic functions like bladder and bowel control and sexual function (Hachmann et al. 2021). However, when it comes to the full restoration of locomotion, among other motor behaviors, the field is still a long way away.

The placement of electrodes in the cord affects motor output, and so mapping how different locations in the cord result in particular motor outputs will better inform the placement of spinal stimulators and the efficacy of spinal stimulation as a treatment. The cat lumbosacral spinal cord has been anatomically and functionally mapped in its intact state. However, it has yet to be mapped in the transected state. It is highly important to understand how the lumbosacral cord responds to electrical stimulation after SCI, but also how those responses have changed as a result of SCI. Previous work has demonstrated that neural properties change with spinal transection, but how these changes affect the functional map is unknown. For instance, it's been demonstrated that following transection of the cord, motoneuron receptive fields broaden and unwanted whole limb reflexes can occur (Hyngstrom et al. 2008). Persistent inward currents are also drastically reduced following SCI, due to the loss of supraspinal input, and particularly monoaminergic input (Harvey et al. 2006; Heckman et al. 2008). Overall, motoneuron excitability drops due to this sudden loss in neuromodulation (Heckman et al. 2009b). Interneuron excitability, however, can increase, as monoaminergic input inhibits some interneurons (Jankowska et al. 2000). This interneuron disinhibition may expand motor pools following SCI. In all, previous

research has demonstrated that spinal circuits change following SCI, and this may affect the cord's functional output.

Therefore, the goal of this study was to examine how the functional map of the lumbosacral spinal cord changes with SCI. Understanding how the functional map changes with SCI will help guide development of more effective electrical stimulation protocols and devices for improving locomotion in individuals with SCI. Based on evidence showing that motor pools may widen following SCI, it is predicted that the functional maps will broaden: stimulation at a particular location will evoke responses in more hindlimb muscles, and hindlimb muscles will respond to stimulation at a greater number of locations. To study this, specifically engineered electrodes sitting on the dorsal root columns stimulated segments spanning from L3 to S1-S2 while activity in hindlimb muscles were measured in cats both before and following spinal transection. Data from the intact spinal cord have been previously presented in Chapter 2. Results herein illustrate that the functional map of the lumbosacral cord broadens following SCI.

Methods

Animals

All experimental procedures were approved by the Institutional Animal Care and Use Committee of Northwestern University. All animals were obtained from a designated breeding establishment for scientific research. Before the experiments, animals were housed and fed within designated areas, which were monitored daily by veterinary staff and trained personnel. The current data set is compiled from 8 adult cats of either sex weighing between 2.5 and 5.0 kg. All animals underwent acute terminal experiments, in which initial surgical procedures were done under deep gaseous anesthesia obtained by a mixture of isoflurane, nitrous oxide, and oxygen. Before data collection,

a precollicular decerebration was performed. This allowed the discontinuation of anesthesia, thus warranting that spinal circuits responded fully to ES without being suppressed by anesthesia.

Surgical preparation

Anesthesia. Anesthesia was induced in a clear cylindrical chamber with a gaseous mixture (1.5–3% isoflurane in a 1:3 mixture of O_2 and N_2O) and then continued with a face mask until a tracheal tube was inserted and secured. Anesthetic gases were then delivered through tracheal tube for the duration of initial procedures. The right common carotid artery and right jugular vein were cannulated to monitor arterial blood pressure and administer intravenous fluids, respectively. Throughout the experiment, arterial blood pressure, heart rate, respiratory rates, reflexes, and muscle tone were recorded every 15 minutes, and used to adjust the level of anesthesia.

EMG recordings. The animal was transferred to a stereotaxic frame (Kopf) for further surgery. The animal's hindlimbs were positioned and rigidly clamped with the ankle at about 90° relative to the tibia, the knee at 130°, and the hip at 105°. Stainless steel fine wire EMG electrodes (A-M Systems, Washington USA) were inserted into nine muscles in the left hindlimb: medial gastrocnemius (MG), lateral gastrocnemius (LG), soleus (SL), tibialis anterior (TA), gluteus medius (GM), sartorious (SR), vastus lateralis (VL), biceps femoris posterior (BF), and pectineus (PT). The EMG data was recorded using custom-built differential amplifiers, and were digitized at 10 KHz per channel using a power 1401 board (CED, UK). The data was acquired through SPIKE2 software (CED, UK), and stored on a computer for offline analysis.

Stimulation locations. A dorsal laminectomy was performed to expose the lumbosacral spinal cord (L4-S2). The dura was incised and retracted to expose the spinal cord tissue and allow identification of exact location of dorsal root entry zones. A Microscribe G2X Digitizer was used to record the 3D location of the identifiable dorsal root entry zones (L4-S2) as well as the border of laminectomy by touching the tip of the microscribe to the root entry zones and the edges of the exposed spinal cord. Great care was taken not to damage the cord during

these recordings. These digitally-recorded locations were used to guide the placement of the stimulation electrode.

Decerebration. Once these above-mentioned initial procedures are completed, a precollicular decerebration was performed while the deep anesthetic plane is maintained. All anterior forebrain structures were removed via an aspirator and replaced with saline-soaked cotton to control bleeding. At this point, animals were considered to have complete lack of sentience (Silverman et al. 2005), and anesthesia was gradually discontinued. The preparation was left to recover for about 60 minutes before data collection commenced. Details of these procedures are provided in previous publications (Lee and Heckman 1998b; Miller et al. 1995).

Electrical stimulation

Stimulus generation and delivery. Electrical stimulation was generated by a custom-built voltage-controlled current source (VCCS) driven by an NI DAQ card. Stimulation was delivered to spinal tissue through a custom-built silver ball bipolar electrode. The voltage command and the delivered current on the spinal cord were measured, and simultaneously recorded into SPIKE2 at 20 KHz to ensure accurate delivery of intended stimuli. The stimulation electrode was fitted in a spring-loaded mechanism to minimize damage to spinal cord whenever vertical movements occurred.

Stimulus parameters.1 Hz square wave electrical stimulation of 1 ms duration was applied to individual dorsal root entry zones at an amplitude of 5 μA. Amplitude was increased until we observed EMG activity within one of the 9 muscles. This amplitude was noted as the response threshold at that stimulation location. The amplitude was then increased 2X, 5X and 10X that response threshold or until a response plateau was reached but below any risk of tissue damage. Using the measured range, threshold to plateau, we designed a stimulation sequence covering that range. Each stimulation amplitude (1xT-10xT) was repeated 5 times at each location, and the average EMG response of each muscle was used for analysis. The electrode was then moved to a new dorsal root entry zone and the protocol was repeated.

Transection

Following a full stimulation protocol in the intact cord, forceps were used to transect the cord at L2. 45 minutes following the transection, the stimulation protocol was repeated.

Data Analysis

The raw time series data from each muscle was split according to stim amplitude, position, etc. in windows of ±0.5 s centered around the stimulus time. Data for the first pulse in each stimulation train at the maximum stimulation amplitude were selected for analysis. Trials with activity 10 ms pre-stimulus through 4 ms post-stimulus were excluded.

The goal of this experiment was to map how different muscles responded to stimulation at different spinal locations before and after spinal transection. To this end, both the short latency and long latency responses were measured in the nine hindlimb muscles. The short latency response was quantified as the maximum peak to peak response within 12 ms post-stimulus using custom Matlab software (The MathWorks, Natick, MA). The long latency response was quantified as the rectified integrated EMG (RIEMG) for two windows: 12-30 ms and 30-400 ms.

Statistical Analysis. The distribution of outcomes of interest was explored through the density plots. Side-by-side boxplots were generated to compare outcomes of interest across stim location and muscle. Generalized linear mixed models were fit on log transformed outcomes for all animals, with fixed effects of muscle, stim position, and transection; the interaction between muscle and stim position and transection; as well as a random intercept of animal and muscle within animal effect. ANOVA was conducted to test the significance of the interaction term. Outcomes of interest were peak to peak, RIEMG 12-30 ms, and RIEMG 30-400 ms. The analysis was performed for both normalized and unnormalized data.

Results

Rostrocaudal Distribution of Short Latency Responses. The first goal of this experiment was to create a map of the rostrocaudal arrangement of the short latency responses in the transected cord of the decerebrate cat. The short latency responses are likely monosynaptic, and so these results are assumed to reflect the direct activation of monosynaptic Ia afferent circuits. To map the short latency responses, we measured the peak to peak response within 4-12 ms post stimulation. Figure 8 shows this distribution of peak to peak responses. Figure 8 A-B presents the raw data and Figure 8 C-D presents the log transformed data. Statistics were performed on the log transformed data, and 95% confidence intervals are presented in Table 4. During the short latency window, the most rostrally responding muscles were the hip flexor SR and the hip adductor PT, followed next by the knee extensor VL. The remainder of muscles studied responded to stimulation applied more caudally. TA did not respond significantly differently to rostral or caudal stimulation.

Comparison of Short Latency Responses to Motor Pools. The next goal was to describe the alignment of the short latency responses to the motor pools. To do this, responses were compared to the cat anatomical motor pool locations determined by Yakovenko et al. 2002. Figure 9 illustrates each muscle's functional map compared to its motor pool. Error bars indicate 95% confidence intervals, which are also listed in Table 4. Responses to stimulation are considered significantly different if their 95% confidence intervals do not overlap. When a location or locations within a muscle's motor pool (indicated in red) has or have a significantly greater response compared to locations outside the motor pool, this would be interpreted as the functional responses aligning with the anatomical motor pool. If a location or locations outside a muscle's motor pool has or have a significantly greater response compared to other locations outside the motor pool, this would be interpreted as the functional responses being broader than the anatomical motor pool.

In addition to mapping the rostrocaudal distribution of functional responses, it is important to note the alignment of the functional responses to the anatomical motor pools. Three muscles—VL, MG, and GM—had significantly greater responses at locations only within the motor pool. Five muscles—SR, PT, SL, LG, and BF—had significantly greater responses at locations both within and outside the motor pool. No muscles had significantly larger responses that specifically aligned only with their motor pools—PT, SL, and BF all had significantly greater responses at all locations within the motor pool, but also had significantly greater responses at locations outside the motor pool too. Further detail of how the functional responses of individual muscles compare to their anatomical motor pools can be found in Figure 9 and Table 4.

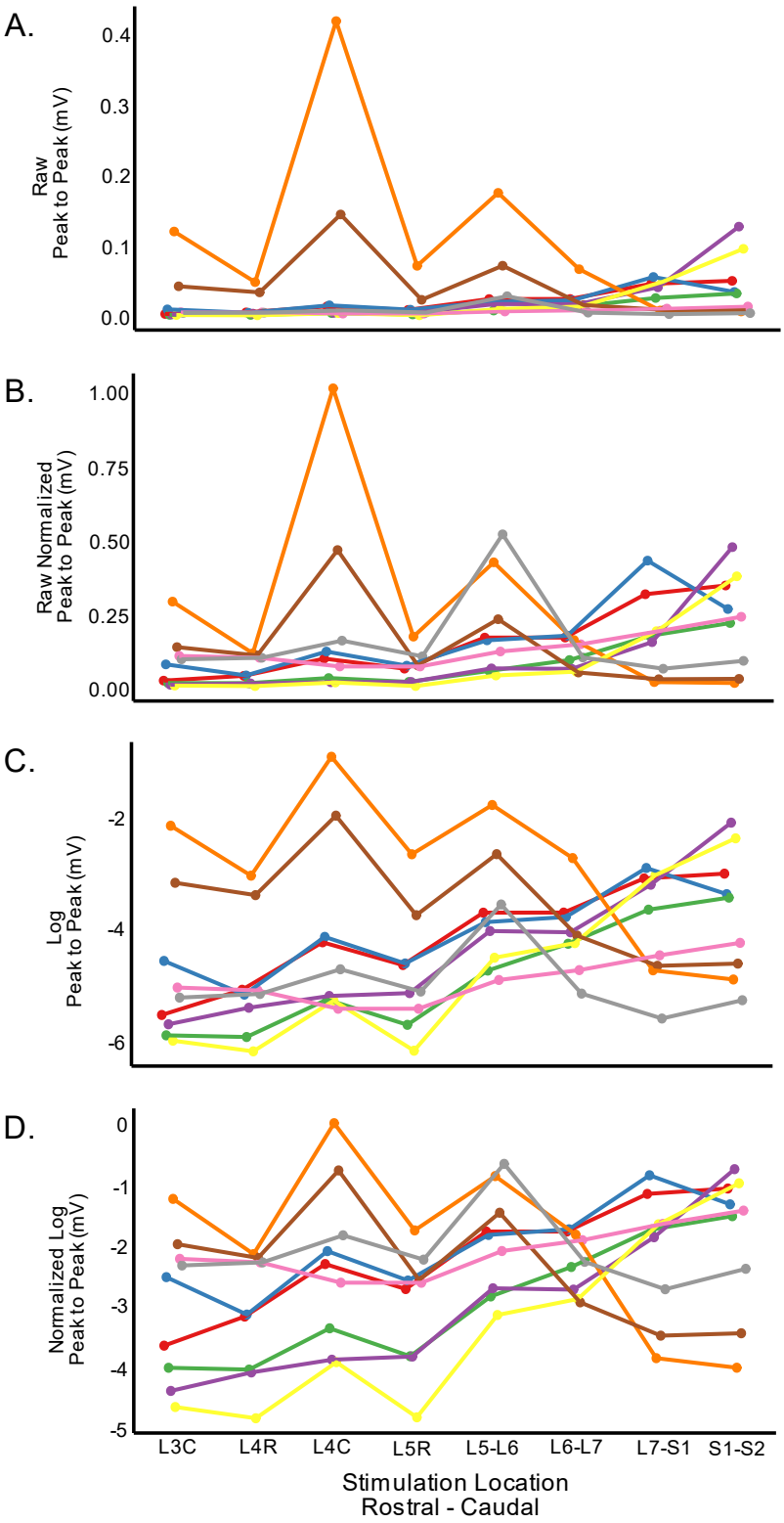

Figure 8. Rostrocaudal Distributions of Transected Short Latency Responses. Each colored line represents the mean peak to peak response of a muscle to electrical stimulation across eight decerebrate cats.

Electrical stimulation was applied to the lumbosacral cord at locations indicated on the x axis (L3C through S1-S2) and the peak to peak response was measured from 4-12 ms using EMG in nine hindlimb muscles. The legend indicates which color line represents which muscle. Each subplot represents a different way of processing the data. A) Raw data. B) Normalized raw data. C) Log transformed data. D) Log transformed normalized data.

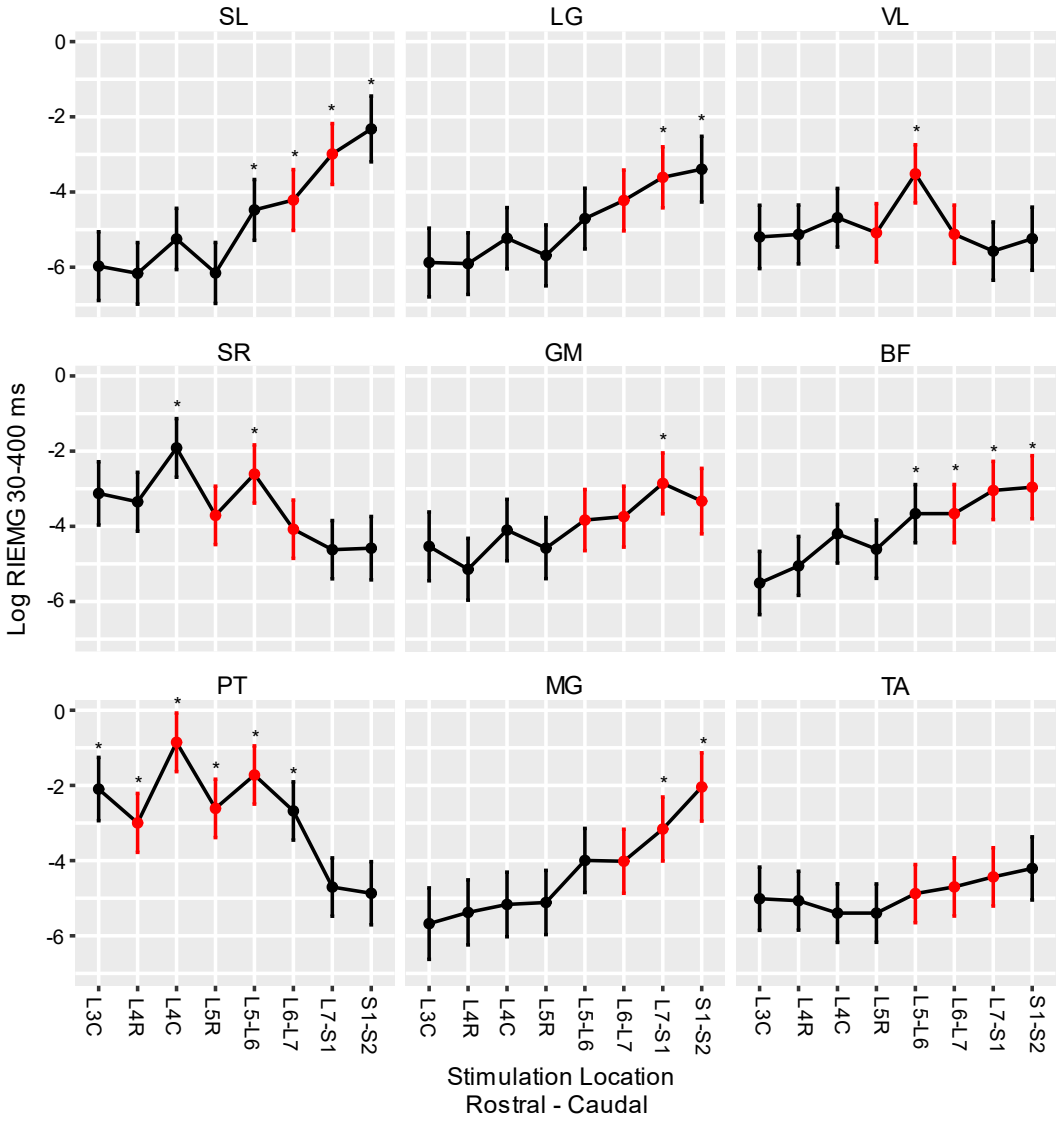

Figure 9. Individual Muscles' Rostrocaudal Distributions of Transected Log Transformed Short Latency Response. Each subplot shows a different hindlimb muscle's mean peak to peak response across eight decerebrate cats. Electrical stimulation was applied to the lumbosacral cord at locations indicated on the x axis (L3C through S1-S2) and the peak to peak response was measured from 4-12 ms using EMG in nine hindlimb muscles. Error bars indicate 95% confidence intervals; lower and upper bounds are listed in Table 4. Responses to stimulation are significantly different if their 95% confidence intervals do not overlap. Stars indicate the response at that stimulation location is significantly different from at least one other location's response. To determine significance, generalized linear mixed models were fit on log transformed outcomes for all animals, with fixed effects of muscle, stim position and the interaction between muscle and stim

position, as well as a random intercept of animal and muscle within animal effect. ANOVA was conducted to test the significance of the interaction term. The anatomical locations of the motor pools are highlighted in red. This figure illustrates how the spread of significant responses compares to the anatomical motor pool.

Muscle	Stimulation Position	Log Peak to Peak	Confidence Interval Lower Bound	Confidence Interval Upper Bound	Peak to Peak
SL	L3C	-5.972	-6.886	-5.058	0.00255
SL	L4R	-6.164	-6.983	-5.345	0.00210
SL	L4C	-5.249	-6.063	-4.434	0.00525
SL	L5R	-6.153	-6.963	-5.342	0.00213
SL	L5-L6	-4.476	-5.284	-3.668	0.01138
SL	L6-L7	-4.213	-5.022	-3.404	0.01480
SL	L7-S1	-2.989	-3.799	-2.180	0.05034
SL	S1-S2	-2.323	-3.198	-1.448	0.09798
LG	L3C	-5.875	-6.790	-4.961	0.00281
LG	L4R	-5.905	-6.724	-5.086	0.00273
LG	L4C	-5.230	-6.044	-4.415	0.00535
LG	L5R	-5.686	-6.496	-4.875	0.00339
LG	L5-L6	-4.707	-5.515	-3.900	0.00903
LG	L6-L7	-4.224	-5.034	-3.415	0.01464
LG	L7-S1	-3.609	-4.421	-2.798	0.02708
LG	S1-S2	-3.393	-4.266	-2.519	0.03361
VL	L3C	-5.195	-6.037	-4.353	0.00554
VL	L4R	-5.129	-5.912	-4.346	0.00592
VL	L4C	-4.684	-5.464	-3.905	0.00924
VL	L5R	-5.085	-5.862	-4.309	0.00619
VL	L5-L6	-3.517	-4.290	-2.743	0.02969
VL	L6-L7	-5.123	-5.898	-4.348	0.00596
VL	L7-S1	-5.572	-6.347	-4.797	0.00380
VL	S1-S2	-5.242	-6.082	-4.402	0.00529
SR	L3C	-3.125	-3.966	-2.283	0.04394
SR	L4R	-3.348	-4.131	-2.564	0.03515
SR	L4C	-1.914	-2.694	-1.135	0.14749
SR	L5R	-3.709	-4.485	-2.933	0.02450
SR	L5-L6	-2.609	-3.382	-1.835	0.07361
SR	L6-L7	-4.077	-4.852	-3.302	0.01696
SR	L7-S1	-4.622	-5.397	-3.847	0.00983
SR	S1-S2	-4.582	-5.425	-3.739	0.01023
GM	L3C	-4.534	-5.448	-3.619	0.01074

GM	L4R	-5.142	-5.964	-4.320	0.00585
GM	L4C	-4.100	-4.917	-3.283	0.01657
GM	L5R	-4.580	-5.392	-3.767	0.01025
GM	L5-L6	-3.834	-4.648	-3.021	0.02162
GM	L6-L7	-3.742	-4.553	-2.932	0.02371
GM	L7-S1	-2.858	-3.668	-2.048	0.05738
GM	S1-S2	-3.330	-4.201	-2.459	0.03579
BF	L3C	-5.508	-6.350	-4.666	0.00405
BF	L4R	-5.053	-5.837	-4.270	0.00639
BF	L4C	-4.198	-4.977	-3.418	0.01503
BF	L5R	-4.608	-5.384	-3.832	0.00997
BF	L5-L6	-3.664	-4.437	-2.890	0.02563
BF	L6-L7	-3.662	-4.437	-2.888	0.02568
BF	L7-S1	-3.046	-3.821	-2.272	0.04755
BF	S1-S2	-2.960	-3.800	-2.120	0.05182
PT	L3C	-2.097	-2.938	-1.255	0.12282
PT	L4R	-2.997	-3.780	-2.213	0.04994
PT	L4C	-0.853	-1.633	-0.074	0.42613
PT	L5R	-2.611	-3.387	-1.835	0.07346
PT	L5-L6	-1.723	-2.496	-0.949	0.17853
PT	L6-L7	-2.679	-3.454	-1.905	0.06863
PT	L7-S1	-4.703	-5.478	-3.928	0.00907
PT	S1-S2	-4.869	-5.708	-4.029	0.00768
MG	L3C	-5.676	-6.626	-4.726	0.00343
MG	L4R	-5.378	-6.242	-4.513	0.00462
MG	L4C	-5.166	-6.025	-4.307	0.00571
MG	L5R	-5.114	-5.967	-4.260	0.00601
MG	L5-L6	-3.995	-4.847	-3.143	0.01841
MG	L6-L7	-4.017	-4.869	-3.166	0.01801
MG	L7-S1	-3.160	-4.011	-2.308	0.04243
MG	S1-S2	-2.041	-2.949	-1.133	0.12990
TA	L3C	-5.014	-5.855	-4.172	0.00664
TA	L4R	-5.066	-5.849	-4.283	0.00631
TA	L4C	-5.396	-6.175	-4.616	0.00453
TA	L5R	-5.396	-6.172	-4.620	0.00453
TA	L5-L6	-4.877	-5.651	-4.104	0.00762
TA	L6-L7	-4.699	-5.474	-3.925	0.00910
TA	L7-S1	-4.433	-5.208	-3.658	0.01188
TA	S1-S2	-4.208	-5.048	-3.368	0.01488

Table 4. Transected Short Latency Confidence Intervals. Each row outlines the mean log peak to peak, lower and upper bounds of the 95% confidence interval, as well as the raw mean peak to peak for each muscle and stimulation position for 8 decerebrate cats combined. Means and 95% confidence intervals determined by fitting generalized linear mixed models on log transformed outcomes for all animals, with fixed effects of muscle, stim position and the interaction between muscle and stim position, as well as a random intercept of animal and muscle within animal effect. The mean log peak to peak values for each muscle and stimulation location are displayed in Figure 8B and Figure 9. In Figure 9, the confidence interval lower and upper bounds are displayed as error bars. The raw peak to peak measurements are displayed in Figure 8A.

Rostrocaudal Distribution of Long Latency Window I Responses. The next goal of this experiment was to create a rostrocaudal map of long latency responses, and to compare these long latency responses to the anatomical motor pools. For the long latency responses, the outcome measure was RIEMG: Window I is 12-30 ms and Window II is 30-400 ms. The long latency responses are polysynaptic, so likely involve more circuits that may span multiple segments compared to the short latency response. Figure 10 shows the rostrocaudal distribution of muscle activity 12-30 ms following subdural spinal stimulation. Figure 10 A-B presents the raw data and Figure 10 C-D presents the log transformed data. Statistics were performed on the log transformed data, and 95% confidence intervals are presented in Table 5. As shown in Figure 10, during this time window, there is no apparent rostrocaudal organization in the transected cord.

Comparison of Long Latency Window I Responses to Motor Pools. Next, we wanted to determine if the long latency responses aligned with the motor pools. To determine whether the map of long latency responses and the anatomical map are aligned, responses were compared to the cat anatomical motor pool locations. Figure 11 illustrates each muscle's functional map compared to its motor pool. Just as with the short latency figure, error bars indicate 95% confidence intervals, which are also listed in Table 5. Responses to stimulation are considered significantly different if their 95% confidence intervals do not overlap. As with the short latency response, when a location or locations within a muscle's motor pool has or have a significantly greater response compared to locations outside the motor pool, this would be interpreted as the functional responses aligning with the anatomical motor pool.

As shown in Figure 11, only four muscles—PT, TA, MG, and BF— had significantly greater responses at any location, and only at one location each at that. The location that TA responded significantly greater at was not within its motor pool, but the significantly greater locations in the other three muscles was within each's motor pool. The remaining five muscles did not have significantly different responses at any stimulation locations.

Rostrocaudal Distribution of Long Latency Window II Responses. We also looked at the rostrocaudal organization of the latest window: 30-400 ms. Figure 12 shows the rostrocaudal distribution of muscle activity 30-400 ms following subdural spinal stimulation. Figure 12 A-B presents the raw data and Figure 12 C-D presents the log transformed data. Statistics were performed on the log transformed data, and 95% confidence intervals are presented in Table 6. As shown in Figure 12, during this time window, there is no apparent rostrocaudal organization.

Comparison of Long Latency Window II Responses to Motor Pools. Finally, we compared the latest window's responses to the motor pools. Figure 13 illustrates each muscle's functional map of the RIEMG response from 30-400 ms compared to its motor pool. Error bars indicate 95% confidence intervals, which are also listed in Table 6. As shown in Figure 13, three muscles—PT, TA, GM—had a significantly greater response at any location. PT had significantly greater responses at two locations within the motor pool and two locations outside the motor pool, compared to other locations. TA had a significantly greater response at one location outside the motor pool, and GM had a significantly greater response at one location within the motor pool. All other muscles had no significantly higher response to stimulation at any location compared to other locations.

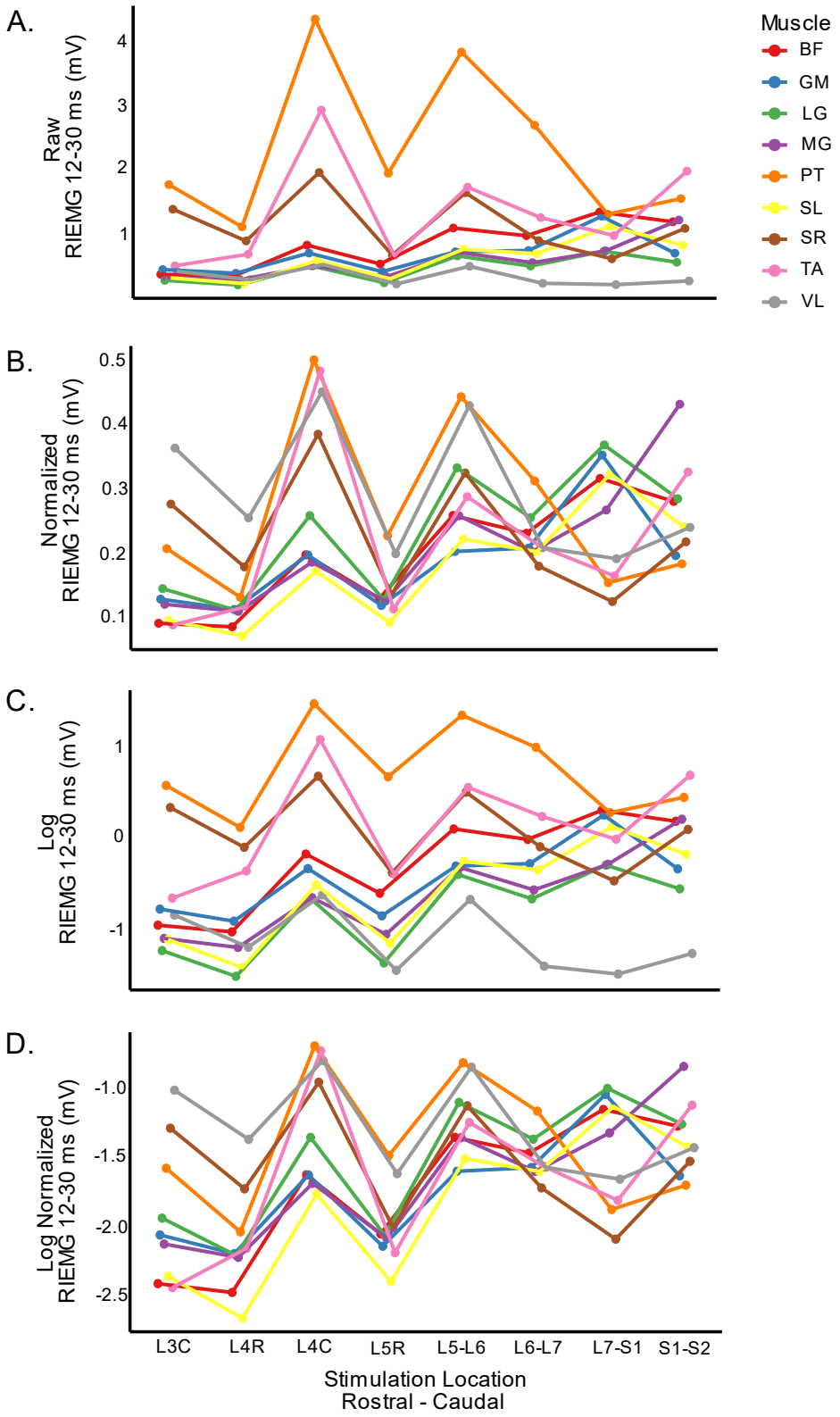
A.
Raw
RIEMG 12-30 ms (mV)
4
3
2
1
Muscle
BF
GM
LG
MG
PT
SL
SR
TA
VL
B.
Normalized
RIEMG 12-30 ms (mV)
0.5
0.4
0.3
0.2
0.1
C.
Log
RIEMG 12-30 ms (mV)
1
0
-1
D.
Log Normalized
RIEMG 12-30 ms (mV)
-1.0
-1.5
-2.0
-2.5
L3C
L4R
L4C
L5R
L5-L6
L6-L7
L7-S1
S1-S2
Stimulation Location
Rostral - Caudal

Figure 10. Rostrocaudal Distributions of Transected Long Latency (12-30 ms) Responses. Each colored line represents the mean RIEMG response of a muscle to electrical stimulation across eight decerebrate cats. Electrical stimulation was applied to the lumbosacral cord at locations indicated on the x axis (L3C through S1-S2) and the RIEMG response was measured from 12-30 ms using EMG in nine hindlimb muscles. The legend indicates which color line represents which muscle. Each subplot represents a different way of processing the data. A) Raw data. B) Normalized raw data. C) Log transformed data. D) Log transformed normalized data.

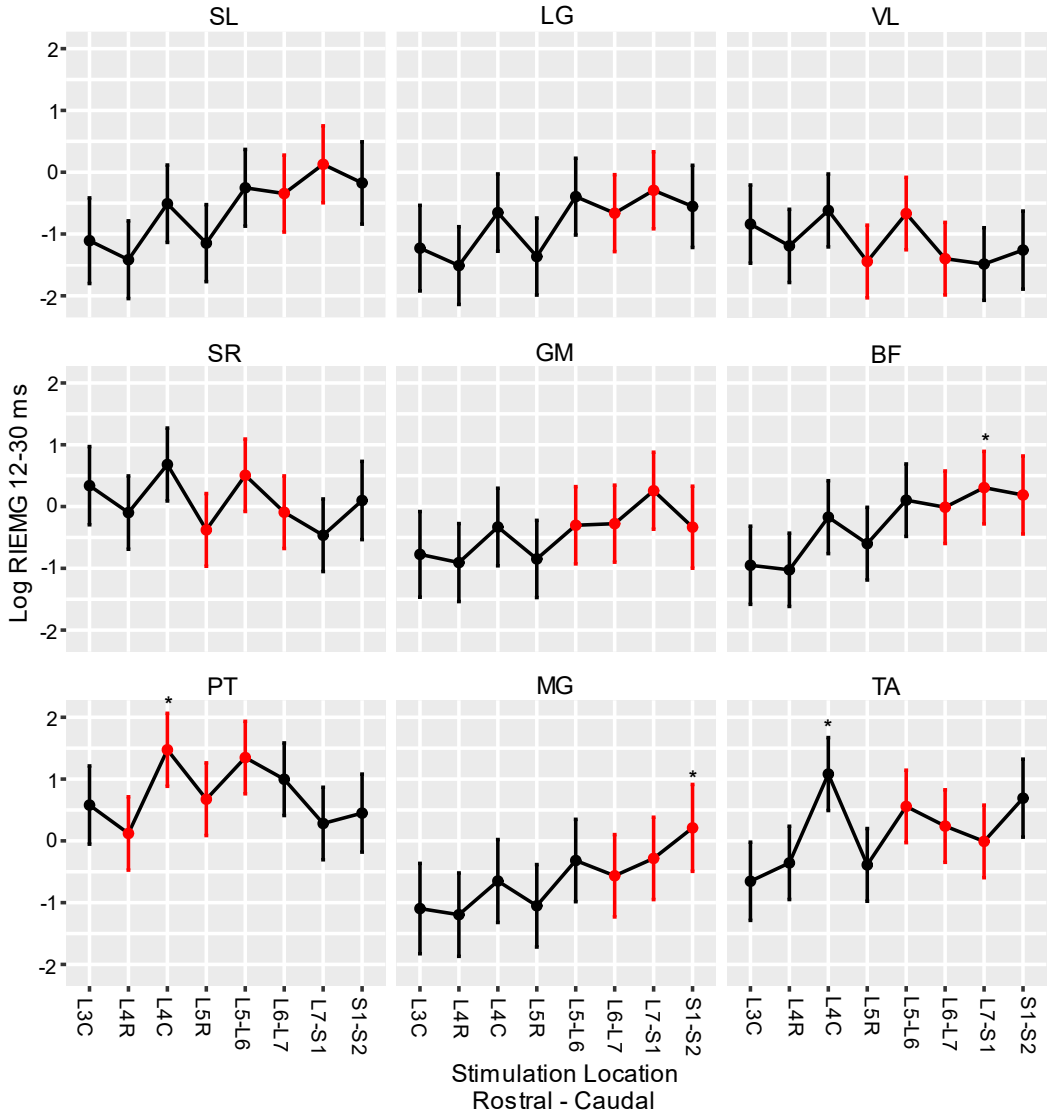

Figure 11. Individual Muscles' Rostrocaudal Distributions of Transected Log Transformed Long Latency (12-30 ms) Response. Each subplot shows a different hindlimb muscle's mean RIEMG response across eight decerebrate cats. Electrical stimulation was applied to the lumbosacral cord at locations indicated on the x axis (L3C through S1-S2) and the RIEMG response was measured from 12-30 ms using EMG in nine hindlimb muscles. Error bars indicate 95% confidence intervals; lower and upper bounds are listed in Table 2. Responses to stimulation are significantly different if their 95% confidence intervals do not overlap. Stars indicate the response at that stimulation location is significantly different from at least one other location's

response. To determine significance, generalized linear mixed models were fit on log transformed outcomes for all animals, with fixed effects of muscle, stim position and the interaction between muscle and stim position, as well as a random intercept of animal and muscle within animal effect. ANOVA was conducted to test the significance of the interaction term. The anatomical locations of the motor pools are highlighted in red. This figure illustrates how the spread of significant responses compares to the anatomical motor pool.

Muscle	Stimulation Position	Log RIEMG 12-30 ms	Confidence Interval Lower Bound	Confidence Interval Upper Bound	RIEMG 12-30 ms
SL	L3C	-1.108	-1.801	-0.416	0.33022
SL	L4R	-1.416	-2.045	-0.787	0.24268
SL	L4C	-0.510	-1.136	0.116	0.60050
SL	L5R	-1.148	-1.771	-0.525	0.31727
SL	L5-L6	-0.252	-0.873	0.369	0.77724
SL	L6-L7	-0.345	-0.968	0.277	0.70822
SL	L7-S1	0.128	-0.494	0.750	1.13655
SL	S1-S2	-0.174	-0.840	0.492	0.84030
LG	L3C	-1.229	-1.922	-0.536	0.29259
LG	L4R	-1.511	-2.140	-0.882	0.22069
LG	L4C	-0.653	-1.279	-0.028	0.52048
LG	L5R	-1.365	-1.988	-0.741	0.25538
LG	L5-L6	-0.395	-1.017	0.226	0.67368
LG	L6-L7	-0.663	-1.285	-0.040	0.51530
LG	L7-S1	-0.293	-0.916	0.331	0.74602
LG	S1-S2	-0.553	-1.218	0.112	0.57522
VL	L3C	-0.840	-1.472	-0.207	0.43171
VL	L4R	-1.192	-1.785	-0.600	0.30361
VL	L4C	-0.619	-1.209	-0.029	0.53848
VL	L5R	-1.445	-2.033	-0.857	0.23575
VL	L5-L6	-0.669	-1.255	-0.083	0.51222
VL	L6-L7	-1.399	-1.986	-0.812	0.24684
VL	L7-S1	-1.486	-2.073	-0.899	0.22628
VL	S1-S2	-1.260	-1.892	-0.629	0.28365
SR	L3C	0.338	-0.295	0.970	1.40214
SR	L4R	-0.098	-0.691	0.495	0.90665
SR	L4C	0.680	0.090	1.270	1.97388
SR	L5R	-0.378	-0.966	0.210	0.68523
SR	L5-L6	0.506	-0.080	1.092	1.65864

SR	L6-L7	-0.092	-0.679	0.495	0.91211
SR	L7-S1	-0.465	-1.052	0.122	0.62814
SR	S1-S2	0.098	-0.535	0.731	1.10296
GM	L3C	-0.774	-1.467	-0.081	0.46116
GM	L4R	-0.907	-1.538	-0.276	0.40373
GM	L4C	-0.331	-0.959	0.296	0.71821
GM	L5R	-0.848	-1.473	-0.224	0.42827
GM	L5-L6	-0.303	-0.928	0.322	0.73860
GM	L6-L7	-0.277	-0.900	0.346	0.75805
GM	L7-S1	0.256	-0.367	0.879	1.29175
GM	S1-S2	-0.334	-0.998	0.329	0.71605
BF	L3C	-0.951	-1.583	-0.318	0.38635
BF	L4R	-1.024	-1.617	-0.431	0.35916
BF	L4C	-0.172	-0.762	0.418	0.84198
BF	L5R	-0.601	-1.189	-0.013	0.54826
BF	L5-L6	0.103	-0.483	0.689	1.10849
BF	L6-L7	-0.011	-0.598	0.575	0.98906
BF	L7-S1	0.306	-0.281	0.893	1.35798
BF	S1-S2	0.187	-0.444	0.818	1.20563
PT	L3C	0.579	-0.053	1.212	1.78425
PT	L4R	0.120	-0.473	0.713	1.12750
PT	L4C	1.474	0.883	2.064	4.36667
PT	L5R	0.674	0.086	1.262	1.96207
PT	L5-L6	1.348	0.762	1.935	3.84972
PT	L6-L7	0.997	0.410	1.584	2.71014
PT	L7-S1	0.281	-0.306	0.867	1.32445
PT	S1-S2	0.449	-0.182	1.080	1.56674
MG	L3C	-1.096	-1.827	-0.365	0.33421
MG	L4R	-1.195	-1.869	-0.520	0.30270
MG	L4C	-0.650	-1.321	0.021	0.52205
MG	L5R	-1.051	-1.718	-0.384	0.34959
MG	L5-L6	-0.318	-0.984	0.348	0.72760
MG	L6-L7	-0.565	-1.231	0.101	0.56836
MG	L7-S1	-0.284	-0.950	0.382	0.75277
MG	S1-S2	0.210	-0.493	0.913	1.23368
TA	L3C	-0.654	-1.287	-0.022	0.51996
TA	L4R	-0.357	-0.949	0.236	0.69977
TA	L4C	1.081	0.491	1.671	2.94763
TA	L5R	-0.389	-0.977	0.199	0.67773
TA	L5-L6	0.557	-0.029	1.143	1.74543

TA	L6-L7	0.239	-0.347	0.826	1.26998
TA	L7-S1	-0.009	-0.596	0.578	0.99104
TA	S1-S2	0.691	0.060	1.322	1.99571

Table 5. Transected Long Latency Latency (12-30 ms) Confidence Intervals. Each row outlines the mean log RIEMG, lower and upper bounds of the 95% confidence interval, as well as the raw mean RIEMG for each muscle and stimulation position for 8 decerebrate cats combined. Means and 95% confidence intervals determined by fitting generalized linear mixed models on log transformed outcomes for all animals, with fixed effects of muscle, stim position and the interaction between muscle and stim position, as well as a random intercept of animal and muscle within animal effect. The mean log RIEMG values for each muscle and stimulation location are displayed in Figure 10B and Figure 11. In Figure 11, the confidence interval lower and upper bounds are displayed as error bars. The raw RIEMG measurements are displayed in Figure 10A.

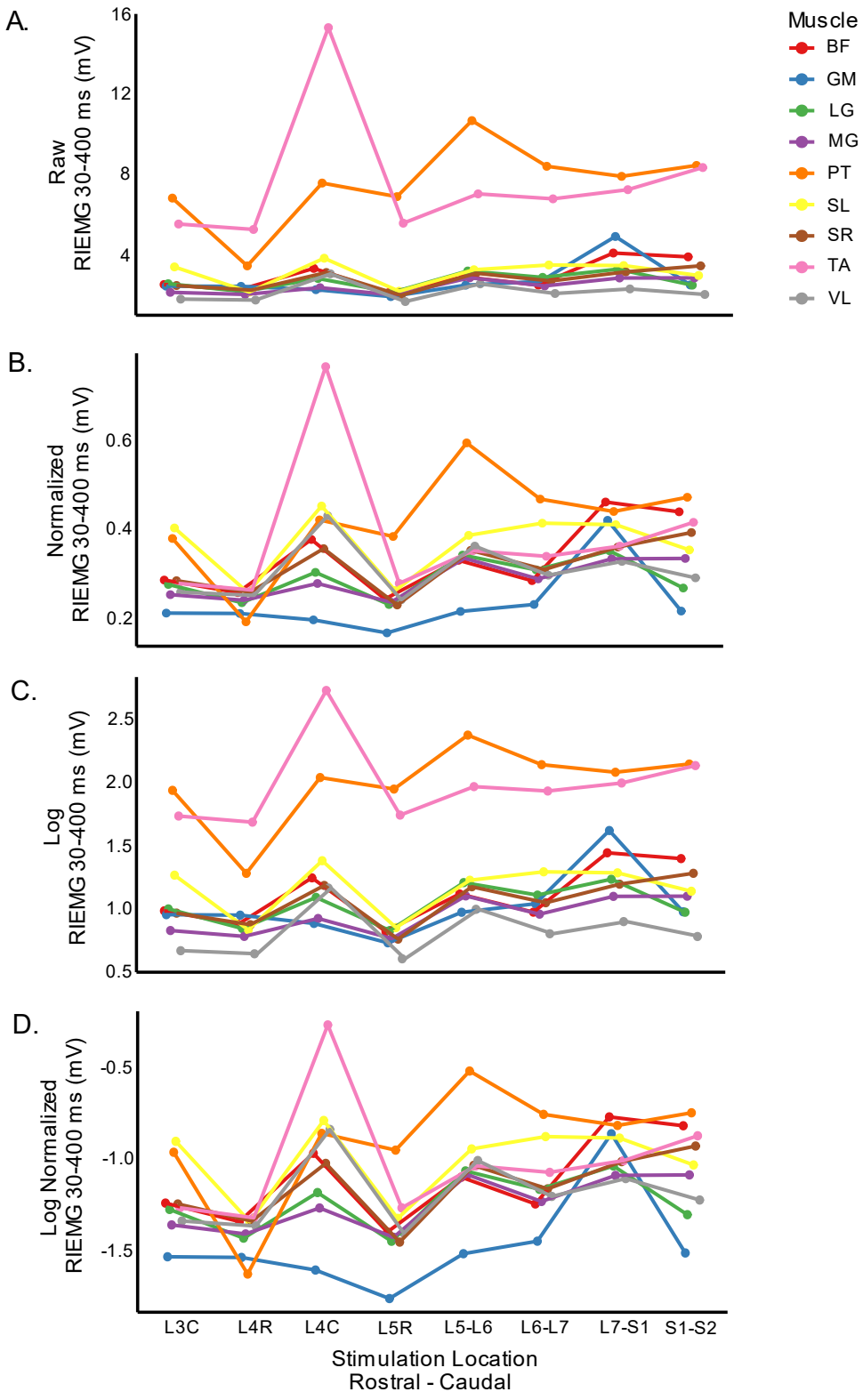
A.
Raw
RIEMG 30-400 ms (mV)
16
12
8
4
Muscle
BF
GM
LG
MG
PT
SL
SR
TA
VL
B.
Normalized
RIEMG 30-400 ms (mV)
0.6
0.4
0.2
C.
Log
RIEMG 30-400 ms (mV)
2.5
2.0
1.5
1.0
0.5
D.
Log Normalized
RIEMG 30-400 ms (mV)
-0.5
-1.0
-1.5
L3C
L4R
L4C
L5R
L5-L6
L6-L7
L7-S1
S1-S2
Stimulation Location
Rostral - Caudal

Figure 12. Rostrocaudal Distributions of Transected Long Latency (30-400 ms) Responses. Each colored line represents the mean RIEMG response of a muscle to electrical stimulation across eight decerebrate cats. Electrical stimulation was applied to the lumbosacral cord at locations indicated on the x axis (L3C through S1-S2) and the RIEMG response was measured from 30-400 ms using EMG in nine hindlimb muscles. The legend indicates which color line represents which muscle. Each subplot represents a different way of processing the data. A) Raw data. B) Normalized raw data. C) Log transformed data. D) Log transformed normalized data.

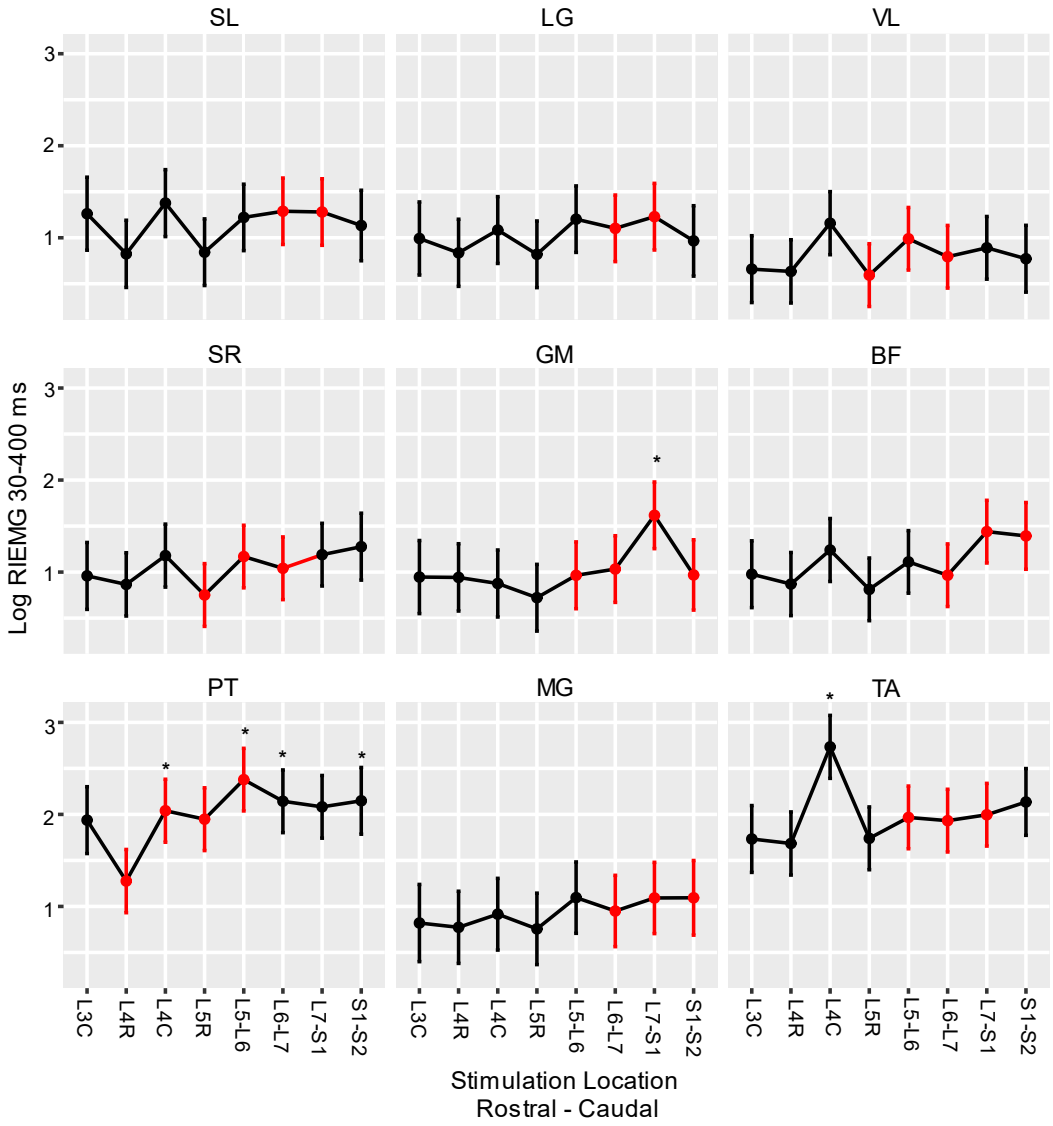

Figure 13. Individual Muscles' Rostrocaudal Distributions of Transected Log Transformed Long Latency (30-400 ms) Response. Each subplot shows a different hindlimb muscle's mean RIEMG response across eight decerebrate cats. Electrical stimulation was applied to the lumbosacral cord at locations indicated on the x axis (L3C through S1-S2) and the RIEMG response was measured from 30-400 ms using EMG in nine hindlimb muscles. Error bars indicate 95% confidence intervals; lower and upper bounds are listed in Table 6. Responses to stimulation are significantly different if their 95% confidence intervals do not overlap. Stars indicate the response at that stimulation location is significantly different from at least one other

location's response. To determine significance, generalized linear mixed models were fit on log transformed outcomes for all animals, with fixed effects of muscle, stim position and the interaction between muscle and stim position, as well as a random intercept of animal and muscle within animal effect. ANOVA was conducted to test the significance of the interaction term. The anatomical locations of the motor pools are highlighted in red. This figure illustrates how the spread of significant responses compares to the anatomical motor pool.

Muscle	Stimulation Position	Log RIEMG 13-400 ms	Confidence Interval Lower Bound	Confidence Interval Upper Bound	RIEMG 13-400 ms
SL	L3C	1.261	0.865	1.658	3.52895
SL	L4R	0.825	0.460	1.190	2.28188
SL	L4C	1.377	1.013	1.740	3.96299
SL	L5R	0.843	0.481	1.205	2.32333
SL	L5-L6	1.221	0.860	1.582	3.39058
SL	L6-L7	1.288	0.927	1.649	3.62553
SL	L7-S1	1.280	0.918	1.641	3.59664
SL	S1-S2	1.133	0.750	1.516	3.10496
LG	L3C	0.992	0.595	1.389	2.69662
LG	L4R	0.836	0.472	1.201	2.30712
LG	L4C	1.084	0.721	1.447	2.95648
LG	L5R	0.820	0.458	1.182	2.27050
LG	L5-L6	1.202	0.841	1.563	3.32676
LG	L6-L7	1.102	0.741	1.464	3.01018
LG	L7-S1	1.229	0.867	1.591	3.41781
LG	S1-S2	0.966	0.583	1.348	2.62741
VL	L3C	0.659	0.296	1.022	1.93286
VL	L4R	0.634	0.291	0.978	1.88514
VL	L4C	1.158	0.816	1.501	3.18356
VL	L5R	0.594	0.253	0.935	1.81122
VL	L5-L6	0.989	0.649	1.329	2.68854
VL	L6-L7	0.794	0.453	1.134	2.21223
VL	L7-S1	0.891	0.550	1.231	2.43757
VL	S1-S2	0.772	0.409	1.135	2.16409
SR	L3C	0.959	0.595	1.322	2.60909
SR	L4R	0.866	0.523	1.210	2.37738
SR	L4C	1.179	0.837	1.521	3.25112
SR	L5R	0.751	0.410	1.092	2.11912
SR	L5-L6	1.169	0.829	1.509	3.21877
SR	L6-L7	1.041	0.701	1.382	2.83205

SR	L7-S1	1.189	0.849	1.530	3.28380
SR	S1-S2	1.276	0.913	1.640	3.58228
GM	L3C	0.946	0.549	1.343	2.57539
GM	L4R	0.942	0.577	1.308	2.56511
GM	L4C	0.876	0.512	1.240	2.40128
GM	L5R	0.722	0.359	1.084	2.05855
GM	L5-L6	0.965	0.602	1.328	2.62479
GM	L6-L7	1.033	0.671	1.395	2.80948
GM	L7-S1	1.617	1.255	1.979	5.03795
GM	S1-S2	0.969	0.587	1.351	2.63531
BF	L3C	0.977	0.614	1.340	2.65647
BF	L4R	0.870	0.527	1.213	2.38691
BF	L4C	1.240	0.898	1.582	3.45561
BF	L5R	0.812	0.472	1.153	2.25241
BF	L5-L6	1.111	0.771	1.451	3.03739
BF	L6-L7	0.966	0.626	1.306	2.62741
BF	L7-S1	1.440	1.099	1.780	4.22070
BF	S1-S2	1.393	1.031	1.756	4.02691
PT	L3C	1.938	1.575	2.301	6.94485
PT	L4R	1.276	0.932	1.619	3.58228
PT	L4C	2.040	1.698	2.382	7.69061
PT	L5R	1.948	1.607	2.289	7.01464
PT	L5-L6	2.378	2.038	2.718	10.78331
PT	L6-L7	2.143	1.802	2.483	8.52497
PT	L7-S1	2.082	1.742	2.423	8.02049
PT	S1-S2	2.148	1.785	2.510	8.56771
MG	L3C	0.820	0.400	1.239	2.27050
MG	L4R	0.773	0.381	1.165	2.16626
MG	L4C	0.916	0.526	1.305	2.49927
MG	L5R	0.756	0.368	1.144	2.12974
MG	L5-L6	1.096	0.708	1.483	2.99217
MG	L6-L7	0.950	0.563	1.338	2.58571
MG	L7-S1	1.092	0.705	1.479	2.98023
MG	S1-S2	1.094	0.688	1.499	2.98619
TA	L3C	1.733	1.370	2.096	5.65760
TA	L4R	1.684	1.341	2.027	5.38706
TA	L4C	2.734	2.392	3.076	15.39434
TA	L5R	1.740	1.399	2.081	5.69734
TA	L5-L6	1.967	1.627	2.308	7.14920
TA	L6-L7	1.932	1.592	2.273	6.90330

TA	L7-S1	1.996	1.656	2.337	7.35956
TA	S1-S2	2.135	1.773	2.498	8.45705

Table 6. Transected Long Latency Latency (12-30 ms) Confidence Intervals. Each row outlines the mean log RIEMG, lower and upper bounds of the 95% confidence interval, as well as the raw mean RIEMG for each muscle and stimulation position for 8 decerebrate cats combined. Means and 95% confidence intervals determined by fitting generalized linear mixed models on log transformed outcomes for all animals, with fixed effects of muscle, stim position and the interaction between muscle and stim position, as well as a random intercept of animal and muscle within animal effect. The mean log RIEMG values for each muscle and stimulation location are displayed in Figure 12B and Figure 13. In Figure 13, the confidence interval lower and upper bounds are displayed as error bars. The raw RIEMG measurements are displayed in Figure 12A.

Comparison of Intact and Transected States

After building a map of the transected cord on its own to understand its individual trends, we then compared the transected map to the intact map. The goal was to understand if transection had a significant impact on the rostrocaudal organization of the lumbosacral cord in the decerebrate cat. This comparison was made for the three windows previously analyzed: short latency (4-12 ms), long latency Window I (12-30 ms), and long latency Window II (30-400 ms).

Comparison of Short Latency Responses. Figure 14 illustrates the similarities and differences between the intact and transected short latency responses. For most muscles at most locations, there was no significant difference between the intact and transected responses. The muscles and locations that did have a significant difference between the intact and transected responses are as follows: SR, PT, TA, LG, and BF. SR, TA, and BF all had significantly different responses at one location outside the motor pool. PT had significantly different responses at two locations within the motor pool and one location outside the motor pool. BF had significantly different responses at one location within the motor pool and three locations outside the motor pool.

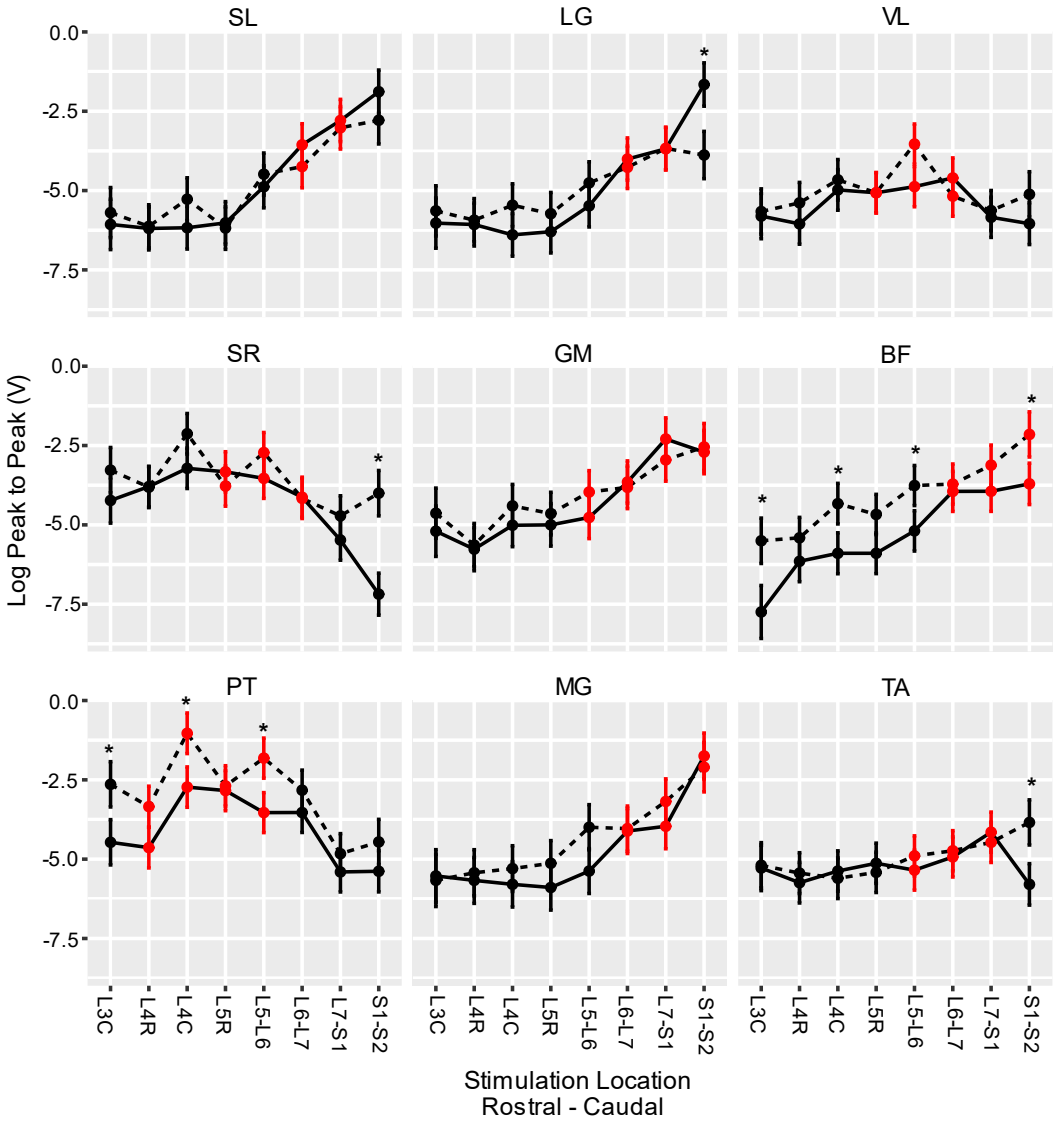

Figure 14. Comparison of Intact and Transected Muscle Maps of Log Transformed Short Latency Response. Each subplot shows a different hindlimb muscle's mean peak to peak responses across eight decerebrate cats: both in the intact cord (solid line) and the transected cord (dotted line). Intact and transected responses were measured within the same animal: the protocol was performed on the intact cord, and then the cord was transected, and the protocol was repeated. Electrical stimulation was applied to the lumbosacral cord at locations indicated on the x axis (L3C through S1-S2) and the peak to peak response was measured from 4-12 ms using EMG in nine hindlimb muscles. Error bars indicate 95% confidence intervals; lower and upper bounds are listed in Table 1 for the intact and Table 4 for the transected. The intact and transected responses are significantly different if their 95% confidence intervals do not overlap at a particular location; this is indicated by a star. To determine significance, generalized linear mixed models were fit on log transformed outcomes for all animals, with fixed effects of muscle, stim position and the interaction between muscle and stim position, as well as a random intercept of animal and muscle within animal effect. ANOVA was conducted to test the significance of the interaction term. The

anatomical locations of the motor pools are highlighted in red. This figure illustrates how the intact and transected responses are similar.

Comparison of Long Latency Window I Responses. Figure 15 illustrates how the intact and transected responses compare for the first window of the long latency response (12-30 ms). For most muscles at most locations, there was no significant difference between the intact and transected responses. The muscles and locations that did have a significant difference between the intact and transected responses are as follows: SR, PT, TA, SL, and LG. SR, PT, SL, and LG all had significantly different responses at one location outside the motor pool. TA had significantly different responses at two locations within the motor pool.

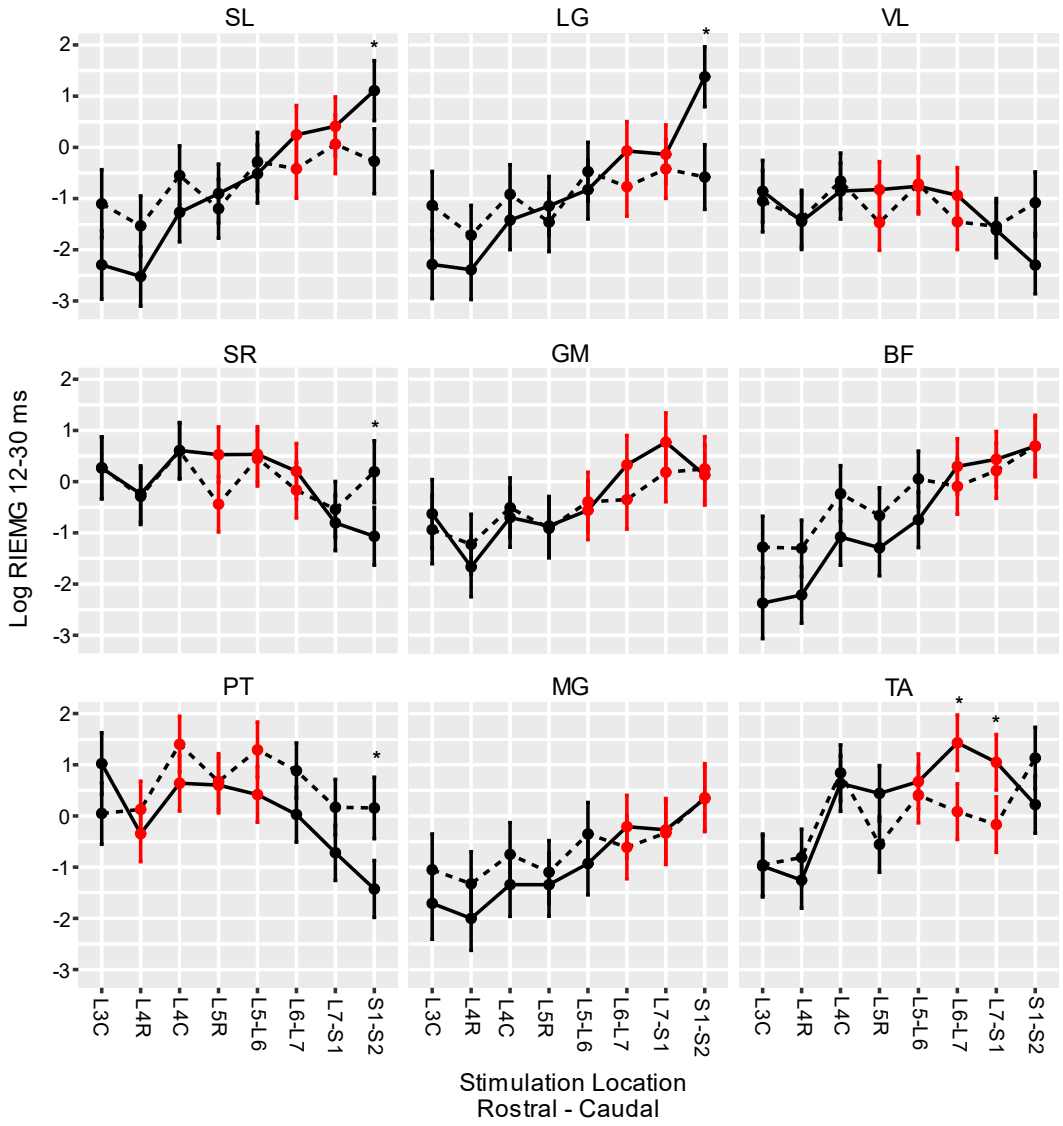

Figure 15. Comparison of Intact and Transected Muscle Maps of Log Transformed Long Latency (12-30 ms) Response. Each subplot shows a different hindlimb muscle's mean RIEMG responses across eight decerebrate cats: both in the intact cord (solid line) and the transected cord (dotted line). Intact and transected responses were measured within the same animal: the protocol was performed on the intact cord, and then the cord was transected, and the protocol was repeated. Electrical stimulation was applied to the lumbosacral cord at locations indicated on the x axis (L3C through S1-S2) and the RIEMG response was measured from 12-30 ms using EMG in nine hindlimb muscles. Error bars indicate 95% confidence intervals; lower and upper bounds are listed in Table 2 for the intact and Table 5 for the transected. The intact and transected responses are significantly different if their 95% confidence intervals do not overlap at a particular location; this is indicated by a star. To determine significance, generalized linear mixed models were fit on log transformed outcomes for all animals, with fixed effects of muscle, stim position and the interaction between muscle and stim position, as well as a random intercept of animal and muscle within animal effect. ANOVA was conducted to test the significance of the interaction term. The anatomical

locations of the motor pools are highlighted in red. This figure illustrates how the intact and transected responses are similar.

Comparison of Long Latency Window II Responses. Figure 16 compares the intact and transected responses for the second window of the long latency response (30-400 ms). For most muscles—PT, TA, VL, SL, LG, and MG—there was a significant difference between the intact and transected responses. SL and LG both had significant different responses at two locations within the motor pool and two locations outside the motor pool. MG had significantly different responses at one location within the motor pool. PT and VL had significantly different responses at one location each outside the motor pool, and TA had significantly different responses at two locations outside the motor pool.

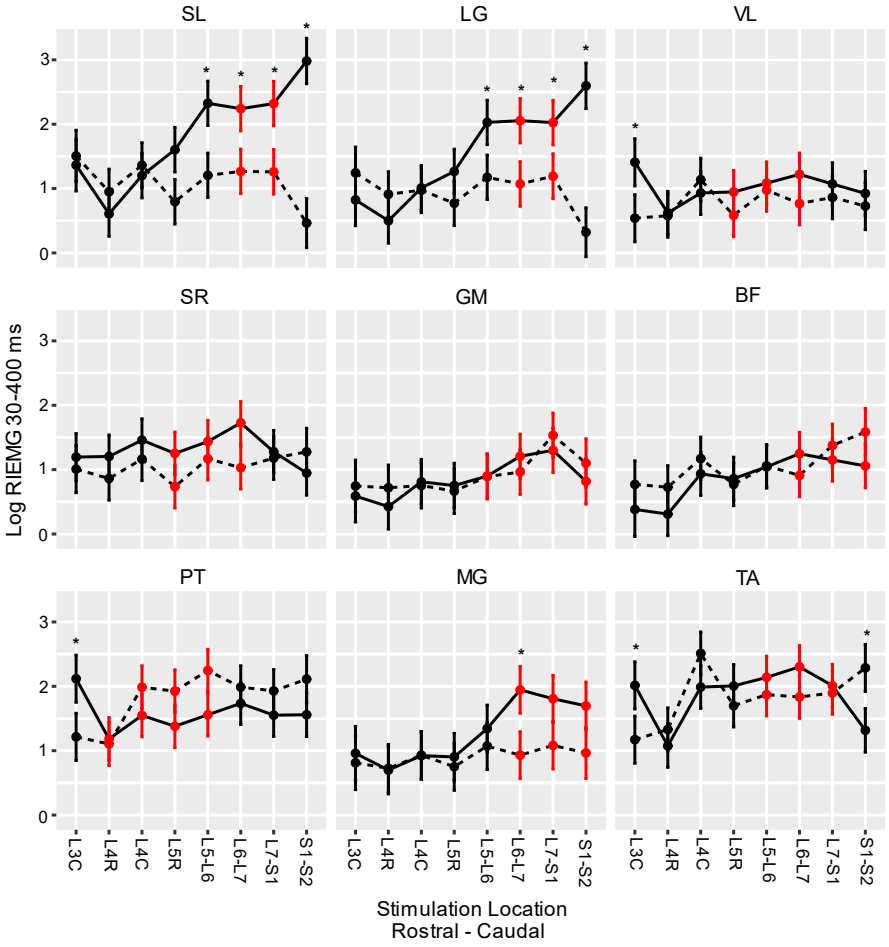

Figure 16. Comparison of Intact and Transected Muscle Maps of Log Transformed Long Latency (30-400 ms) Response. Each subplot shows a different hindlimb muscle's mean RIEMG responses across eight decerebrate cats: both in the intact cord (solid line) and the transected cord (dotted line). Intact and transected responses were measured within the same animal: the protocol was performed on the intact cord, and then the cord was transected, and the protocol was repeated. Electrical stimulation was applied to the lumbosacral cord at locations indicated on the x axis (L3C through S1-S2) and the RIEMG response was measured from 30-400 ms using EMG in nine hindlimb muscles. Error bars indicate 95% confidence intervals; lower and upper bounds are listed in Table 3 for the intact and Table 6 for the transected. The intact and transected responses are significantly different if their 95% confidence intervals do not overlap at a particular location; this is indicated by a star. To determine significance, generalized linear mixed models were fit on log transformed outcomes for all animals, with fixed effects of muscle, stim position and the interaction between muscle and stim position, as well as a random intercept of animal and muscle within animal effect. ANOVA was conducted to test the significance of the interaction term. The anatomical locations of the motor pools are highlighted in red. This figure illustrates how the intact and transected responses are divergent in this later window.

Discussion

The intact decerebrate cat lumbosacral cord had been previously mapped using subdural stimulation (See Chapter 2), so the objective of this study was to map the transected cord with subdural stimulation and observe how it compares to the intact map. To do so, electrical stimulation was applied at seven spinal locations ranging from L3-S2 while intramuscular EMG was recorded in nine hindlimb muscles. Our first main result is a map of the rostrocaudal distribution of hindlimb EMG activity in response to subdural stimulation in the transected lumbosacral cord of the decerebrate cat. Our second main result is a comparison of the rostrocaudal maps of the intact cord and transected cord.

Rostrocaudal Organization of the Transected Cord

For the short latency window, responses of muscles with more rostrally situated motor pools (SR, PT) tended to have significantly higher responses at more rostral stimulation locations compared to other locations, while the rest of the muscles with more caudally situated motor pools tended to have significantly higher responses at more caudal stimulation locations compared to other locations. TA did not show any differences in response based on stimulation location. SR, PT, SL, LG, and BF all had significant responses at locations neighboring but outside the motor pool compared to other locations. Otherwise, short latency responses largely aligned with the motor pool. This coincides with findings in the intact cord (using intraspinal stimulation in the anesthetized cat) showing that functional responses largely align with the anatomical map (Mushahwar et al. 2002; Mushahwar and Horch 1998b, 2000; Saigal et al. 2004; Toossi et al. 2019; Vanderhorst and Holstege 1997; Yakovenko et al. 2002).

For the long latency 12-30 ms window in the transected cord, responses were less aligned with the motor pools. For one, SR, VL, LG, MG, and GM all showed no significant difference in

responses between stimulation locations, meaning that there was no rostrocaudal distribution of responses in these muscles, including over the motor pools. TA had significant responses at two locations outside its motor pool compared to other locations, and no significantly different responses within the motor pool compared to other locations. For the other muscles—PT and SL—there were significantly higher responses at 1-2 locations within the motor pool compared to other locations. For the long latency 30-400 ms window in the transected cord, six of the nine muscles—SR, VL, SL, LG, MG, BF-- showed no significant difference in responses between stimulation locations, so did not have a rostrocaudal distribution. TA had a significantly different response at one location outside its motor pool compared to other locations. PT and GM had a significantly different response at one location in the motor pool compared to other locations. In all, the long latency responses were generally more broad than the anatomical motor pools. This suggests that stimulation-induced action potentials propagated rostrally and caudally, activating afferents, interneurons, and motoneurons along the lumbosacral cord, culminating in activating multiple motor pools and muscles at later latencies. This finding aligns with previous work showing at polysynaptic latencies, many muscles showed responses to spinal stimulation (Gaunt et al. 2006).

Comparison of Intact and Transected Rostrocaudal Distributions

This is the first study to directly compare the stimulation maps of the lumbosacral cord before and after transection. Statistically, transection was found to have a significant effect on motor output in response to stimulation. When looking at the individual muscle maps for the short and long latency responses, however, there is much overlap in the responses. For the short latency responses, only five of the nine muscles showed any difference between the intact and transected responses, and only at a single stimulation location at that. The types of muscles that had these difference varied in their functions as well-- hip flexors (SR and PT), knee flexor (BF), ankle

extensor (LG), and ankle flexor (TA). Notably, BF showed differences at the most stimulation locations that ranged across the rostrocaudal spectrum, which is fitting with research showing bias towards activation of flexor muscles after spinal cord injury (Hofstoetter et al. 2015; McPherson et al. 2015). For the long latency 12-30 ms response, only three out of nine muscles showed a difference between the intact and transected responses, and also only at one location each. These muscles also varied from hip flexors to ankle extensors. The long latency 30-400 ms response was distinct-- six out of the nine muscles had a significant difference between the intact and transected responses, and half of those muscles showed a difference across multiple stimulation locations. SL and LG, in congruence with their motor pools, had divergent responses with more caudal stimulation locations. The divergence was not entirely aligned with the motor pool, as caudal stimulation locations outside the motor pool showed differences too. MG, also had divergence over its caudal motor pool, although only at one of the stimulation locations. The other three muscles—PT, VL, and TA—had differences between intact and transected responses outside of their motor pools.

In all, only a few muscles showed a significant difference in response to stimulation at multiple locations, and even that was only in the longest latency window. As this is the first instance of mapping the lumbosacral cord of the cat after transection, there is not substantial previous research to compare with. A single study has looked at classifying motor output using electrical stimulation in the acute transected cord of the cat (Mushahwar et al. 2004). This study found that after transection, intraspinal stimulation changed significantly and evoked predominantly flexion movements compared to very few extensor movements, suggesting that motor output depended significantly on descending input (Mushahwar et al. 2004). We did not find a significant change after transection, nor a bias towards activation of extensor muscles. A second previous study demonstrated that in the decerebrate, transected cat, the receptive fields of hindlimb motor pools

broadened compared to those in the intact cat (Hyngstrom et al. 2008). This suggests that with the loss of descending control over afferent pathways, these converging pathways become disinhibited and contribute to additional limb responses (Hyngstrom et al. 2008). Given these previous findings, we expected to find the intact and transected maps to significantly differ, and for the transected map to be broader. Instead, we found the intact and transected maps to largely overlap. This could be due to the fact that the intact maps were already fairly broad due to the decreased specificity of subdural stimulation, so that any further broadening with transection was not significant. Physiologically, in the intact cord, the lower resolution of subdural stimulation may have activated afferents across multiple motor pools at a single stimulation site. Following transection, the loss of supraspinal input may have disinhibited convergent afferent pathways, leading to the activation of afferents across multiple motor pools, but it's possible that this did not lead to a significant change in afferents and motor pools activated with the already broad subdural stimulation in the intact cord. In addition, that there was more difference between the maps as latency increased points to the polysynaptic pathways being more greatly impacted by transection than monosynaptic pathways. One potential explanation is that the disinhibition of Ia afferents did not significantly change the monosynaptic pathways activated as described previously, but did activate a significantly broader range of polysynaptic pathways. As the loss of supraspinal monoaminergic input tends to increase the excitability of interneurons, this may have led to more interneuronal pathways activated and then more motor pools activated at later latencies by stimulation at a single site. In all, while previous studies suggested that the transected map would be significantly broader than the intact maps, it's possible that the type of stimulation and pathways activated did not alter the maps significantly, save for at later latencies.

Comparison of Intact and Transected Stimulation Thresholds

We also looked at stimulation threshold to understand any changes occurring in the cord. Stimulation threshold is defined as the stimulation amplitude that evoked a response that was ten times greater than baseline. A more depolarized motoneuron would be expected to require less stimulation current to bring it to threshold and fire an action potential. A lower stimulation threshold signals a more excitable state. The transected cord demonstrated lower stimulation thresholds than the intact cord, indicating the transected cord has greater excitability. When spinal cord injury severs descending monoaminergic input to below the level of injury, interneurons become disinhibited (Heckman et al. 2009b). Lower stimulation thresholds in the transected cord suggests that when this disinhibition occurs, there is a net depolarization in the acute cord, leading to greater excitability and less stimulation current needed to reach threshold.

Limitations

A limitation of this study is the use of a single stimulation protocol. Varying the duration, frequency, and amplitude of stimulation may activate different neural pathways that alter the maps in the intact and transected cord. It is possible that stimulation activating different pathways may result in a different intact and transected maps, as those pathways may be more effected by the loss of supraspinal input than those activated by the current protocol. Second, some muscles did show significant differences between the maps, especially at longer latencies. It's possible that testing a wider range of hindlimb muscles may have captured more muscles with significant differences.

Clinical Relevance

Electrical spinal cord stimulation is an emerging tool in the treatment of movement impairments after spinal cord injury (Angeli et al. 2014; Ievins and Moritz 2017; Nagel et al. 2017). Understanding how the location of stimulation effects motor output is an important step in improving the efficacy of this treatment. However, studies mapping the lumbosacral cord have

only been performed in the intact cord of the cat, and not in the cord following spinal cord injury (Saigal et al. 2004; Yakovenko et al. 2002). Thus, the results of this study better inform the placement of spinal stimulators in the treatment of spinal cord injury. Additionally, this study builds a map using subdural stimulation, a type of electrical stimulation that shows promise as it may be more precise than epidural or transcutaneous stimulation, but less invasive than intraspinal stimulation (Anderson et al. 2019; Ievins and Moritz 2017). By increasing our understanding of subdural stimulation, this study improves its efficacy as a potential treatment for spinal cord injury.

Conclusions

This study is the first to develop a rostrocaudal map of the lumbosacral cord in the cat after spinal cord injury, and the first to compare how this transected map relates to the intact map. We found that overall, transection did not have a significant impact on the rostrocaudal organization on the lumbosacral cord. Looking at individual muscles, some muscles showed significant differences between the intact and transected states, particularly at longer latencies. These findings indicate that we may be able to rely upon the intact rostrocaudal map of the cord to inform the placement of spinal stimulators after spinal cord injury. However, further research is needed to understand if different types of stimulation—epidural, intraspinal, etc.—also do not see a significant change in rostrocaudal mapping after transection.

IV. Concluding Remarks

Spinal cord injury (SCI) impacts an estimated 282,000 people in the United States and can lead to impairments in mobility and even paralysis (Ievins and Moritz 2017). There is a great need for research into developing rehabilitation practices and tools to improve mobility for individuals with SCI. The spinal cord is an excellent therapeutic target as spinal networks below the level of the injury largely remain intact even as SCI disrupts the connection between supraspinal and spinal neurons (Musienko et al. 2012). Electrical stimulation targeting these intact networks shows therapeutic promise to help restore sensorimotor function. Advances in spinal electrical stimulation over the past few decades have produced functional improvement in locomotion, breathing, bladder function, and pain management (Angeli et al. 2014; Jilge et al. 2004; Martens and Heesakkers 2011; Nagel et al. 2017; Toossi et al. 2019). But more research is still needed to improve the efficacy of spinal electrical stimulation as a treatment for SCI, particularly for restoring or improving individuals' ability to walk. Developing a functional map of the spinal cord with subdural stimulation is essential to its development as a clinical tool in the treatment of paralysis after spinal cord injury and other disorders.

The goal of the first paper was to build a functional map of the intact spinal cord using subdural stimulation in the decerebrate cat. Previous research had built maps using intraspinal stimulation in the anesthetized cat, so this would be the first map built using subdural stimulation and in the decerebrate cat. Data from eight cats showed that during the short latency window, the most rostrally responding muscles were the hip flexor SR, the hip adductor PT, and the knee extensor VL; the remainder of muscles studied responded to stimulation applied more caudally. All muscles had functional activity that aligned with their anatomical pools, although to different extents. During the long latency window, the most rostrally responding muscles were the hip flexor SR, the hip adductor PT, and the knee extensor VL; the ankle flexor TA responded to stimulation both more rostrally and caudally; and the remainder of muscles studied responded to stimulation

applied more caudally. All muscles had functional activity that aligned with their anatomical pools, with a trend towards the functional maps broadening at longer latencies. These findings generally aligned with previous findings using intraspinal stimulation, although were more broad. This is likely because subdural stimulation likely does not activate motoneurons directly but instead activates Ia afferents, potentially from multiple motor pools or traveling through multiple spinal segments (Capogrosso et al. 2013; Gaunt et al. 2006).

The goal of the second paper was to build a functional map of the transected spinal cord using subdural stimulation in the decerebrate cat, and then compare this to the map of the intact cord. Only a single previous study has looked at classifying motor output using electrical stimulation in the acute transected cord of the cat, and that was with intraspinal stimulation (Mushahwar et al. 2004). This study found that the map changed significantly after transection (Mushahwar et al. 2004). Other research had also indicated that the maps may broaden after transection (Hyngstrom et al. 2008). However, we found the transected maps to be generally in alignment with the intact maps. In all, only a few muscles showed a significant difference in response to stimulation at multiple locations, and even that was only in the longest latency window. This could be due to the fact that the intact maps were already fairly broad due to the decreased specificity of subdural stimulation, so that any further broadening with transection was not significant. Additionally, because the difference increased with latency, one potential explanation is that the disinhibition of Ia afferents did not significantly change the monosynaptic pathways activated as described previously, but did activate a significantly broader range of polysynaptic pathways.

The results of these two studies increase our understanding of the functional responses of the lumbosacral spinal cord and better inform the placement of spinal stimulators in the treatment of spinal cord injury. Understanding how the location of stimulation effects motor output

is an important step in improving the efficacy of this treatment. Additionally, this study builds a map using subdural stimulation, a type of electrical stimulation that shows promise as it may be more precise than epidural or transcutaneous stimulation, but less invasive than intraspinal stimulation (Anderson et al. 2019; Ievins and Moritz 2017). By increasing our understanding of subdural stimulation, this study improves its efficacy as a potential treatment for spinal cord injury.

V. References

Anderson DJ, **Kipke DR**, **Nagel SJ**, **Lempka SF**, **Machado AG**, **Holland MT**, **Gillies GT**, **Howard MA**, **Wilson S**. Intradural Spinal Cord Stimulation: Performance Modeling of a New Modality. *Front Neurosci* 13: 253, 2019.

Angeli CA, **Boakye M**, **Morton RA**, **Vogt J**, **Benton K**, **Chen Y**, **Ferreira CK**, **Harkema SJ**. Recovery of Over-Ground Walking after Chronic Motor Complete Spinal Cord Injury. *N Engl J Med* 379: 1244–1250, 2018.

Angeli CA, **Edgerton VR**, **Gerasimenko YP**, **Harkema SJ**. Altering spinal cord excitability enables voluntary movements after chronic complete paralysis in humans. *Brain* 137: 1394–1409, 2014.

AnonFacts and Figures at a Glance [Online]. National Spinal Cord Injury Statistical Center, University of Alabama at Birmingham2020.https://www.nscisc.uab.edu/Public/Facts%20and%20Figures%202020.pdf [6 Apr. 2022].

Boger AS, **Bhadra N**, **Gustafson KJ**. High frequency sacral root nerve block allows bladder voiding. *Neurourol Urodyn* 31: 677–682, 2012.

Bourbeau D, **Creasey G**, **French J**, **Grill WM**, **Howley S**, **Krassioukov A**, **Moritz C**, **Santacruz B**, **Thor K**, **Wheeler T**. A roadmap for advancing neurostimulation approaches for bladder and bowel function after spinal cord injury. *Spinal Cord* 58: 1227–1232, 2020.

Brown AG. Organization in the Spinal Cord: the Anatomy and Physiology of Identified Neurones [Online]. Springer London.https://doi.org/10.1007/978-1-4471-1305-8 [9 Aug. 2021].

Campos RJ, **Dimitrijevic MM**, **Faganel J**, **Sharkey PC**. Clinical evaluation of the effect of spinal cord stimulation on motor performance in patients with upper motor neuron lesions. *Appl Neurophysiol* 44: 141–151, 1981.

Capogrosso M, **Milekovic T**, **Borton D**, **Wagner F**, **Moraud EM**, **Mignardot J-B**, **Buse N**, **Gandar J**, **Barraud Q**, **Xing D**, **Rey E**, **Duis S**, **Jianzhong Y**, **Ko WKD**, **Li Q**, **Detemple P**, **Denison T**, **Micera S**, **Bezard E**, **Bloch J**, **Courtine G**. A brain–spine interface alleviating gait deficits after spinal cord injury in primates. *Nature* 539: 284–288, 2016.

Capogrosso M, **Wenger N**, **Raspopovic S**, **Musienko P**, **Beauparlant J**, **Bassi Luciani L**, **Courtine G**, **Micera S**. A Computational Model for Epidural Electrical Stimulation of Spinal Sensorimotor Circuits. *J Neurosci* 33: 19326–19340, 2013.

Carhart MR, **He J**, **Herman R**, **D'Luzansky S**, **Willis WT**. Epidural spinal-cord stimulation facilitates recovery of functional walking following incomplete spinal-cord injury. *IEEE Trans Neural Syst Rehabil Eng* 12: 32–42, 2004.

Cook A, **Taylor J**, **Nidzgorski F**. Functional stimulation of the spinal cord in multiple sclerosis. *J Med Eng Technol* 3: 18–23, 1979.

Cook A, **Weinstein S**. Chronic dorsal column stimulation in multiple sclerosis. Preliminary report. *NY State J Med* 73: 2868–2872, 1973.

Cruce WLR. The anatomical organization of hindlimb motoneurons in the lumbar spinal cord of the frog, Rana catesbiana. *J Comp Neurol* 153: 59–76, 1974.

Danner SM, **Krenn M**, **Hofstoetter US**, **Toth A**, **Mayr W**, **Minassian K**. Body Position Influences Which Neural Structures Are Recruited by Lumbar Transcutaneous Spinal Cord Stimulation. *PLOS ONE* 11: e0147479, 2016.

Darrow D, **Balser D**, **Netoff TI**, **Krassioukov A**, **Phillips A**, **Parr A**, **Samadani U**. Epidural Spinal Cord Stimulation Facilitates Immediate Restoration of Dormant Motor and Autonomic Supraspinal Pathways after Chronic Neurologically Complete Spinal Cord Injury. *J Neurotrauma* 36: 2325–2336, 2019.

Dimitrijevic MM, **Dimitrijevic MR**, **Illis LS**, **Nakajima K**, **Sharkey PC**, **Sherwood AM**. Spinal Cord Stimulation for the Control of Spasticity in Patients with Chronic Spinal Cord Injury: I. Clinical Observations. *Cent Nerv Syst Trauma* 3: 129–143, 1986.

Dimitrijevic MR, **Gerasimenko Y**, **Pinter MM**. Evidence for a Spinal Central Pattern Generator in Humansa. *Ann N Y Acad Sci* 860: 360–376, 1998.

Dooley DM. Spinal cord stimulation. *AORN J* 23: 1209–1212, 1976.

Edgerton VR, **Courtine G**, **Gerasimenko YP**, **Lavrov I**, **Ichiyama RM**, **Fong AJ**, **Cai LL**, **Otoshi CK**, **Tillakaratne NJK**, **Burdick JW**, **Roy RR**. Training locomotor networks. *Brain Res Rev* 57: 241–254, 2008.

Gad P, **Choe J**, **Shah P**, **Garcia-Alias G**, **Rath M**, **Gerasimenko Y**, **Zhong H**, **Roy RR**, **Edgerton VR**. Sub-threshold spinal cord stimulation facilitates spontaneous motor activity in spinal rats. *J NeuroEngineering Rehabil* 10: 108, 2013.

Gad PN, **Roy RR**, **Zhong H**, **Lu DC**, **Gerasimenko YP**, **Edgerton VR**. Initiation of Bladder Voiding with Epidural Stimulation in Paralyzed, Step Trained Rats. *PLoS ONE* 9: 1–9, 2014.

Gaunt RA, **Prochazka A**, **Mushahwar VK**, **Guevremont L**, **Ellaway PH**. Intraspinal Microstimulation Excites Multisegmental Sensory Afferents at Lower Stimulus Levels Than Local α-Motoneuron Responses. *J Neurophysiol* 96: 2995–3005, 2006.

Gerasimenko Y, **Gorodnichev R**, **Moshonkina T**, **Sayenko D**, **Gad P**, **Reggie Edgerton V**. Transcutaneous electrical spinal-cord stimulation in humans. *Ann Phys Rehabil Med* 58: 225–231, 2015a.

Gerasimenko YP, **Lu DC**, **Modaber M**, **Zdunowski S**, **Gad P**, **Sayenko DG**, **Morikawa E**, **Haakana P**, **Ferguson AR**, **Roy RR**, **Edgerton VR**. Noninvasive Reactivation of Motor Descending Control after Paralysis. *J NEUROTRAUMA* 32: 1968–1980, 2015b.

Hachmann JT, **Yousak A**, **Wallner JJ**, **Gad PN**, **Edgerton VR**, **Gorgey AS**. Epidural spinal cord stimulation as an intervention for motor recovery after motor complete spinal cord injury. *J Neurophysiol* 126: 1843–1859, 2021.

Hamid S, **Hayek R**. Role of electrical stimulation for rehabilitation and regeneration after spinal cord injury: an overview. *Eur Spine J* 17: 1256–1269, 2008.

Harkema S, **Gerasimenko Y**, **Hodes J**, **Burdick J**, **Angeli C**, **Chen Y**, **Ferreira C**, **Willhite A**, **Rejc E**, **Grossman RG**, **Edgerton VR**. Effect of Epidural stimulation of the lumbosacral spinal cord on voluntary movement, standing, and assisted stepping after motor complete paraplegia: a case study. *Lancet* 377: 1938–1947, 2011.

Harvey PJ, **Li X**, **Li Y**, **Bennett DJ**. Endogenous Monoamine Receptor Activation Is Essential for Enabling Persistent Sodium Currents and Repetitive Firing in Rat Spinal Motoneurons. *J Neurophysiol* 96: 1171–1186, 2006.

Heckman CJ, **Johnson M**, **Mottram C**, **Schuster J**. Persistent inward currents in spinal motoneurons and their influence on human motoneuron firing patterns. *The Neuroscientist* 14: 264–275, 2008.

Heckman CJ, **Mottram C**, **Quinlan K**, **Theiss R**, **Schuster J**. Motoneuron excitability: The importance of neuromodulatory inputs. *Clin Neurophysiol* 120: 2040–2054, 2009a.

Heckman CJ, **Mottram C**, **Quinlan K**, **Theiss R**, **Schuster J**. Motoneuron excitability: The importance of neuromodulatory inputs. *Clin Neurophysiol* 120: 2040–2054, 2009b.

Herda TJ, **Ryan ED**, **Costa PB**, **Walter AA**, **Hoge KM**, **Uribe BP**, **McLagan JR**, **Stout JR**, **Cramer JT**. Acute effects of passive stretching and vibration on the electromechanical delay and musculotendinous stiffness of the plantar flexors. *Electromyogr Clin Neurophysiol* 50: 277–288, 2010.

Herman R, **He J**, **D'Luzansky S**, **Willis W**, **Dilli S**. Spinal cord stimulation facilitates functional walking in a chronic, incomplete spinal cord injured. *Spinal Cord* 40: 65–68, 2002.

Hochman S. Spinal Cord. *Curr Biol* 17: R950–R955, 2007.

Hofstoetter US, **Krenn M**, **Danner SM**, **Hofer C**, **Kern H**, **McKay WB**, **Mayr W**, **Minassian K**. Augmentation of Voluntary Locomotor Activity by Transcutaneous Spinal Cord Stimulation in Motor-Incomplete Spinal Cord-Injured Individuals. *Artif Organs* 39: E176–E186, 2015.

Hofstoetter US, **McKay WB**, **Tansey KE**, **Mayr W**, **Kern H**, **Minassian K**. Modification of spasticity by transcutaneous spinal cord stimulation in individuals with incomplete spinal cord injury. *J Spinal Cord Med* 37: 202–211, 2014.

Holinski BJ, **Mazurek KA**, **Everaert DG**, **Toossi A**, **Lucas-Osma AM**, **Troyk P**, **Etienne-Cummings R**, **Stein RB**, **Mushahwar VK**. Intraspinal microstimulation produces over-ground walking in anesthetized cats. *J Neural Eng* 13: 056016, 2016.

Holland MT, **Seaman SC**, **Woodroffe RW**, **Fredericks DC**, **Kovach CK**, **Gibson-Corley KN**, **Gillies GT**, **Howard MA**. In Vivo Testing of a Prototype Intradural Spinal Cord Stimulator in a Porcine Model. *World Neurosurg* 137: e634–e641, 2020.

Huang H, **He J**, **Herman R**, **Carhart MR**. Modulation effects of epidural spinal cord stimulation on muscle activities during walking. *IEEE Trans Neural Syst Rehabil Eng* 14: 14–23, 2006.

Hyngstrom A, **Johnson M**, **Schuster J**, **Heckman CJ**. Movement-related receptive fields of spinal motoneurones with active dendrites. *J Physiol* 586: 1581–1593, 2008.

Ievins A, **Moritz CT**. Therapeutic Stimulation for Restoration of Function After Spinal Cord Injury. *Physiology* 32: 391–398, 2017.

Imai Y, **Kusama T**. Distribution of the dorsal root fibers in the cat. An experimental study with the Nauta method. *Brain Res* 13: 338–359, 1969.

Ishizuka N, **Mannen H**, **Hongo T**, **Sasaki S**. Trajectory of group Ia afferent fibers stained with horseradish peroxidase in the lumbosacral spinal cord of the cat: Three dimensional reconstructions from serial sections. *J Comp Neurol* 186: 189–211, 1979.

Iwahara T, **Atsuta Y**, **Garcia-Rill E**, **Skinner RD**. Spinal cord stimulation-induced locomotion in the adult cat. *Brain Res Bull* 28: 99–105, 1992.

Jankowska E. Interneuronal relay in spinal pathways from proprioceptors. *Prog Neurobiol* 38: 335–378, 1992.

Jankowska E. Spinal interneuronal systems: identification, multifunctional character and reconfigurations in mammals. *J Physiol* 533: 31–40, 2001.

Jankowska E, **Edgley SA**. Functional subdivision of feline spinal interneurons in reflex pathways from group Ib and II muscle afferents; an update. *Eur J Neurosci* 32: 881–893, 2010.

Jankowska E, **Hammar I**, **Chojnicka B**, **Hedén CH**. Effects of monoamines on interneurons in four spinal reflex pathways from group I and/or group II muscle afferents. *Eur J Neurosci* 12: 701–714, 2000.

Jilge B, **Minassian K**, **Rattay F**, **Pinter MM**, **Gerstenbrand F**, **Binder H**, **Dimitrijevic MR**. Initiating extension of the lower limbs in subjects with complete spinal cord injury by epidural lumbar cord stimulation. *Exp Brain Res* 154: 308–326, 2004.

Kato K, **Nishihara Y**, **Nishimura Y**. Stimulus outputs induced by subdural electrodes on the cervical spinal cord in monkeys. *J Neural Eng* 17: 016044, 2020.

Kubo K, **Kanehisa H**, **Fukunaga T**. Effects of transient muscle contractions and stretching on the tendon structures in vivo. *Acta Physiol Scand* 175: 157–164, 2002.

Kubo K, **Kanehisa H**, **Kawakami Y**, **Fukunaga T**. Influence of static stretching on viscoelastic properties of human tendon structures in vivo. *J Appl Physiol* 90: 520–527, 2001.

Kumar K, **Bishop S**. Financial impact of spinal cord stimulation on the healthcare budget: a comparative analysis of costs in Canada and the United States: Clinical article. *J Neurosurg Spine* 10: 564–573, 2009.

Lee RH, **Heckman CJ**. Bistability in Spinal Motoneurons In Vivo: Systematic Variations in Rhythmic Firing Patterns. *J Neurophysiol* 80: 572–582, 1998.

Lu DC, **Edgerton VR**, **Modaber M**, **AuYong N**, **Morikawa E**, **Zdunowski S**, **Sarino ME**, **Sarrafzadeh M**, **Nuwer MR**, **Roy RR**, **Gerasimenko Y**. Engaging Cervical Spinal Cord Networks to Reenable Volitional Control of Hand Function in Tetraplegic Patients. *Neurorehabil Neural Repair* 30: 951–962, 2016.

Martens FMJ, **Heesakkers JPFA**. Clinical Results of a Brindley Procedure: Sacral Anterior Root Stimulation in Combination with a Rhizotomy of the Dorsal Roots. *Adv Urol* 1–7, 2011.

McPherson JG, **Miller RR**, **Perlmutter SI**. Targeted, activity-dependent spinal stimulation produces long-lasting motor recovery in chronic cervical spinal cord injury. *Proc Natl Acad Sci* 112: 12193–12198, 2015.

Mendell LM, **Sassoon EM**, **Wall PD**. Properties of synaptic linkage from long ranging afferents onto dorsal horn neurones in normal and deafferented cats. *J Physiol* 285: 299–310, 1978.

Meunier S, **Pierrot-Deseilligny E**, **Simonetta M**. Pattern of monosynaptic heteronymous Ia connections in the human lower limb. *Exp Brain Res* 96: 534–544, 1993.

Minassian K, **Hofstoetter US**, **Danner SM**, **Mayr W**, **Bruce JA**, **McKay WB**, **Tansey KE**. Spinal Rhythm Generation by Step-Induced Feedback and Transcutaneous Posterior Root Stimulation in Complete Spinal Cord–Injured Individuals. *Neurorehabil Neural Repair* 30: 233–243, 2016.

Minassian K, **Jilge B**, **Rattay F**, **Pinter MM**, **Binder H**, **Gerstenbrand F**, **Dimitrijevic MR**. Stepping-like movements in humans with complete spinal cord injury induced by epidural stimulation of the lumbar cord: electromyographic study of compound muscle action potentials. *Spinal Cord* 42: 401–416, 2004.

Mondello SE, **Kasten MR**, **Horner PJ**, **Moritz CT**. Therapeutic intraspinal stimulation to generate activity and promote long-term recovery. *Front Neurosci* 8, 2014.

Moritz CT, **Lucas TH**, **Perlmutter SI**, **Fetz EE**. Forelimb Movements and Muscle Responses Evoked by Microstimulation of Cervical Spinal Cord in Sedated Monkeys. *J Neurophysiol* 97: 110–120, 2007.

Moss CW, **Kilgore KL**, **Peckham PH**. A Novel Command Signal for Motor Neuroprosthetic Control. *Neurorehabil Neural Repair* 25: 847–854, 2011.

Mushahwar V. Spinal Cord Microstimulation Generates Functional Limb Movements in Chronically Implanted Cats. *Exp Neurol* 163: 422–429, 2000.

Mushahwar VK, **Aoyagi Y**, **Stein RB**, **Prochazka A**. Movements generated by intraspinal microstimulation in the intermediate gray matter of the anesthetized, decerebrate, and spinal cat. *Can J Physiol Pharmacol* 82: 702–714, 2004.

Mushahwar VK, **Gillard DM**, **Gauthier MJA**, **Prochazka A**. Intraspinal micro stimulation generates locomotor-like and feedback-controlled movements. *IEEE Trans Neural Syst Rehabil Eng* 10: 68–81, 2002.

Mushahwar VK, **Horch KW**. Selective activation and graded recruitment of functional muscle groups through spinal cord stimulation. *Ann N Y Acad Sci* 860: 531–535, 1998a.

Mushahwar VK, **Horch KW**. Selective Activation and Graded Recruitment of Functional Muscle Groups through Spinal Cord Stimulation. *Ann N Y Acad Sci* 860: 531–535, 1998b.

Mushahwar VK, **Horch KW**. Selective activation of muscle groups in the feline hindlimb through electrical microstimulation of the ventral lumbo-sacral spinal cord. *IEEE Trans Rehabil Eng* 8: 11–21, 2000.

Musienko P, **Heutschi J**, **Friedli L**, **den Brand R van**, **Courtine G**. Multi-system neurorehabilitative strategies to restore motor functions following severe spinal cord injury. *Exp Neurol* 235: 100–109, 2012.

Nagel SJ, **Wilson S**, **Johnson MD**, **Machado A**, **Frizon L**, **Chardon MK**, **Reddy CG**, **Gillies GT**, **Howard MA**. Spinal Cord Stimulation for Spasticity: Historical Approaches, Current Status, and Future Directions. *Neuromodulation Technol Neural Interface* 20: 307–321, 2017.

Nichols TR, **Cope TC**, **Abelew TA**. 8 Rapid Spinal Mechanisms of Motor Coordination. *Exerc Sport Sci Rev* 27: 255–284, 1999.

Nishimura Y, **Perlmutter SI**, **Fetz EE**. Restoration of upper limb movement via artificial corticospinal and musculospinal connections in a monkey with spinal cord injury. *Front Neural Circuits* 7, 2013.

Peña Pino I, **Hoover C**, **Venkatesh S**, **Ahmadi A**, **Sturtevant D**, **Patrick N**, **Freeman D**, **Parr A**, **Samadani U**, **Balser D**, **Krassioukov A**, **Phillips A**, **Netoff TI**, **Darrow D**. Long-Term Spinal Cord Stimulation After Chronic Complete Spinal Cord Injury Enables Volitional Movement in the Absence of Stimulation. *Front Syst Neurosci* 14: 35, 2020.

Rasmussen S, **Chan AK**, **Goslow Jr. GE**. The cat step cycle: electromyographic patterns for hindlimb muscles during posture and unrestrained locomotion. 155: 253–269, 1978.

Rejc E, **Angeli C**, **Harkema S**. Effects of Lumbosacral Spinal Cord Epidural Stimulation for Standing after Chronic Complete Paralysis in Humans. *PLOS ONE* 10: e0133998, 2015.

Rejc E, **Angeli CA**, **Atkinson D**, **Harkema SJ**. Motor recovery after activity-based training with spinal cord epidural stimulation in a chronic motor complete paraplegic. *Sci Rep* 7: 13476, 2017a.

Rejc E, **Angeli CA**, **Bryant N**, **Harkema SJ**. Effects of Stand and Step Training with Epidural Stimulation on Motor Function for Standing in Chronic Complete Paraplegics. *J Neurotrauma* 34: 1787–1802, 2017b.

Romanes GJ. The motor cell columns of the lumbo-sacral spinal cord of the cat. *J Comp Neurol* 94: 313–363, 1951.

Romanes GJ. The Motor Pools of the Spinal Cord. In: *Progress in Brain Research*. Elsevier, p. 93–119.

Ryan ED, **Beck TW**, **Herda TJ**, **Hull HR**, **Hartman MJ**, **Costa PB**, **Defreitas JM**, **Stout JR**, **Cramer JT**. The time course of musculotendinous stiffness responses following different durations of passive stretching. *J Orthop Sports Phys Ther* 38: 632–639, 2008.

Saigal R, **Renzi C**, **Mushahwar VK**. Intraspinal microstimulation generates functional movements after spinal-cord injury. *IEEE Trans Neural Syst Rehabil Eng* 12: 430–440, 2004.

Sharpe AN, **Jackson A**. Upper-limb muscle responses to epidural, subdural and intraspinal stimulation of the cervical spinal cord. *J Neural Eng* 11: 016005, 2014.

Shealy CN, **Mortimer JT**, **Reswick JB**. Electrical Inhibition of Pain by Stimulation of the Dorsal Columns: Preliminary Clinical Report. *Anesth Analg* 46: 489???491, 1967a.

Shealy CN, **Taslitz N**, **Mortimer T**, **Becker DP**. Electrical Inhibition of Pain: Experimental Evaluation. *Anesth Analg-Curr Res* 46: 299–305, 1967b.

Sherrington CS. Notes on the Arrangement of some Motor Fibres in the Lumbo-Sacral Plexus. *J Physiol* 13: 621-772.17, 1892.

Silva NA, **Sousa N**, **Reis RL**, **Salgado AJ**. From basics to clinical: A comprehensive review on spinal cord injury. *Prog Neurobiol* 114: 25–57, 2014.

Silverman J, **Garnett NL**, **Giszter SF**, **Heckman CJ**, **Kulpa-Eddy JA**, **Lemay MA**, **Perry CK**, **Pinter M**. Decerebrate mammalian preparations: unalleviated or fully alleviated pain? A review and opinion. *Contemp Top Lab Anim Sci* 44: 34–36, 2005.

Taylor DC, **Brooks DE**, **Ryan JB**. Viscoelastic characteristics of muscle: Passive stretching versus muscular contractions. *Med Sci Sports Exerc* 29: 1619–1624, 1997.

Thiriez C, **Gurruchaga J-M**, **Goujon C**, **Fénelon G**, **Palfi S**. Spinal Stimulation for Movement Disorders. *Neurotherapeutics* 11: 543–552, 2014.

Toossi A, **Everaert DG**, **Perlmutter SI**, **Mushahwar VK**. Functional organization of motor networks in the lumbosacral spinal cord of non-human primates. *Sci Rep* 9: 13539, 2019.

Vanderhorst VGJM, **Holstege G**. Organization of lumbosacral motoneuronal cell groups innervating hindlimb, pelvic floor, and axial muscles in the cat. *J Comp Neurol* 382: 46–76, 1997.

Vincent JA, **Gabriel HM**, **Deardorff AS**, **Nardelli P**, **Fyffe REW**, **Burkholder T**, **Cope TC**. Muscle proprioceptors in adult rat: mechanosensory signaling and synapse distribution in spinal cord. *J Neurophysiol* 118: 2687–2701, 2017.

Wall PD, **Werman R**. The physiology and anatomy of long ranging afferent fibres within the spinal cord. *J Physiol* 255: 321–334, 1976.

Waltz J. Spinal cord stimulation: a quarter century of development and investigation. A review of its development and effectiveness in 1,336 cases. *Stereotact Funct Neurosurg* 69: 288–299, 1997.

Yakovenko S, **Mushahwar V**, **VanderHorst V**, **Holstege G**, **Prochazka A**. Spatiotemporal Activation of Lumbosacral Motoneurons in the Locomotor Step Cycle. *J Neurophysiol* 87: 1542–1553, 2002.

Zimmermann JB, **Seki K**, **Jackson A**. Reanimating the arm and hand with intraspinal microstimulation. *J Neural Eng* 8: 054001, 2011.

Appendix

Impact of Voluntary Muscle Activation on Stretch Reflex Excitability

in Individuals with Hemiparetic Stroke

Abstract

Objective: To characterize how, following a stretch-induced attenuation, volitional muscle activation impacts stretch reflex activity in individuals with stroke.

Methods: A robotic device rotated the paretic elbow of individuals with hemiparetic stroke from 70° to 150°, and then back to 70° elbow flexion at an angular speed of 120°/s. This stretching sequence was repeated twenty times. Subsequently, participants volitionally activated their elbow musculature or rested. Finally, the stretching sequence was repeated another twenty times. The flexors' stretch reflex activity was quantified as the net torque measured at 135°.

Results: Data from fifteen participants indicated that the stretching sequence attenuated the flexion torque ($p<0.001$) and resting sustained the attenuation ($p=1.000$). Contrastingly, based on data from fourteen participants, voluntary muscle activation increased the flexion torque ($p<0.001$) to an initial pre-stretch torque magnitude ($p=1.000$).

Conclusions: Stretch reflex attenuation induced by repeated fast stretches may be nullified when individuals post-stroke volitionally activate their muscles. In contrast, resting may enable a sustained reflex attenuation if the individual remains relaxed.

Significance: Stretching is commonly implemented to reduce hyperactive stretch reflexes following a stroke. These findings suggest that stretch reflex accommodation arising from repeated fast stretching may be reversed once an individual volitionally moves their paretic arm.

Introduction

An estimated 20-40% of survivors of a stroke exhibit hyperactive stretch reflexes, or spasticity, defined as a position- and velocity-dependent resistance to muscle stretch (Lance, 1980; Li, 2017; McPherson et al., 2019; Sommerfeld et al., 2004; Urban et al., 2010; Wissel et al., 2010; Zorowitz et al., 2013). Hypertonia and associated spasticity are thought to originate from increased spinal motoneuron excitability (Brown, 1994; Li et al., 2014; Li, 2017; Li et al., 2019; McPherson et al., 2008; McPherson, McPherson, et al., 2018; Mottram et al., 2010) and are shown to impair mobility, posture, and hygiene (Sommerfeld et al., 2004; Wissel et al., 2010; Zorowitz et al., 2013). One common approach to reduce hyperactive stretch reflexes is to stretch the affected limb (Naro et al., 2017; Schmit et al., 2000; Triandafilou et al., 2011; Vecchio et al., 2017). For example, fast consecutive stretches fast enough to elicit stretch reflexes, as confirmed by surface electromyography (sEMG), have been shown to induce reflex accommodation when the limb is relaxed (Schmit et al., 2000). Even so, it remains unknown whether the reflex accommodation that arises from stretching is sustained once an individual volitionally activates their muscles.

Evidence indicates that subsequent volitional muscle activation may negate the stretch-induced accommodation. Previous work established that norepinephrine, which alters stretch reflex activity, increases in cats with volitional movement (Pavlenko & Kulichenko, 2003). Additional experiments in humans revealed that volitional muscle activation prior to and during a task amplifies stretch reflex responses (McPherson, McPherson, et al., 2018; McPherson, Stienen, et al., 2018). Combined, these findings indicate that volitional muscle activation increases stretch reflex activity (McPherson, McPherson, et al., 2018; McPherson, Stienen, et al., 2018; Pavlenko & Kulichenko, 2003). Even so, the question remains whether volitional muscle activation impacts stretch reflex excitability after stretch-induced accommodation.

The current study investigated the impact of voluntary muscle activation on stretch reflex activity following stretch-induced accommodation in individuals with stroke. A protocol that has been shown to accommodate the stretch reflex in the stroke population was used, specifically applying fast consecutive stretches that induce stretch reflexes to a relaxed arm (Schmit et al., 2000). Research suggests that muscle activation amplifies motoneuron excitability and, in turn, stretch reflex activity (Heckman et al., 2009; McPherson, McPherson, et al., 2018; Pavlenko & Kulichenko, 2003). Hence, we hypothesized that voluntary muscle activation would increase stretch reflex activity when compared to the accommodated level induced from the fast consecutive stretches.

Materials And Methods

Participants

This investigation was approved by the Northwestern University Institutional Review Board and complies with the 1964 Declaration of Helsinki. Participants provided written informed consent and were evaluated by a licensed clinician. Eligibility criteria included: >1 year post-stroke; paresis confined to one side; passive range-of-motion about the paretic elbow between 70° and 150°, with 180° being full extension; volitional control about the paretic elbow in extension and flexion; no use of anti-spastic agents in the previous six months; absence of severe cognitive deficits and contractures; and ability to detect a movement at the paretic arm (Lincoln et al., 1998).

Experimental Setup

Participants sat in a Biodex chair (System 3 ProTM; Shirley, NY, USA) with their trunk stabilized (Figure A1A). Their paretic forearm was fixed to a manipulandum at 85° shoulder abduction and 30° shoulder flexion, and its weight was fully supported. A Harmonic Drive FHA-17C-100 motor with attached US250 encoder (Peabody, MA, USA) rotated the paretic forearm and measured its

angular position with a resolution of 0.000225°. A Futek reaction torque sensor (Model Number TFF600; Irvine, CA, USA) measured torques with a resolution of 0.013Nm. Surface electromyography (sEMG) electrodes (Delsys, 16-channel Bagnoli EMG System; Boston, MA) placed on the muscle bellies quantified activity of the elbow flexors (biceps brachii, brachioradialis) and extensors (triceps brachii lateral head). The software ran at 4kHz, and data were saved at 1kHz.

Procedures

A plethora of stretching approaches exist, which vary in angular range, velocity, repetitions, and frequency (Bovend'Eerdt et al., 2008). The stretching protocol selected for this study was modeled after one protocol that demonstrated stretch reflex accommodation in the stroke population (Schmit et al., 2000); this approach is commonly used in quantitative ramp stretching protocols (Condliffe et al., 2005; McPherson et al., 2019; McPherson, Stienen, et al., 2018). Using this protocol, participants completed a two-hour session on two separate days (Figure A1B-C).

Slow Stretches: First Set

The paretic forearm was extended from 70° to 150°, held for 10s, flexed from 150° to 70°, and held for 10s. This stretching sequence was repeated five times at an angular speed of 6°/s to avoid stretch reflex activity, as confirmed with sEMG. In turn, we could quantify passive musculoskeletal properties (Levin & Feldman, 1994; Schmit et al., 2000).

Fast Stretches: First Set

The stretching sequence described above was repeated twenty times at an angular speed of 120°/s to evoke flexor and extensor stretch reflex activity, as determined with sEMG (Levin & Feldman, 1994; McPherson et al., 2019; Schmit et al., 2000).

Testing Condition

Voluntary Muscle Activation: During the first session, participants extended and flexed about their paretic elbow through their active range-of-motion five times as quickly as possible.

Rest: This session was included to determine whether the time elapsed, rather than the voluntary muscle activation, elicited a change in the stretch reflex activity. Participants rested at 70° elbow flexion for an equal duration to the time that elapsed between the first set and second set of fast 120°/s stretches for the voluntary muscle activation session.

Fast Stretches: Second Set

The stretching sequence was repeated twenty times at 120°/s.

Slow Stretches: Second Set

The stretching sequence was repeated five times at 6°/s.

Data Analyses

Quantifying Passive Musculoskeletal Stiffness – Slow Stretches

We aimed to quantify the passive musculoskeletal stiffness at the beginning and end of each session. This was achieved by analyzing the data acquired during the slow stretches, which were implemented to avoid stretch reflex activity as determined by an absence of sEMG activity. Data were removed for a participant's entire session if the muscle activity during these slow stretches was not deemed quiescent, based on the sEMG data. Since the stiffness profile is nonlinear for the range of angles that we tested, we used a proxy measure to describe the passive musculoskeletal stiffness. Specifically, we quantified the difference in the mean torque when the forearm was held at two discrete positions, 150° and 70° ($\bar{\boldsymbol{\tau}}_{\mathbf{150}^\circ} - \bar{\boldsymbol{\tau}}_{\mathbf{70}^\circ}$). Using this approach, we could ensure that the difference in the mean torque was based on consistent angular positions

for all participants, permitting this outcome measure to be a good proxy for passive musculoskeletal stiffness.

Quantifying Stretch Reflex Activity – Fast Stretches

Modeling: We used the following two outcome measures so that subsequent analyses could identify changes in reflex activity: 1) net torque for any stretch, $\boldsymbol{i}$, and 2) change in net torque between any two stretches, $\boldsymbol{i}$ and $\boldsymbol{j}$ (not necessarily consecutive).

To begin, we modeled the net torque ($\boldsymbol{\tau}_{\text{Net}}$) about the elbow for every 120°/s stretch in extension or flexion as a summation of the neural stretch reflex ($\boldsymbol{\tau}_{\text{Reflex}}$) component and passive musculoskeletal inertial ($\boldsymbol{\tau}_{\text{Inertia}}$), damping ($\boldsymbol{\tau}_{\text{Damping}}$), and stiffness ($\boldsymbol{\tau}_{\text{Stiffness}}$) components:

$$\boldsymbol{\tau}_{\text{Net}}(\boldsymbol{\theta}(\boldsymbol{t})) = \boldsymbol{\tau}_{\text{Inertia}}(\boldsymbol{\theta}(\boldsymbol{t})) + \boldsymbol{\tau}_{\text{Damping}}(\boldsymbol{\theta}(\boldsymbol{t})) + \boldsymbol{\tau}_{\text{Stiffness}}(\boldsymbol{\theta}(\boldsymbol{t})) + \boldsymbol{\tau}_{\text{Reflex}}(\boldsymbol{\theta}(\boldsymbol{t})). \quad (1)$$

θ and $\boldsymbol{t}$ indicate angular position and time.

To avoid the influence of the passive musculoskeletal inertial and damping components, we extracted and analyzed torque data during the constant velocity portion of each stretch. Since the robotic device implemented each stretch using the same control algorithm, the passive musculoskeletal inertial and damping components can be assumed to be comparable within a testing session for each participant such that for any two stretches, $\boldsymbol{i}$ and $\boldsymbol{j}$:

$$\boldsymbol{\tau}_{Inertia_i}(\boldsymbol{\theta}(\boldsymbol{t})) - \boldsymbol{\tau}_{Inertia_j}(\boldsymbol{\theta}(\boldsymbol{t})) = 0 \text{ and}$$

$$\boldsymbol{\tau}_{Damping_i}(\boldsymbol{\theta}(\boldsymbol{t})) - \boldsymbol{\tau}_{Damping_j}(\boldsymbol{\theta}(\boldsymbol{t})) = 0. \quad (2)$$

Prior research indicates that the passive musculoskeletal stiffness can be modified with stretching, particularly when using much longer stretching durations than those used in our study (Herda et al. 2010; Kubo et al. 2001, 2002; Ryan et al. 2008; Taylor et al. 1997). Whether changes in passive musculoskeletal stiffness occur for the shorter stretching duration used in our protocol

remains unknown (Ryan et al. 2008). As such, analyses were needed to determine whether the passive musculoskeletal stiffness did change due to the 120°/s stretches used in our protocol. We refer the reader to Sections 2.4.1, 2.5.1, and 3.2 for information regarding how we obtained our outcome measures for the passive musculoskeletal stiffness and, subsequently, ran our analyses. If the passive musculoskeletal stiffness was not found to significantly change within one testing session, we could conclude that the passive musculoskeletal stiffness for any two stretches, $\boldsymbol{i}$ and $\boldsymbol{j}$, within that testing session was comparable such that the difference between them would cancel one another out:

$$\boldsymbol{\tau}_{Stiffness_i}\big(\boldsymbol{\theta}(\boldsymbol{t})\big) - \boldsymbol{\tau}_{Stiffness_j}\big(\boldsymbol{\theta}(\boldsymbol{t})\big) = 0. \quad (3)$$

Therefore, a comparison of the net torque for any two stretches, $\boldsymbol{i}$ and $\boldsymbol{j}$, within one testing session becomes a comparison of solely the reflex component.

While we can use the logic provided above to indicate that the passive musculoskeletal inertial, damping, and stiffness components remain comparable within a testing session, the same assumption cannot be made between testing sessions. The measurements obtained for the passive musculoskeletal inertial, damping, and stiffness components of Equation 1 may not be comparable between testing sessions due to day-to-day measurement errors related to the set up of the participant. To address this limitation, the outcome measure used to compare changes in the reflex activity between testing sessions was the change in the net torque between any two stretches, $\boldsymbol{i}$ and $\boldsymbol{j}$, within one testing session:

$$\boldsymbol{\tau}_{\boldsymbol{Diff}_{(i,j)}}\big(\boldsymbol{\theta}(\boldsymbol{t})\big) = \Big(\boldsymbol{\tau}_{Inertia_i}\big(\boldsymbol{\theta}(\boldsymbol{t})\big) + \boldsymbol{\tau}_{Damping_i}\big(\boldsymbol{\theta}(\boldsymbol{t})\big) + \boldsymbol{\tau}_{Stiffness_i}\big(\boldsymbol{\theta}(\boldsymbol{t})\big) + \boldsymbol{\tau}_{Reflex_i}\big(\boldsymbol{\theta}(\boldsymbol{t})\big)\Big) - \Big(\boldsymbol{\tau}_{Inertia_j}\big(\boldsymbol{\theta}(\boldsymbol{t})\big) + \boldsymbol{\tau}_{Damping_j}\big(\boldsymbol{\theta}(\boldsymbol{t})\big) + \boldsymbol{\tau}_{Stiffness_j}\big(\boldsymbol{\theta}(\boldsymbol{t})\big) + \boldsymbol{\tau}_{Reflex_j}\big(\boldsymbol{\theta}(\boldsymbol{t})\big)\Big). \quad (4)$$

If the passive musculoskeletal inertial, damping, and stiffness components remain similar within a single testing session, as discussed above, then the change in the net torque between the two stretches, $\boldsymbol{i}$ and $\boldsymbol{j}$, simplifies to the change in the stretch reflex activity:

$$\boldsymbol{\tau_{Diff_{(i,j)}}(\theta(t)) = \tau_{Reflex_i}(\theta(t)) - \tau_{Reflex_j}(\theta(t))}. \quad (5)$$

As such, the change in net torque can be used to compare the impact of volitional muscle activation versus rest on changes in stretch reflex activity.

Reflex Elicitation: Data related to the flexors and/or extensors were removed for a participant's session if the muscle activity was deemed insufficient, based on sEMG data, during the first stretch of the first set of fast 120°/s stretches.

Torque Extraction: The torque data were filtered using a forward-backward low-pass filter with a 5Hz cut-off frequency (Dewald et al., 1996; Herda et al., 2010; Kamper et al., 2003; McPherson et al., 2019; McPherson, McPherson, et al., 2018). Following, torque values at the angles of 135° and 88° were extracted during each stretch in extension and flexion, respectively, to quantify stretch reflex activity of the flexor and extensor muscles, respectively. These empirically selected angles permitted consistent extraction of torque responses across all participants during the constant velocity portion of each stretch.

Short- and Long-Latency Response: In addition to examining the torque response, we analyzed the participants' sEMG data to identify the short-latency response, arising from spinal-cord circuitry, and long-latency response, potentially involving cortical circuitry. We extracted the sEMG data at time points corresponding to the response time from the spinal cord (20-50ms) and transcortexical (50-150ms) components of the stretch reflex (McPherson, Stienen, et al., 2018). The relevant sEMG data were first prepared for these analyses by subtracting the mean sEMG activity from each movement so that the signal had a mean value of zero. Following, the signal was rectified and then smoothed using a low-pass forward-backward filter with a cutoff frequency

of 5Hz. Next, the baseline, pre-activation signal was determined by taking the mean of this processed sEMG signal for the 500ms prior to the movement, and averaging it across every stretch in extension and flexion, respectively, within a 120°/s fast stretching set. The corresponding pre-activation signal prior to the movement in extension or flexion was removed from the average sEMG signal between 20ms and 50ms and between 50ms and 150ms, respectively, of every stretch within that fast 120°/s stretching set to give the short-latency response (SLR) and long-latency response (LLR) for the flexors and extensors.

We highlight that the LLR is comprised of both transcortical and spinal components since the sEMG spinal component of the stretch reflex is present from approximately 20ms post perturbation intiation. Thus, to deduce contributions arising from the transcortical component, we needed to confirm that the spinal component was comparable during the measurements occurring at 20-50ms (SLR) and 50-150ms (LLR) after perturbation initiation. The spinal component would only be comparable if the angular speed at which the forearm rotated was the same during each of these respective time windows. If the angular speed of rotation was not comparable, then we would not be able to deduce whether changes from the SLR to the LLR arise due to changes in the spinal versus the transcortical component. For this reason, we report the mean angular speed of rotation of the forearm during the SLR and LLR and summarize our results accordingly.

Statistical Analyses

Analysis of Passive Musculoskeletal Stiffness – Slow Stretches

We aimed to indicate whether the passive musculoskeletal stiffness remained consistent within a single testing session. This was achieved by using a pairwise t-test to determine whether, across all participants, the difference in the mean torque $\bar{\boldsymbol{\tau}}_{\mathbf{150}^\circ} - \bar{\boldsymbol{\tau}}_{\mathbf{70}^\circ}$) as defined in the previous section, significantly changed between the first and second set of slow stretches for a single

testing session. If the difference in the mean torque was found to significantly change, then the proposed analyses in the previous section would not hold.

Analysis of Stretch Reflex Activity – Fast Stretches

Impact Across All Stretches: We aimed to indicate whether the torque arising due to stretch reflex activity was impacted by the fast 120°/s stretchesing before and after volitional muscle activation and rest. To do so, the net torque outcome measure, defined in Section 2.4.2, was fit to a linear mixed-effects model, with participant as a random effect. We identified whether the net torque depended on the stretch repetition (1-20) and set (first, second) for each testing condition (volitional muscle activation, rest) and muscle group (flexors, extensors). An analysis of variance with a Tukey adjustment identified significant fixed effects.

Impact Across Pairs of Stretches: In addition to identifying effects across all stretches, we also identified effects for specific pairs of stretches. For these pairs, data were analyzed across all participants using a pairwise t-test with a Bonferroni correction.

To begin, we indicated whether the net torque significantly differed between the following pairs of stretches for each testing condition and muscle group. We compared the first set's final stretch and second set's first stretch to determine whether volitional muscle activation and rest had an immediate effect on stretch-induced accommodated reflex activity. Additionally, we compared the first stretch of the first set to the first stretch of the second set to determine the impact of volitional muscle activation and rest on reflex activity when compared to the reflex activity prior to stretching. Moreover, we compared the final stretch of the first set to the final stretch of the second set to determine whether volitional muscle activation and rest affected the extent to which the reflex could be accommodated with the fast 120°/s stretches.

Following, for each muscle group we determined whether the difference in the net torque between each of these pairs of stretches within each session depended on the testing condition.

Short- and Long-Latency Response: We aimed to indicate whether the short- and/or long-latency response corresponding to spinal reflexes and potentially cortical circuitry, respectively, were affected by the fast 120°/s stretching after the participant volitionally activated their muscles or relaxed. To do so, we fit the short-latency response (SLR) and long-latency response (LLR) outcome measures described in Section 2.4.2 to a linear mixed-effects model, with participant as a random effect. Subsequently, we determined whether the SLR and LLR depended on the stretch repetition (1-20) and set (first, second) for each testing condition (volitional muscle activation, rest) and muscle group (flexors, extensors). An analysis of variance with a Tukey adjustment identified significant fixed effects.

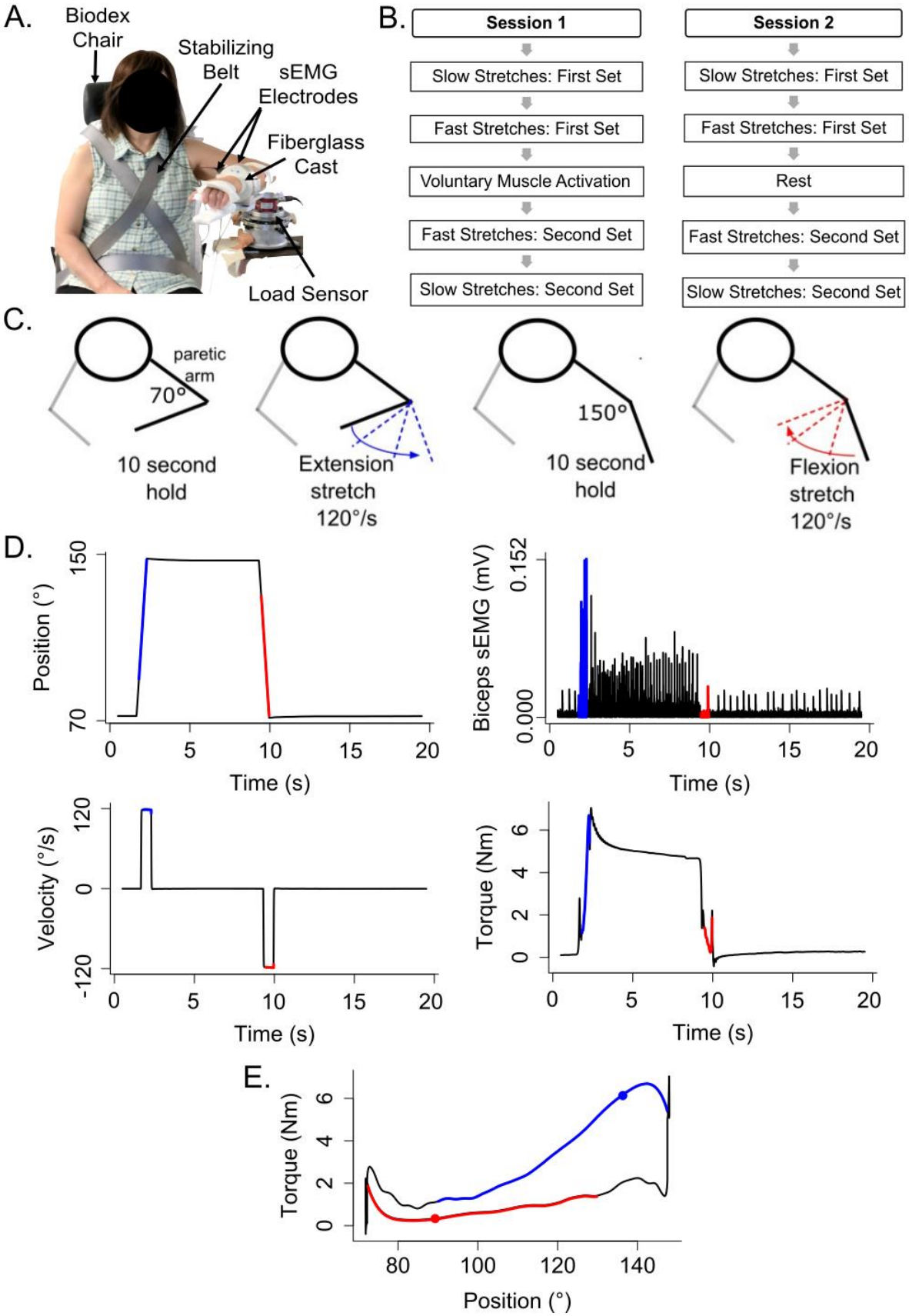
A.
Biodex Chair
Stabilizing Belt
sEMG Electrodes
Fiberglass Cast
Load Sensor
B.
Session 1
Slow Stretches: First Set
Fast Stretches: First Set
Voluntary Muscle Activation
Fast Stretches: Second Set
Slow Stretches: Second Set
Session 2
Slow Stretches: First Set
Fast Stretches: First Set
Rest
Fast Stretches: Second Set
Slow Stretches: Second Set
C.
paretic arm
70°
10 second hold
Extension stretch 120°/s
150°
10 second hold
Flexion stretch 120°/s
D.
Position (°)
150
70
0
5
10
15
20
Time (s)
Biceps sEMG (mV)
0.152
0.000
Velocity (°/s)
120
0
-120
Torque (Nm)
0
2
4
6
E.
Torque (Nm)
80
100
120
140
Position (°)

Figure A1. Experimental setup and procedures. A. Participant sitting with their paretic forearm affixed to the robotic device. B. Five tasks of each session. C. Representation of one repetition of the stretching sequence. D. Example angular position, angular velocity, biceps brachii sEMG activity, and torque data during one repetition of the fast stretching sequence. Blue and red lines indicate the constant velocity portion in elbow extension and flexion, respectively. E. Example torque versus angular position data. The blue filled circle identifies the flexion torque at 135°, and the red filled circle identifies the extension torque at 88°. Blue and red lines indicate the constant velocity portion in elbow extension and flexion, respectively.

Results

Participants

Seventeen individuals 12±9 (μ±σ) years post-stroke participated (Table 1). Participants had upper-extremity Fugl-Meyer motor assessment (UE FMA) scores spanning 12-48 (μ±σ UE FMA: 28±11).

Participant	Gender	Age	Years Post Stroke	Lesion Location	UE FMA Score	Biceps Brachii MAS
1	M	70	14	R: F,BG,I	29	1+
2	M	51	29	NA	26	1+
3	M	61	3	R: IC	39	1
4	M	70	22	L: Th,IC,BG,T,I	12	2
5	M	47	10	R: Th,IC,BG	18	2
6	F	69	14	L: Th,IC,BG	12	2
7	F	66	32	L: Th,IC,BG	16	1+
8	M	48	13	R: Th,IC,BG	38	2
9	M	43	4	L: Th,IC,BG,F,P	39	1+
10	M	63	14	L: IC	48	1+
~~11~~	~~M~~	~~59~~	~~7~~	~~L: IC~~	~~22~~	~~3~~
12	M	73	15	NA	27	1+
13	M	48	7	R: Th,BG	33	1+
14	F	49	11	R: IC,F,P	28	1+
15	M	64	8	R: IC	17	1+
16	M	62	4	NA	36	2
17	M	58	1	NA	N/A	1+

Table A1. Study participants. UE-FMA: upper-extremity score of Fugl-Meyer motor assessment (max=66); MAS: modified Ashworth scale score (max=4); M: male; F: female; R: right; L: left; Th: thalamus; IC: internal capsule; BG: basal ganglia; F: frontal; P: parietal; O: occipital; T: temporal; T-P: tempo-parietal; I: insula; NA: not available. Participant 11 was removed due to the presence of muscle activity during the slow stretches.

Passive Musculoskeletal Stiffness

To address whether the passive musculoskeletal stiffness changed within each testing session, we compared the difference in the mean torque ($\bar{\tau}$(150°)- $\bar{\tau}$(70°)) for the first and second slow stretching set of that testing session (Figure A2). Data for one participant were removed from both testing sessions due to the presence of muscle activity during the slow stretches, as determined from analyses of the sEMG signals. Therefore, the remaining analyses are based on the remaining sixteen participants.

During the voluntary muscle activation session, muscle activity was observed for a second participant during the slow stretches, as determined from the sEMG signals; hence, data for this participant were removed from further analyses of this testing session. In turn, future analyses for the voluntary muscle activation session were based on the remaining fifteen participants.

Finally, during the rest session, there was a data storage error during the slow stretches of the second set for one participant, and, hence, data for this participant were not included in the analyses relevant to the passive musculoskeletal stiffness. The data analyzed for this participant for the first set of this session, as well as both sets of the voluntary muscle activation session, did not reveal the presence of muscle activity. Hence, while we excluded this participant from the analyses relevant to the passive musculoskeletal stiffness, we did include this participant's data in the remaining analyses for the fast 120°/s stretches.

Analyses of the passive musculoskeletal stiffness during the slow stretches were based on fifteen participants for each session since two participants were excluded from each session, as discussed above. Results shown in Figure A2 indicate that the difference in the mean torque $\bar{\boldsymbol{\tau}}_{\mathbf{150^\circ}} - \bar{\boldsymbol{\tau}}_{\mathbf{70^\circ}}$), as defined in the previous section, did not significantly change between the first and second set of slow stretches of the voluntary muscle activation (t(14)=-0.37; p=0.718) and rest (t(14)=0.06; p=0.951) sessions. Consequently, we conclude that the passive musculoskeletal

stiffness remained similar throughout each session, providing support that the outcome measures described in the previous section are reasonable.

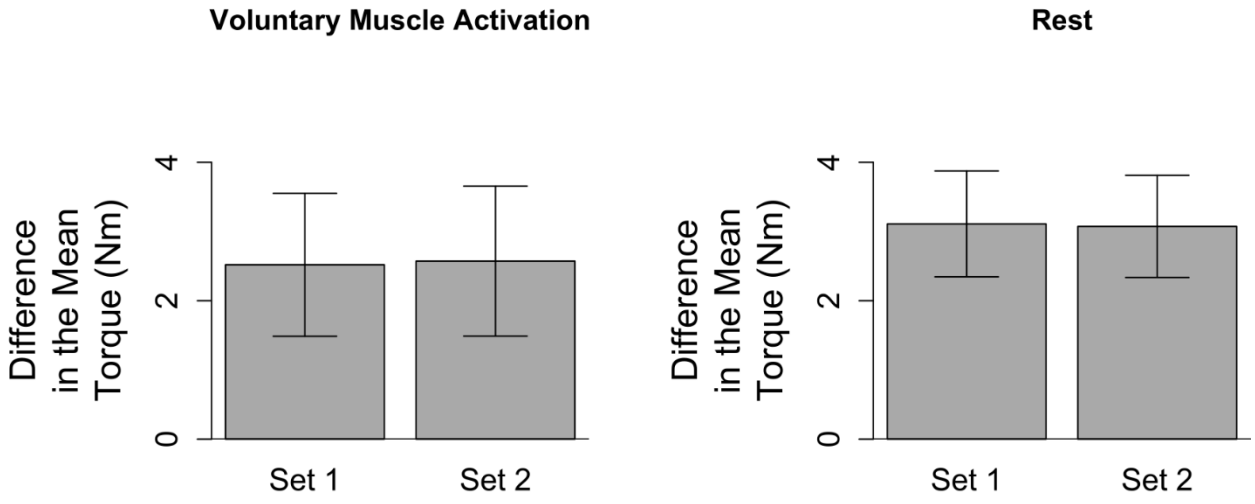

Figure A2. Difference in the mean torque, a proxy for the passive musculoskeletal stiffness, across each session. Mean (bar height) and lower and upper 95th percentile confidence intervals (error bars) are identified for participants' difference in the mean torque during each slow stretching set (Set 1 and Set 2) of every session (voluntary muscle activation and rest).

Preparation of Fast Stretch Data for Analyses

For the 120°/s fast stretching data, separate analyses were run for the different muscle groups (flexors and extensors). That is, when the forearm extended from 70° to 150°, we obtained information about how the stretched flexor muscles responded. Likewise, when the forearm flexed from 150° to 70°, we obtained information about how the stretched extensor muscles responded. Hereafter, results will be presented by the muscle group stretched, i.e., flexors and extensors.

As discussed previously, data from two participants for the volitional muscle activation session and one participant for the rest session were excluded due to the presence of muscle activity during the slow stretches. Given that the baseline muscle activity existed, we could not clearly determine how the 120°/s stretching impacted these participants' reflex activity. Therefore, results presented for the volitional muscle activation and rest sessions are based on the remaining fifteen and sixteen participants, respectively.

Flexors: We confirmed that muscle flexor activity was present in the first stretch of the first 120°/s fast stretching set of each testing session for every participant. In this way, we could confirm that attenuation of the stretch reflex activity was occurring. Data for one participant in each testing session were removed due to quiescent flexor muscle activity. Therefore, results for the flexors during the volitional muscle activation and rest sessions are based on fourteen and fifteen participants, respectively. Results comparing these testing sessions are based on thirteen participants for whom data existed in both.

Extensors: We confirmed that muscle extensor activity was present in the first stretch of the first 120°/s fast stretching set of each testing session for every participant. In this way, we could confirm that attenuation of the stretch reflex activity was occurring. Data for nine participants in the volitional muscle activation session and eleven participants in the rest session were removed from the analyses for the extensors due to quiescent extensor muscle activity. Therefore, results for the extensors during the volitional muscle activation session and rest session are based on six and five participants, respectively. Results comparing these sessions are based on four participants for whom data existed in both.

Impact of Voluntary Muscle Activation and Rest on Reflex Activity Across All Fast Stretches

Results are summarized in Figure A3 and Figure A4.

Flexors: During the voluntary muscle activation session, the net torque reduced as the stretch repetition increased ($F(19,526)=14.78$; $p<0.001$), being greater on the first two fast stretches than subsequent stretches ($p<0.050$). Additionally, the net torque was greater across the second set of 120°/s fast stretches following voluntary muscle activation than the first set ($F(1,526)=9.64$; $p=0.002$). Therefore, volitional muscle activation amplified stretch reflex activity across subsequent fast stretches.

During the rest session, the net torque decreased with stretch repetition ($F(19,565)=8.34$; $p<0.001$), being greater on the first two fast stretches than on subsequent stretches ($p<0.050$). Additionally, the net torque was less across the second set of fast stretches following rest than the first set ($F(1,565)=116.73$; $p<0.001$). Therefore, the stretch reflex activity was not found to be noticeably affected by the rest.

Extensors: During the voluntary muscle activation session, the net torque depended on the stretch repetition ($F(19,214)=2.62$; $p<0.001$), with a significant difference between the eighth and subsequent fast stretches ($p>0.050$), yet did not depend on the stretching set ($F(1,214)=2.13$; $p=0.146$). Therefore, the 120°/s fast stretches did not notably attenuate extensor reflex activity.

During the rest session, the net torque did not significantly depend on the stretch repetition ($F(19,175)=0.11$; $p=1.000$); yet, the net torque was less across the second fast stretching set

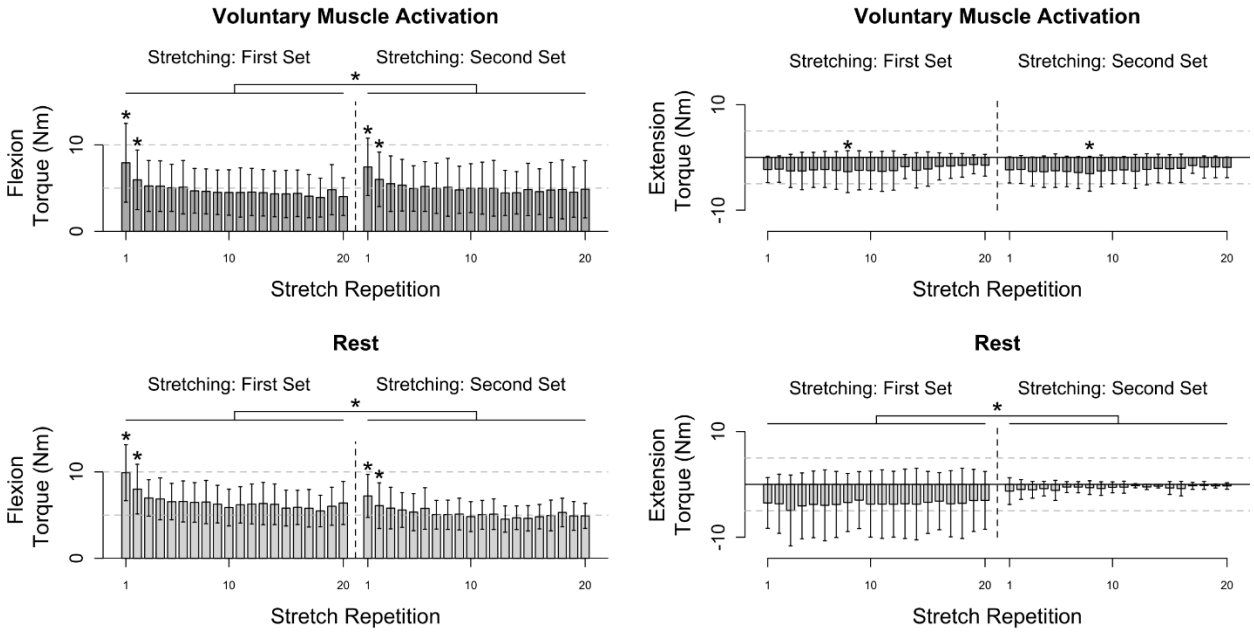

Figure A3. Participants' flexion and extension torque as a function of stretch repetition prior to and following voluntary muscle activation and rest. Mean (bar height) and lower and upper 95th percentile confidence intervals (error bars) are identified. A line with a star above indicates a significant difference between sets. An individual star indicates stretch repetitions that significantly differ from subsequent stretch repetition(s). Post hoc comparisons for each significant stretch repetition are provided in Figure A4.

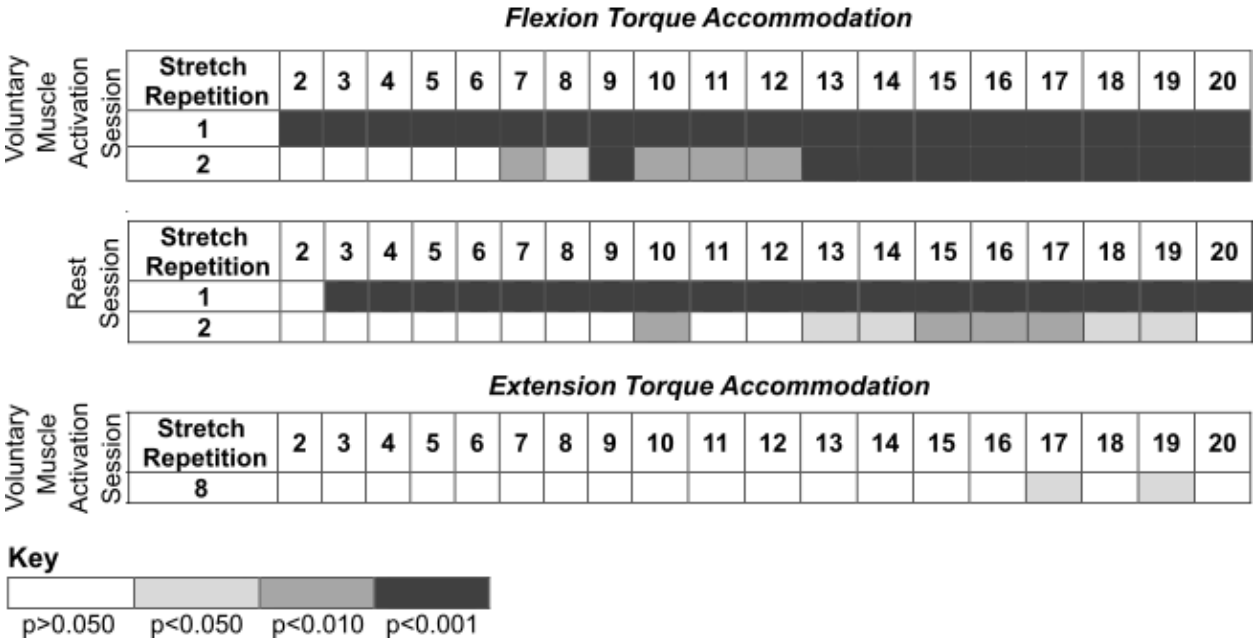

Figure A4. Post hoc comparisons for the results presented in Figure A3 during the voluntary muscle activation and rest sessions. Rows identify the **i**th stretch repetition, and columns identify subsequent stretch repetitions. Rows are not included for stretch repetitions that did not have significance. Significance is represented using shading — white: p>0.050; light gray: p<0.050; darker gray: p<0.010; darkest gray: p<0.001.

following rest than the first ($F(1,175)=56.96$; $p<0.001$). Therefore, each individual 120°/s fast stretch did not noticeably attenuate the extensor reflex activity whereas there was a cumulative effect.

Pairwise Comparisons

Figure A5 summarizes the impact of voluntary muscle activation and rest on specific pairs of fast stretches.

Immediate Impact of Voluntary Muscle Activation and Rest on Reflex Activity when Compared to Stretch-Attenuated Level

We compared the net torque of the second set's first fast stretch to the first set's final fast stretch to determine the immediate impact of volitional muscle activation and rest on stretch-induced attenuated stretch reflex activity (Figure A5A).

Flexors: The net torque increased following voluntary muscle activation ($t(13)=-5.22$; $p<0.001$), but not rest ($t(14)=-1.09$; $p=0.879$). The difference in the net torque between these two fast stretches did not significantly differ between the voluntary muscle activation and rest sessions ($t(12)=2.62$; $p=0.067$), albeit there was a trend towards significance. Combined, these results suggest that flexor reflex activity increased immediately with volitional muscle activation, but not rest.

Extensors: No significant difference in the net torque was found between these two 120°/s fast stretches following voluntary muscle activation ($t(5)=2.04$; $p=0.289$) and rest ($t(4)=-1.15$; $p=0.948$). Therefore, extensor reflex activity was sustained regardless of volitional muscle activation or rest.

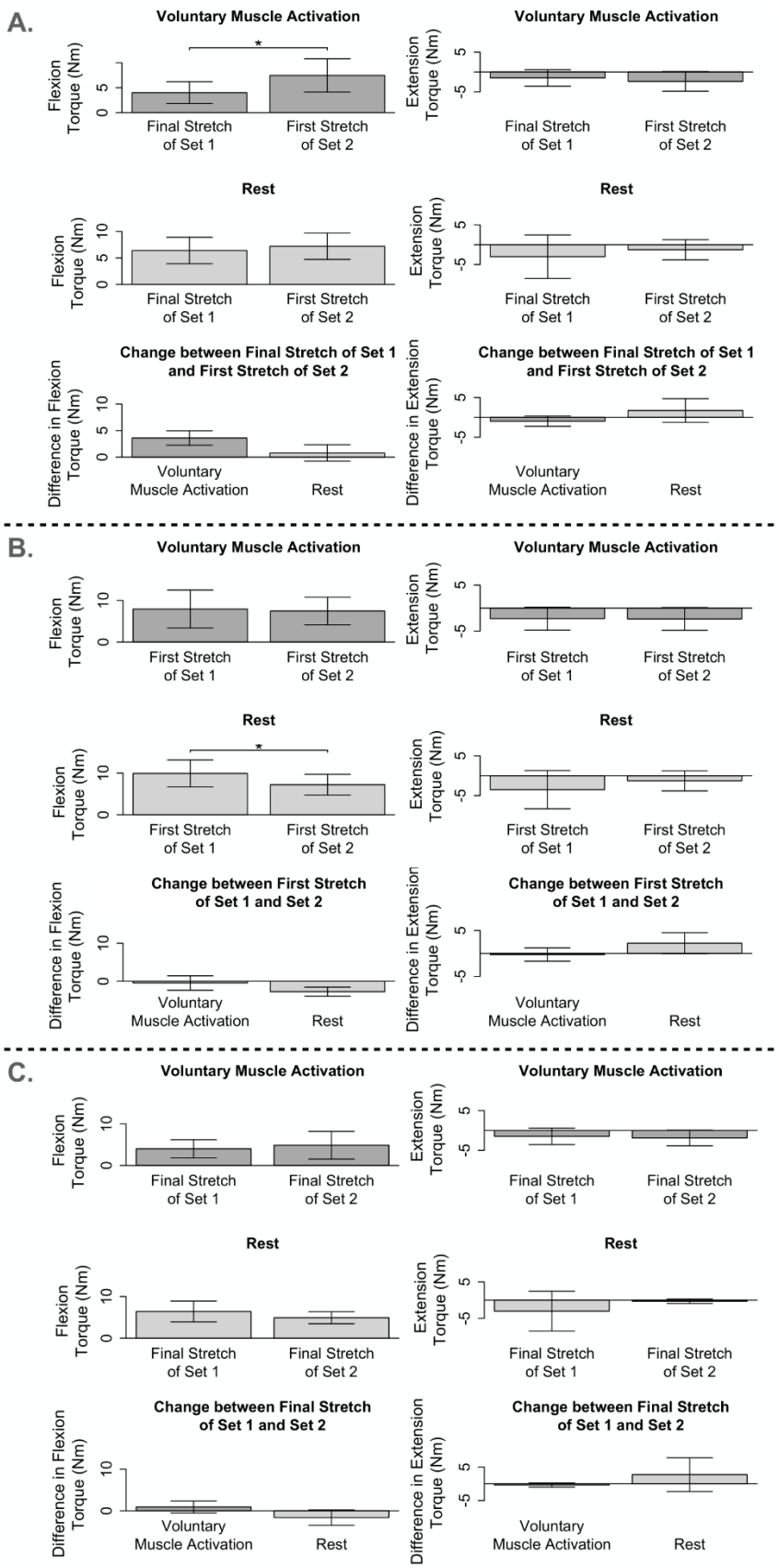
A.
Voluntary Muscle Activation
Flexion Torque (Nm)
Final Stretch of Set 1
First Stretch of Set 2
Extension Torque (Nm)
Rest
Change between Final Stretch of Set 1 and First Stretch of Set 2
Difference in Flexion Torque (Nm)
Difference in Extension Torque (Nm)
Voluntary Muscle Activation
Rest
B.
First Stretch of Set 1
First Stretch of Set 2
Change between First Stretch of Set 1 and Set 2
C.
Final Stretch of Set 1
Final Stretch of Set 2

Figure A5. Comparison of the flexion and/or extension torque during specific stretches. Mean (bar height) and lower and upper 95th percentile confidence intervals (error bars) are identified. A line with a star above indicates a significant difference. Comparison between the: A. final fast stretch of set 1 and initial fast stretch of set 2, B. initial fast stretch of set 1 and initial fast stretch of set 2, and C. final fast stretch of set 1 and final fast stretch of set 2.

Immediate Impact of Voluntary Muscle Activation and Rest on Reflex Activity when Compared to Pre-Stretching Level

We compared the net torque of the second set's first fast stretch to the first set's first fast stretch to determine the immediate impact of volitional muscle activation and rest on stretch reflex activity when compared to pre-accommodation levels (Figure A5B).

Flexors: The net torque from the first 120°/s fast stretch was greater for the first set than the second set for the rest session ($t(14)=4.78$; $p<0.001$), but not the voluntary muscle activation session ($t(13)=0.53$; $p=1.000$). Even so, the difference in the net torque between these two fast stretches did not significantly differ when comparing the voluntary muscle activation and rest sessions ($t(12)=2.02$; $p=0.198$). Combined, these results suggest that volitional muscle activation restored flexor reflex activity to pre-stretch levels whereas rest maintained the stretch-induced flexor reflex accommodation.

Extensors: The net torque did not significantly change between these two fast stretches during the voluntary muscle activation ($t(5)=0.14$; $p=1.000$) and rest ($t(4)=-1.91$; $p=0.388$) sessions. Therefore, extensor stretch reflex activity was at a pre-stretch level immediately following volitional muscle activation and rest.

Impact of Voluntary Muscle Activation and Rest on Reflex Activity of Final Fast Stretches

We compared the net torque from the final fast stretch of each set to determine whether voluntary muscle activation and rest impacted the level to which our stretching protocol accommodated reflex activity (Figure A5C).

Flexors: The net torque did not significantly differ between these two fast stretches during the voluntary muscle activation ($t(13)=-1.27$; $p=0.679$) and rest ($t(14)=1.69$; $p=0.339$) sessions. Therefore, our stretching protocol accommodated flexor stretch reflex activity to similar levels regardless of the testing condition.

Extensors: The net torque did not significantly differ between these two fast stretches during the voluntary muscle activation ($t(5)=1.99$; $p=0.954$) and rest ($t(4)=-1.06$; $p=1.000$) sessions. Therefore, our stretching protocol accommodated extensor stretch reflex activity to similar levels regardless of the testing condition.

Short- and Long-Latency Reflex Response

Flexors: To describe the flexors' SLR and LLR, we analyzed the sEMG data captured from the biceps brachii. Across all fast stretches, the average speed at which the forearm rotated during the time segment corresponding to the SLR and LLR was 94.7º/s and 117.9º/s, respectively. Hence, the spinal contribution to the SLR and LLR could have differed due to the change in the angular speed at which the forearm rotated during each respective time window. Therefore, we cannot draw conclusions regarding contributions arising from the transcortical input since the spinal input was still changing during the LLR time window due to the ramping up of the angular speed.

During the voluntary muscle activation session, the biceps brachii SLR ($F(19,526)=8.28$; $p<0.001$) and LLR ($F(19,526)=8.28$; $p<0.001$) reduced with stretch repetition, with muscle activity being greater on the first fast stretch than subsequent stretches ($p<0.050$). The stretching set did not

significantly affect the SLR ($F(1,526)=0.02$; $p=0.895$) and LLR ($F(1,526)=0.08$; $p=0.772$). These results indicate that a short-latency response could explain changes in the biceps brachii reflex activity throughout the voluntary muscle activation session; due to the change in the angular speed at which the forearm rotated during the SLR and LLR time windows, the contributions during from the long-latency response remain inconclusive.

During the rest session, the biceps brachii SLR ($F(19,565)=1.95$; $p=0.010$) and LLR ($F(19,565)=2.45$; $p<0.001$) reduced with stretch repetition, with muscle activity being greater on the first fast stretch than subsequent stretches ($p<0.050$). Additionally, the SLR increased increased from the first to the second fast stretching set ($F(1,565)=4.80$; $p=0.029$), whereas the LLR did not significantly change ($F(1,565)=0.98$; $p=0.323$). These results, again, indicate that the short-latency response can explain changes in the biceps brachii reflex activity throughout the rest session; due to the change in the angular speed at which the forearm rotated during the SLR and LLR time windows, the contributions during the long-latency response remain inconclusive.

Extensors: To describe the extensors' SLR and LLR, we analyzed the sEMG data captured from the lateral head of the triceps brachii. Across all fast stretches, the average speed at which the forearm rotated during the time segment corresponding to the SLR and LLR was 94.5º/s and 118.2º/s, respectively. Hence, the spinal contribution to the SLR and LLR could have differed due to the change in the angular speed at which the forearm rotated during each respective time window. Therefore, we cannot draw conclusions regarding contributions arising from the transcortical input since the spinal input was still changing during the LLR time window due to the ramping up of the angular speed.

During the voluntary muscle activation session, the triceps brachii SLR ($F(19,214)=2.51$; $p<0.001$) and LLR ($F(19,214)=2.45$; $p=0.001$) reduced with stretch repetition, being greater on the eighth fast stretch than the seventeenth fast stretch and nineteenth fast stretch ($p<0.050$). Additionally,

the triceps brachii activity was greater on the second fast stretching set, after volitional muscle activation, than the first set for the SLR ($F(1,214)=72.06$; $p<0.001$) and LLR ($F(1,214)=65.54$; $p<0.001$). These results suggest that the short-latency response can explain changes in the triceps brachii reflex activity throughout the voluntary muscle activation session; due to the change in the angular speed at which the forearm rotated during the SLR and LLR time windows, the contributions during from the long-latency response remain inconclusive.

During the rest session, the triceps brachii activity was less on the second fast stretching set, after rest, than the first fast stretching set for the SLR ($F(1,175)=61.66$; $p<0.001$) and LLR ($F(1,175)=60.94$; $p<0.001$). The triceps brachii activity was not found to be significantly affected by the stretch repetition for the SLR ($F(19,175)=0.13$; $p=1.000$) and LLR ($F(19,175)=0.13$; $p=1.000$). These results demonstrate that the short-latency response can explain changes in the triceps brachii reflex activity during the rest session; due to the change in the angular speed at which the forearm rotated during the SLR and LLR time windows, the contributions from the long-latency response remain inconclusive.

Discussion

We examined whether volitional muscle activation altered stretch reflex activity following consecutive fast stretches in individuals with stroke. To begin, we demonstrated that the fast stretches attenuated stretch reflex activity in the flexor muscles. Following, we showed, for the first time, that subsequent voluntary muscle activation reverses stretch-induced reflex accommodation of the flexors.

The majority of the data for our participants' extensor muscles were excluded due to quiescent extensor muscle activity during the 120°/s fast stretches;. the absence of extensor reflex activity is likely due to the stretching speed of 120°/s not being fast enough (McPherson, Stienen, et al., 2018; Powers et al., 1989). Therefore, analyses for the extensors were based on a very low

number of participants. Prior research corroborates this finding that, in the upper limb, the extensors are not as affected with motor deficits, including spasticity, as the flexors (Davidson et al., 2007; Davidson & Buford, 2006; Kably & Drew, 1998; Miller & Dewald, 2012; Zaaimi et al., 2012). Given the limitation of the quiescent muscle activity and, in turn, small sample size for the extensors, we chose to not discuss and draw conclusions based on these data. Therefore, the following discussion only reflects our findings for the elbow flexors.

We also highlight that the mechanism governing stretch-induced reflex accommodation remains unclear; existing literature points to possible neural and mechanical origins (Guissard & Duchateau, 2006; Schmit et al., 2000; Smania et al., 2010; Tsai et al., 2001). Hence, we discuss our results in light of these potential reflex-accommodating mechanisms.

Impact of Voluntary Muscle Activation on Flexor Reflex Activity Following Stretch-Induced Accommodation

Our results indicate that volitional muscle activation restores flexor stretch reflex activity to initial hyperactive levels, despite stretch-induced reflex accommodation. Here, we consider four three mechanisms that potentially underly this restoration: 1) motoneuron excitability and monoaminergic drive; 2) spindle afferent activity; 3) passive musculoskeletal stiffness.

Motoneuron Excitability and Monoaminergic Drive. Research shows that descending noradrenergic and serotonergic neural activity, and, subsequently, motoneuron excitability, increases with voluntary movement (Jacobs et al., 2002; Pavlenko & Kulichenko, 2003; Wei et al., 2014). Noradrenergic neurons increased firing before and during voluntary muscle activation in cats and monkeys, while serotonergic neurons increased firing corresponding to the voluntary motor output in cats (Jacobs et al., 2002; Pavlenko & Kulichenko, 2003; Wei et al., 2014). Norepinephrine and serotonin are monoamines that heighten motoneuron excitability by increasing resting membrane potential, decreasing firing threshold, and contributing to persistent

inward currents (Fedirchuk & Dai, 2004; Heckman et al., 2003, 2008). As hyperactive stretch reflexes arise from increased motoneuron excitability, it follows that increased monoaminergic input with voluntary movement would heighten motoneuron excitability and, thus, stretch reflex activity. Post-stroke, bulbospinal pathways containing these monoaminergic neurons are upregulated, such that this proposed mechanism becomes especially relevant for explaining our results (Fisher et al., 2012; Li, 2017; Li et al., 2019; McPherson, Chen, et al., 2018; McPherson et al., 2008; McPherson, McPherson, et al., 2018).

Spindle Afferent Activity. Muscle contraction can lead to postcontraction sensory discharge, or a prolonged increased firing rate and dynamic stretch sensitivity in muscle spindles from persistent actin-myosin cross-bonds (Brown, MC et al., 1970; Eldred et al., 1976; Enoka et al., 1980; Gregory et al., 1990; Hutton et al., 1973). Increased spindle afferent activity and, thus, excitatory input to spinal motoneurons would increase motoneuron excitability and, in turn, stretch reflex activity. Spinal animals exhibit this elevated activity, suggesting supraspinal input is not necessary for increased motoneuron activity post-contraction (Hutton & Suzuki, 1979). While spindle discharge rates have been shown to increase with voluntary contraction, research has shown that heightened spindle activity does not contribute to spasticity since individuals with stroke have the same spindle sensitivity as individuals who have not had a stroke (Sheean, 2002; Wilson et al., 1999). Therefore, an increase in spindle afferent activity post voluntary contraction is not a likely to contributor to the observed reversal in stretch reflex activity.

Passive Musculoskeletal Stiffness. Passive musculotendon stiffness can change with repeated stretching (Herda et al., 2010; Kubo et al., 2001, 2002; Ryan et al., 2008; Taylor et al., 1997); however, we did not observe a noticeable change in our proxy outcome measure used to identify the passive musculoskeletal stiffness across the span of each session (see Section 3.2). This

finding suggests that the underlying mechanism of the reflex accommodation and its reversal is not musculoskeletal in nature.

In summary, our results suggest that volitional muscle activation restores flexor stretch reflex activity to initial hyperactive levels, despite reflex accommodation induced by repeated fast stretches. Changes in motoneuron excitability post voluntary contraction is the most likely contributor to these findings.

Impact of Rest on Flexor Stretch Reflex Activity Following Stretch-Induced Accommodation

Our results suggest that stretch reflex accommodation is sustained in the absence of volitional muscle activation and that rest does not facilitate noticeable further reflex accommodation with subsequent consecutive 120°/s fast stretches. This finding corroborates previous research that followed a different stretching protocol and showed that accommodated elbow reflex activity was not restored after 3-5 minutes of rest (Turpin et al., 2016). The four mechanisms proposed above, particularly monoaminergic drive and spindle afferent activity, could have been maintained while resting, allowing the decreased stretch reflex activity to be sustained.

Impact of Voluntary Muscle Activation and Rest on Stretch-Induced Flexor Stretch Reflex Accommodation

The impact of the 120°/s fast consecutive stretches on the flexors was most evident within the first few perturbations. This short-lived efficacy may arise from a consistent elevated tonic monoaminergic supply post-stroke, which limits the level of reduction possible such that reflex activity plateaus (Lee & Heckman, 1999; McPherson, McPherson, et al., 2018). As the mechanism underlying stretch-induced accommodation is still uncertain, additional neural and mechanical mechanisms such as Ia synaptic plasticity and reduced motor neuron excitability

following repeated stretch-induced activation could have impacted the level to which the reflex activity accommodated (Guissard & Duchateau, 2006; Schmit et al., 2000; Smania et al., 2010; Tsai et al., 2001).

Short-Latency and Long-Latency Response

While we did not investigate the specific underlying mechanisms of the stretch reflex accomodation, we did analyze the muscle activity over time windows corresponding to the short-latency and long-latency stretch responses associated with spinal and transcortical circuitry, respectively. Our analyses suggest that the short-latency response, associated with the spinal circuitry, contributed to the reflex accommodation and the restoration of heightened stretch reflex activity after volitional muscle activation.

To begin, we observed during the voluntary muscle activation session that the short-latency response decreased with the number of fast 120°/s stretches, yet was not affected by the stretching set. However, during the rest session the short-latency response decreased with the number of fast stretches, as well as the stretching set. Therefore, it appears that the volitional muscle activity increased the short-latency response such that it was comparable across the entire first set of fast stretches when compared to the entire second set of fast stretches. In contrast, during the rest session the short-latency response was significantly less across the entire second set of fast 120°/s stretches when compared to the entire first set of fast stretches. Hence, any noticeable increase in the short-latency response due to rest was not observed.

Conclusions about the impact of the voluntary muscle activation and rest on the long-latency response, which is associated with transcortical circuitry, cannot be deduced. This is because the angular speed differed during the time windows corresponding to the short- and long-latency response, potentially contributing to a speed-dependent change in spinal activity that was greater than the change in a transcortical activity.

Future work is needed to improve our understanding for the mechanism contributing to the impact of volitional muscle activation on reversing stretch-induced reflex accommodation.

Limitations

One limitation of this study is that the angular speed of 120°/s did not elicit a stretch reflex in all participants. This speed was selected since it is faster than speeds used in previous research; yet, using even faster speeds may have been more effective for eliciting responses in the flexors as well as extensors of all participants (Schmit et al., 2000). Second, only one stretching protocol was examined in this experiment. Different stretching interventions, including of varying angular range, velocity, repetitions, and frequency, may lead to different results with regards to the rate of reflex accommodation and the impact of volitional muscle activation and rest. Third, only a ballistic movement, selected for its functional relevance, was tested; other voluntary movement types (e.g. slow, isometric) could induce different effects on stretch reflex activity. Fourth, this study examined the immediate impact of voluntary movement on stretch reflex activity without addressing long-term effects. Currently, the bulk of the literature examines the effects of stretching within a single session and neglects the long-term effects. Further research is needed to understand the effect of stretching, and volitional muscle activation after stretching, on spasticity in the long term.

Concluding Remarks

Our findings indicate that stretch reflex accommodation can be altered by volitional muscle activation. Clinically, our findings suggest that the therapeutic benefit of accommodating stretch reflex activity in individuals with stroke through fast consecutive stretches may be reversed once the individual volitionally activates their paretic arm. This study examined a single, precisely-controlled, robot-mediated stretching protocol, whereas there is a plethora of stretching protocols utilized in the clinical setting that have much greater stretch- to- stretch variances. Further testing

is needed to determine if voluntary muscle activation yields similar results with other stretching protocols. Even so, as long as the stretch reflex threshold is reached, the results of the current study are likely to persist. Moreover, additional research is needed to elucidate the mechanism(s) contributing to increased stretch reflex activity post-volitional muscle activation, in addition to determining the exact neural mechanism(s) contributing to the accommodation of the stretch reflex when stretching. For individuals with a unilateral brain injury due to a stroke who cannot volitionally activate their paretic arm, the stretch-induced reflex accommodation arising from fast consecutive stretching may remain beneficial. To conclude, future work is needed to understand the long-term implications of fast consecutive stretches as an effective treatment for stretch reflex hyperactivity, or spasticity, in individuals with stroke.

References

Bovend'Eerdt, T. J., Newman, M., Barker, K., Dawes, H., Minelli, C., & Wade, D. T. (2008). The effects of stretching in spasticity: A systematic review. Archives of Physical Medicine and Rehabilitation, 89(7), 1395–1406. https://doi.org/10.1016/j.apmr.2008.02.015

Brown, MC, Goodwin, GM, & Matthews, PB. (1970). The persistence of stable bonds between actin and myosin filaments of intrafusal muscle fibers following their activation. The Journal of Physiology, 210(1), 9.

Brown, P. (1994). Pathophysiology of spasticity. Journal of Neurology, Neurosurgery & Psychiatry, 57(7), 773–777. https://doi.org/10.1136/jnnp.57.7.773

Condliffe, E. G., Clark, D. J., & Patten, C. (2005). Reliability of elbow stretch reflex assessment in chronic post-stroke hemiparesis. Clinical Neurophysiology, 116(8), 1870–1878. https://doi.org/10.1016/j.clinph.2005.02.030

Davidson, A. G., & Buford, J. A. (2006). Bilateral actions of the reticulospinal tract on arm and shoulder muscles in the monkey: Stimulus triggered averaging. Experimental Brain Research, 173(1), 25–39. https://doi.org/10.1007/s00221-006-0374-1

Davidson, A. G., Schieber, M. H., & Buford, J. A. (2007). Bilateral spike-triggered average effects in arm and shoulder muscles from the monkey pontomedullary reticular formation. Journal of Neuroscience, 27(30), 8053–8058. https://doi.org/10.1523/JNEUROSCI.0040-07.2007

Dewald, J. P. A., Given, J. D., & Rymer, W. Z. (1996). Long-lasting reductions of spasticity induced by skin electrical stimulation. IEEE Transactions on Rehabilitation Engineering, 4(4), 231–242. https://doi.org/10.1109/86.547923

Eldred, E., Hutton, R. S., & Smith, J. L. (1976). Nature of the persisting changes in afferent discharge from muscle following its contraction. In Progress in Brain Research (Vol. 44, pp. 157–170). https://doi.org/10.1016/S0079-6123(08)60731-1

Enoka, R. M., Hutton, R. S., & Eldred, E. (1980). Changes in excitability of tendon tap and Hoffmann reflexes following voluntary contractions. Electroencephalography and Clinical Neurophysiology, 48(6), 664–672. https://doi.org/10.1016/0013-4694(80)90423-X

Fedirchuk, B., & Dai, Y. (2004). Monoamines increase the excitability of spinal neurones in the neonatal rat by hyperpolarizing the threshold for action potential production. The Journal of Physiology, 557(2), 355–361. https://doi.org/10.1113/jphysiol.2004.064022

Fisher, K. M., Zaaimi, B., & Baker, S. N. (2012). Reticular formation responses to magnetic brain stimulation of primary motor cortex. The Journal of Physiology, 590(16), 4045–4060. https://doi.org/10.1113/jphysiol.2011.226209

Gregory, J. E., Mark, R. F., Morgan, D. L., Patak, A., Polus, B., & Proske, U. (1990). Effects of muscle history on the stretch reflex in cat and man. The Journal of Physiology, 424(1), 93–107. https://doi.org/10.1113/jphysiol.1990.sp018057

Guissard, N., & Duchateau, J. (2006). Neural aspects of muscle stretching. Exercise and Sport Sciences Reviews, 34(4), 154–158. https://doi.org/10.1249/01.jes.0000240023.30373.eb

Heckman, C. J., Johnson, M., Mottram, C., & Schuster, J. (2008). Persistent inward currents in spinal motoneurons and their influence on human motoneuron firing patterns. The Neuroscientist, 14(3), 264–275. https://doi.org/10.1177/1073858408314986

Heckman, C. J., Lee, R. H., & Brownstone, R. M. (2003). Hyperexcitable dendrites in motoneurons and their neuromodulatory control during motor behavior. Trends in Neurosciences, 26(12), 688–695. https://doi.org/10.1016/j.tins.2003.10.002

Heckman, C. J., Mottram, C., Quinlan, K., Theiss, R., & Schuster, J. (2009). Motoneuron excitability: The importance of neuromodulatory inputs. Clinical Neurophysiology, 120(12), 2040–2054. https://doi.org/10.1016/j.clinph.2009.08.009

Herda, T. J., Ryan, E. D., Costa, P. B., Walter, A. A., Hoge, K. M., Uribe, B. P., McLagan, J. R., Stout, J. R., & Cramer, J. T. (2010). Acute effects of passive stretching and vibration on the electromechanical delay and musculotendinous stiffness of the plantar flexors. Electromyography and Clinical Neurophysiology, 50(6), 277–288. https://doi.org/10.1111/j.1600-0838.2008.00787.x

Hutton, R. S., Smith, J. L., & Eldred, E. (1973). Postcontraction sensory discharge from muscle and its source. Journal of Neurophysiology, 36(6), 1090–1103. https://doi.org/10.1152/jn.1973.36.6.1090

Hutton, R. S., & Suzuki, S. (1979). Postcontraction discharge of motor neurons in spinal animals. Experimental Neurology, 64(3), 567–578. https://doi.org/10.1016/0014-4886(79)90232-2

Jacobs, B. L., Martín-Cora, F. J., & Fornal, C. A. (2002). Activity of medullary serotonergic neurons in freely moving animals. Brain Research Reviews, 40(1–3), 45–52. https://doi.org/10.1016/S0165-0173(02)00187-X

Kably, B., & Drew, T. (1998). Corticoreticular pathways in the cat. I. Projection patterns and collaterization. Journal of Neurophysiology, 80(1), 389–405. https://doi.org/10.1152/jn.1998.80.1.389

Kamper, D. G., Harvey, R. L., Suresh, S., & Rymer, W. Z. (2003). Relative contributions of neural mechanisms versus muscle mechanics in promoting finger extension deficits following stroke. Muscle & Nerve, 28(3), 309–318. https://doi.org/10.1002/mus.10443

Krakauer, J. W. (2009). Motor learning and consolidation: The case of visuomotor rotation. In D. Sternad (Ed.), Progress in Motor Control (Vol. 629, pp. 405–421). Springer, Boston, MA. https://doi.org/10.1007/978-0-387-77064-2_21

Krakauer, J. W., & Shadmehr, R. (2006). Consolidation of motor memory. Trends in Neurosciences, 29(1), 58–64. https://doi.org/10.1016/j.tins.2005.10.003

Kubo, K., Kanehisa, H., & Fukunaga, T. (2002). Effects of transient muscle contractions and stretching on the tendon structures in vivo. Acta Physiologica Scandinavica, 175(2), 157–164. https://doi.org/10.1046/j.1365-201X.2002.00976.x

Kubo, K., Kanehisa, H., Kawakami, Y., & Fukunaga, T. (2001). Influence of static stretching on viscoelastic properties of human tendon structures in vivo. Journal of Applied Physiology, 90(2), 520–527. https://doi.org/10.1152/jappl.2001.90.2.520

Lance, J. W. (1980). The control of muscle tone, reflexes, and movement: Robert Wartenbeg Lecture. Neurology, 30(12), 1303–1313. https://doi.org/10.1212/wnl.30.12.1303

Lee, R. H., & Heckman, C. J. (1999). Enhancement of bistability in spinal motoneurons in vivo by the noradrenergic α1 agonist methoxamine. Journal of Neurophysiology, 81(5), 2164–2174. https://doi.org/10.1152/jn.1999.81.5.2164

Levin, M. F., & Feldman, A. G. (1994). The role of stretch reflex threshold regulation in normal and impaired motor control. Brain Research, 657(1–2), 23–30. https://doi.org/10.1016/0006-8993(94)90949-0

Li, S. (2017). Spasticity, motor recovery, and neural plasticity after stroke. Frontiers in Neurology, 8. https://doi.org/10.3389/fneur.2017.00120

Li, S., Chang, S.-H., Francisco, G. E., & Verduzco-Gutierrez, M. (2014). Acoustic startle reflex in patients with chronic stroke at different stages of motor recovery: A pilot study. Topics in Stroke Rehabilitation, 21(4), 358–370. https://doi.org/10.1310/tsr2104-358

Li, S., Chen, Y.-T., Francisco, G. E., Zhou, P., & Rymer, W. Z. (2019). A unifying pathophysiological account for post-stroke spasticity and disordered motor control. Frontiers in Neurology, 10, 468. https://doi.org/10.3389/fneur.2019.00468

Lincoln, N., Jackson, J., & Adams, S. (1998). Reliability and revision of the Nottingham Sensory Assessment for stroke patients. Physiotherapy, 84(8), 358–365. https://doi.org/10.1016/S0031-9406(05)61454-X

McPherson, J. G., Chen, A., Ellis, M. D., Yao, J., Heckman, C. J., & Dewald, J. P. A. (2018). Progressive recruitment of contralesional cortico-reticulospinal pathways drives motor impairment post stroke. The Journal of Physiology, 596(7), 1211–1225. https://doi.org/10.1113/JP274968

McPherson, J. G., Ellis, M. D., Heckman, C. J., & Dewald, J. P. A. (2008). Evidence for increased activation of persistent inward currents in individuals with chronic hemiparetic stroke. Journal of Neurophysiology, 100(6), 3236–3243. https://doi.org/10.1152/jn.90563.2008

McPherson, J. G., McPherson, L. M., Thompson, C. K., Ellis, M. D., Heckman, C. J., & Dewald, J. P. A. (2018). Altered neuromodulatory drive may contribute to exaggerated tonic vibration reflexes in chronic hemiparetic stroke. Frontiers in Human Neuroscience, 12. https://doi.org/10.3389/fnhum.2018.00131

McPherson, J. G., Stienen, A. H. A., Schmit, B. D., & Dewald, J. P. A. (2019). Biomechanical parameters of the elbow stretch reflex in chronic hemiparetic stroke. Experimental Brain Research, 237(1), 121–135. https://doi.org/10.1007/s00221-018-5389-x

McPherson, J. G., Stienen, A. H., Drogos, J. M., & Dewald, J. P. (2018). Modification of spastic stretch reflexes at the elbow by flexion synergy expression in individuals with chronic hemiparetic stroke. Archives of Physical Medicine and Rehabilitation, 99(3), 491–500. https://doi.org/10.1016/j.apmr.2017.06.019

Miller, L. C., & Dewald, J. P. A. (2012). Involuntary paretic wrist/finger flexion forces and EMG increase with shoulder abduction load in individuals with chronic stroke. Clinical Neurophysiology, 123(6), 1216–1225. https://doi.org/10.1016/j.clinph.2012.01.009

Mottram, C. J., Wallace, C. L., Chikando, C. N., & Rymer, W. Z. (2010). Origins of spontaneous firing of motor units in the spastic–paretic biceps brachii muscle of stroke survivors. Journal of Neurophysiology, 104(6), 3168–3179. https://doi.org/10.1152/jn.00463.2010

Naro, A., Leo, A., Russo, M., Casella, C., Buda, A., Crespantini, A., Porcari, B., Carioti, L., Billeri, L., Bramanti, A., Bramanti, P., & Calabrò, R. S. (2017). Breakthroughs in the spasticity management: Are non-pharmacological treatments the future? Journal of Clinical Neuroscience, 39, 16–27. https://doi.org/10.1016/j.jocn.2017.02.044

Pavlenko, V. B., & Kulichenko, A. M. (2003). Self-initiated motor behavioral act-related neuronal activity in the cat locus coeruleus. Neurophysiology, 35, 29–37. https://doi.org/10.1023/A:1023994205918

Powers, R. K., Campbell, D. L., & Rymer, W. Z. (1989). Stretch reflex dynamics in spastic elbow flexor muscles. Annals of Neurology, 25(1), 32–42. https://doi.org/10.1002/ana.410250106

Ryan, E. D., Beck, T. W., Herda, T. J., Hull, H. R., Hartman, M. J., Costa, P. B., Defreitas, J. M., Stout, J. R., & Cramer, J. T. (2008). The time course of musculotendinous stiffness responses following different durations of passive stretching. Journal of Orthopaedic & Sports Physical Therapy, 38(10), 632–639. https://doi.org/10.2519/jospt.2008.2843

Schmit, B. D., Dewald, J. P. A., & Rymer, W. Z. (2000). Stretch reflex adaptation in elbow flexors during repeated passive movements in unilateral brain-injured patients. Archives of Physical Medicine and Rehabilitation, 81, 10. https://doi.org/10.1016/s0003-9993(00)90070-4

Sheean, G. (2002). The pathophysiology of spasticity. European Journal of Neurology, 9(s1), 3–9. https://doi.org/10.1046/j.1468-1331.2002.0090s1003.x

Smania, N., Picelli, A., Daniele, M., Geroin, C., Ianes, P., Waldner, A., & Gandolfi, M. (2010). Rehabilitation procedures in the management of spasticity. European Journal of Physical and Rehabilitation Medicine, 46, 423–438.

Sommerfeld, D. K., Eek, E. U.-B., Svensson, A.-K., Holmqvist, L. W., & von Arbin, M. H. (2004). Spasticity after stroke: Its occurrence and association with motor impairments and activity limitations. Stroke, 35(1), 134–139. https://doi.org/10.1161/01.STR.0000105386.05173.5E

Taylor, D. C., Brooks, D. E., & Ryan, J. B. (1997). Viscoelastic characteristics of muscle: Passive stretching versus muscular contractions. Medicine & Science in Sports & Exercise, 29(12), 1619–1624.

Triandafilou, K. M., Ochoa, J., Kang, X., Fischer, H. C., Stoykov, M. E., & Kamper, D. G. (2011). Transient impact of prolonged versus repetitive stretch on hand motor control in chronic stroke. Topics in Stroke Rehabilitation, 18(4), 316–324. https://doi.org/10.1310/tsr1804-316

Tsai, K.-H., Yeh, C.-Y., Chang, H.-Y., & Chen, J.-J. (2001). Effects of a single session of prolonged muscle stretch on spastic muscle of stroke patients. Proceedings of the National Science Council, 25(3), 76–81.

Turpin, N. A., Levin, M. F., & Feldman, A. G. (2016). Implicit learning and generalization of stretch response modulation in humans. Journal of Neurophysiology, 115(6), 3186–3194. https://doi.org/10.1152/jn.01143.2015

Urban, P. P., Wolf, T., Uebele, M., Marx, J. J., Vogt, T., Stoeter, P., Bauermann, T., Weibrich, C., Vucurevic, G. D., Schneider, A., & Wissel, J. (2010). Occurence and clinical predictors of spasticity after ischemic stroke. Stroke, 41(9), 2016–2020. https://doi.org/10.1161/STROKEAHA.110.581991

Vecchio, M., Gracies, J.-M., Panza, F., Fortunato, F., Vitaliti, G., Malaguarnera, G., Cinone, N., Beatrice, R., Ranieri, M., & Santamato, A. (2017). Change in coefficient of fatigability following rapid, repetitive movement training in post-stroke spastic paresis: A prospective open-label observational study. Journal of Stroke and Cerebrovascular Diseases, 26(11), 2536–2540. https://doi.org/10.1016/j.jstrokecerebrovasdis.2017.05.046

Wei, K., Glaser, J. I., Deng, L., Thompson, C. K., Stevenson, I. H., Wang, Q., Hornby, T. G., Heckman, C. J., & Kording, K. P. (2014). Serotonin affects movement gain control in the spinal cord. Journal of Neuroscience, 34(38), 12690–12700. https://doi.org/10.1523/JNEUROSCI.1855-14.2014

Wilson, L. R., Gandevia, S. C., Inglis, J. T., Gracies, J.-M., & Burke, D. (1999). Muscle spindle activity in the affected upper limb after a unilateral stroke. Brain, 122(11), 2079–2088. https://doi.org/10.1093/brain/122.11.2079

Wissel, J., Schelosky, L. D., Scott, J., Christe, W., Faiss, J. H., & Mueller, J. (2010). Early development of spasticity following stroke: A prospective, observational trial. Journal of Neurology, 257(7), 1067–1072. https://doi.org/10.1007/s00415-010-5463-1

Zaaimi, B., Edgley, S. A., Soteropoulos, D. S., & Baker, S. N. (2012). Changes in descending motor pathway connectivity after corticospinal tract lesion in macaque monkey. Brain, 135(7), 2277–2289. https://doi.org/10.1093/brain/aws115

Zorowitz, R. D., Gillard, P. J., & Brainin, M. (2013). Poststroke spasticity: Sequelae and burden on stroke survivors and caregivers. Neurology, 80(3), S45–S52. https://doi.org/10.1212/WNL.0b013e3182764c86